

TALLINN UNIVERSITY OF TECHNOLOGY
DOCTORAL THESIS
37/2018

**Application of Activated Persulfate
Processes for the Treatment of Water and
High-Strength Wastewater**

ENELIIS KATTEL



TALLINN UNIVERSITY OF TECHNOLOGY

School of Engineering

Department of Materials and Environmental Technology

This dissertation was accepted for the defence of the degree 11/04/2018

Supervisor: Senior Research Scientist Dr. Niina Dulova
School of Engineering
Tallinn University of Technology
Tallinn, Estonia

Co-supervisor: Prof. Marina Trapido
School of Engineering
Tallinn University of Technology
Tallinn, Estonia

Opponents: Prof. Miray Bekbölet
Institute of Environmental Sciences
Bogazici University
Istanbul, Turkey

Dr. Anne Menert
Chair of Genetics
University of Tartu
Tartu, Estonia

Defence of the thesis: 25/06/2018, Tallinn

Declaration:

Hereby I declare that this doctoral thesis, my original investigation and achievement, submitted for the doctoral degree at Tallinn University of Technology has not been submitted for doctoral or equivalent academic degree.

Eneliis Kattel

signature



European Union
European Regional
Development Fund



Investing
in your future

This work has been partially supported by ASTRA "TUT Institutional Development Programme for 2016-2022" Graduate School of Functional Materials and Technologies (2014-2020.4.01.16-0032).

Copyright: Eneliis Kattel, 2018

ISSN 2585-6898 (publication)

ISBN 978-9949-83-243-9 (publication)

ISSN 2585-6901 (PDF)

ISBN 978-9949-83-244-6 (PDF)

TALLINNA TEHNIKAÜLIKOOL
DOKTORITÖÖ
37/2018

**Aktiveeritud persulfaadi protsesside
kasutamine vee ja raskesti saastatud reovee
puhastamiseks**

ENELIIS KATTEL

CONTENTS

LIST OF PUBLICATIONS	7
AUTHOR'S CONTRIBUTION TO THE PUBLICATIONS	9
INTRODUCTION	10
ABBREVIATIONS	11
1 LITERATURE REVIEW	12
1.1 Properties of persulfate	12
1.2 Persulfate activation mechanisms	12
1.2.1 Transition metal-activated persulfate	13
1.2.2 Heterogeneous metal-bearing species-activated persulfate	14
1.2.3 Carbon-activated persulfate	15
1.2.4 Alkali-activated persulfate	16
1.2.5 Oxidant-activated persulfate	16
1.2.6 Thermally-activated persulfate	17
1.2.7 Radiation-activated persulfate	18
1.2.8 Electrochemically-activated persulfate	19
1.3 Activated persulfate treatment for natural water and high-strength wastewater	20
1.3.1 Groundwater and other natural waters	20
1.3.2 Drinking water	21
1.3.3 Secondly treated wastewater	22
1.3.4 Landfill leachate	23
1.3.5 Industrial wastewaters	23
1.4 Aim of the study	24
2 MATERIALS AND METHODS	25
2.1 Chemicals and materials	25
2.2 Experimental procedure	26
2.3 Analytical methods	27
3 RESULTS AND DISCUSSION	29
3.1 Fe(II)-activated persulfate treatment	29
3.2 UVA/Fe(II)-activated persulfate treatment	35
3.3 H ₂ O ₂ -activated persulfate treatment	38
CONCLUSIONS	40

REFERENCES	41
ACKNOWLEDGEMENTS	46
ABSTRACT	47
LÜHIKOKKUVÕTE.....	49
APPENDIX	51
PAPER I	53
PAPER II	63
PAPER III	75
PAPER IV	87
CURRICULUM VITAE	99
ELULOOKIRJELDUS	102

LIST OF PUBLICATIONS

The list of author's publications, on the basis of which the thesis has been prepared:

- I **Kattel, E.**, Dulova, N., Viisimaa, M., Tenno, T., Trapido, M. Treatment of high-strength wastewater by Fe²⁺-activated persulfate and hydrogen peroxide. – *Environmental Technology*, 2016, 37 (3), 352–359.
- II **Kattel, E.**, Dulova, N. Ferrous ion-activated persulphate process for landfill leachate treatment: removal of organic load, phenolic micropollutants and nitrogen. – *Environmental Technology*, 2017, 38 (10), 1223–1231.
- III **Kattel, E.**, Trapido, M., Dulova, N. Oxidative degradation of emerging micropollutant acesulfame in aqueous matrices by UVA-induced H₂O₂/Fe²⁺ and S₂O₈²⁻/Fe²⁺ processes. – *Chemosphere*, 2017, 171, 528–536.
- IV Dulova, N., **Kattel, E.**, Trapido, M. Degradation of naproxen by ferrous ion-activated hydrogen peroxide, persulfate and combined hydrogen peroxide/persulfate processes: the effect of citric acid addition. – *Chemical Engineering Journal*, 2017, 318, 254–263.

Copies of these articles are included in APPENDIX.

Other publications related to the research:

Trapido, M., Tenno, T., Goi, A., Dulova, N., **Kattel, E.**, Klauson, D., Klein, K., Tenno, T., Viisimaa, M. Bio-recalcitrant pollutants removal from wastewater with combination of the Fenton treatment and biological oxidation. – *Journal of Water Process Engineering*, 2017, 16, 277–282.

Klein, K., **Kattel, E.**, Goi, A., Kivi, A., Dulova, N., Saluste, A., Zekker, I., Trapido, M., Tenno, T. Combined treatment of pyrogenic wastewater from oil shale retorting. – *Oil Shale*, 2017, 34 (1), 82–96.

Kattel, E., Kivi, A., Klein, K., Tenno, T., Dulova, N., Trapido, M. Hazardous waste landfill leachate treatment by combined chemical and biological techniques. – *Desalination and Water Treatment*, 2016, 57(28), 13236–13245.

Kattel, E., Trapido, M., Dulova, N. Treatment of landfill leachate by continuously reused ferric oxyhydroxide sludge-activated hydrogen peroxide. – *Chemical Engineering Journal*, 2016, 304, 646–654.

Klauson, D., Kivi, A., **Kattel, E.**, Klein, K., Viisimaa, M., Bolobajev, J., Velling, S., Goi, A., Tenno, T., Trapido, M. Combined processes for wastewater purification: treatment of a typical landfill leachate with a combination of chemical and biological oxidation processes. – *Journal of Chemical Technology and Biotechnology*, 2015, 90, 1927–1536.

Bolobajev, J., **Kattel, E.**, Viisimaa, M., Goi, A., Trapido, M., Tenno, T., Dulova, N. Reuse of ferric sludge as an iron source for the Fenton-based process in wastewater treatment. – *Chemical Engineering Journal*, 2014, 255, 8–13.

Klauson, D., Klein, K., Kivi, A., **Kattel, E.**, Viisimaa, M., Dulova, N., Velling, S., Trapido, M., Tenno, T. Combined methods for the treatment of a typical hardwood soaking basin wastewater from plywood industry. – *International Journal of Environmental Science and Technology*, 2015, 12(11), 3575–3586.

Kattel, E., Viisimaa, M., Klauson, D., Trapido, M., Dulova, N. Advanced chemical oxidation with pre-coagulation for treatment of paint manufacturing wastewater. – *International Journal of Environmental Engineering*, 2014, 1(4), 103–108.

AUTHOR'S CONTRIBUTION TO THE PUBLICATIONS

Contribution to the papers associated with this thesis are:

- I The author carried out the experiments and respective analyses, interpreted the obtained data and participated in writing of the paper.
- II The author carried out the experiments, further supervising the experimental work of an MSc-student, interpreted the results and wrote the paper. She presented the results at the 15th European Meeting on Environmental Chemistry (EMEC 15), Brno, Czech Republic, December 3–6, 2014.
- III The author carried out the experiments, supervised the experimental work of two MSc students, interpreted the results and wrote the paper. She presented the results at the 1st International Conference on Sustainable Water Processing (SWPG 16), Sitges, Spain, September 11–14, 2016 and partly at the 2nd Summer School on Environmental Applications of Advanced Oxidation Processes and Training School on Advanced Treatment Technologies and Contaminants of Emerging Concern (NEREUS COST Action ES1403), Porto, Portugal, July 10–14, 2017.
- IV The author carried out the experiments, and participated in interpretation of the results and writing of the paper.

INTRODUCTION

Continuous water contamination from anthropogenic sources induces a need for applicable purification methods. The rapid development of chemical synthesis and the demand for diverse chemicals in various fields of production and services causes the presence of recalcitrant and sometimes highly toxic substances in surface waters, groundwater and even in drinking water. The origin and the character of pollution often dictates the choice of feasible treatment processes, which may be physical, biological, chemical or a combination of these.

Conventional water decontamination technologies, such as biological treatment in wastewater treatment, and chlorination in drinking water disinfection are often unsuitable for the treatment of water with varying properties. For example, very low concentrations of organic contaminants (ng/L– μ g/L) or, on the contrary, high organic loads (g/L) are problematic for traditional wastewater processes. In addition, chlorination in drinking water disinfection may produce transformation products of high toxicity. A promising solution of the discussed problems consists of radical-based advanced oxidation technologies (AOTs) mainly based on oxidative properties of hydroxyl and sulfate radicals. These species are effective enough to degrade various recalcitrant organic pollutants.

Activated persulfate processes are among AOTs that reduce organic pollution through sulfate radicals. Persulfate is a strong and stable oxidant that needs extra activation to generate sulfate radicals. These species are much more active than the precursor, and selectively degrading different organic compounds such as pharmaceuticals, dyes, agrochemicals, personal care products components etc. The productivity of sulfate radicals from persulfate can be influenced by the activation types. The activation of persulfate may be implemented in several ways, e.g. metallic ions, heat, radiation, oxidant, increased pH, which generally needs careful adjustment to achieve high efficacy in water purification.

This thesis provides an overview of the most important persulfate activation methods with the application examples for the degradation of different compounds at wide concentration ranges in various aqueous matrices including ultrapure water, groundwater and wastewater. The most viable activators, such as ferrous iron and chelated ferrous iron, and the ultraviolet (UV) light, were chosen for studies in this research with the aim to implement these processes *in situ* in future.

This research focuses on the treatment of real waters containing emerging contaminants in different aqueous matrices. Among the studied pollutants, for the first time, an artificial sweetener acesulfame K, further referred as acesulfame (ACE), is degraded by the activated persulfate process. Also, a new combined persulfate system with chelating agent is applied for the abatement of pharmaceutical naproxen (NPX). The studies about a pyrolysis wastewater and a landfill leachate were performed for the first time, since the real aqueous matrices are not very often used in studies leaving several uncertainties.

The knowledge gained from this doctoral research could be a milestone for the full-scale applications of activated persulfate processes for the purification of wastewater at various pollution levels.

ABBREVIATIONS

AOP	Advanced oxidation process
AOT	Advanced oxidation technology
BOD ₇	7-day biochemical oxygen demand
CA	Citric acid
CNT	Carbon nanotube
COD	Chemical oxygen demand
DBP	Disinfection by-product
DOC	Dissolved organic carbon
DN	Dissolved nitrogen
EDTA	Ethylenedinitrilotetraacetic acid
EDDS	Ethylenediaminedisuccinate
GAC	Granulated activated carbon
EtOH	Ethanol
ACE	Acesulfame
NPX	Naproxen
NPOC	Non-purgeable organic carbon
TOC	Total organic carbon
<i>t</i> -BuOH	<i>Tert</i> -Butanol
UV	Ultraviolet
ZVI	Zero-valent iron
SO ₄ ^{•-} -AOTs	Sulfate radical-based advanced oxidation technologies

1 LITERATURE REVIEW

1.1 Properties of persulfate

Peroxydisulfate or persulfate anion ($S_2O_8^{2-}$) is a strong oxidant ($E^0 = 2.01$ V), which can be found in the form of three salts: ammonia, potassium and sodium (Tsitonaki et al., 2010; Waclawek et al., 2017). The application of sodium persulfate ($Na_2S_2O_8$) is mostly favored since this salt has aqueous solubility as high as 730 g per kg of H_2O at 25 °C. The use of ammonia persulfate can lead to the secondary contamination caused by residual concentrations of ammonia, whereas the use of potassium persulfate may be ineffective especially for *in situ* applications due to its low solubility (Behrman and Dean, 1999).

Persulfate is stable at room temperature and its direct oxidation reactions are slow showing a negligible efficacy for water treatment. Thus, it needs activation, which thereupon results in generation of sulfate radicals ($SO_4^{\bullet-}$) selectively degrading organic pollutants.

1.2 Persulfate activation mechanisms

Without activation, persulfate may react with some organic compounds, although the process efficacy is lower than the one of the activated persulfate. This may be explained by the higher oxidation potential of $SO_4^{\bullet-}$ ($E^0 = 2.60$ V) (Tsitonaki et al., 2010). It is important to note that in addition to $SO_4^{\bullet-}$, another type of highly reactive radical species, hydroxyl radicals (HO^{\bullet}), are always in the activated persulfate system through the reactions between water and $SO_4^{\bullet-}$ (Eqs. 1–2) (Hayon et al., 1972; Liang and Su, 2009):



The output of the two different radicals in the oxidative system depends on pH: at acidic pH, $SO_4^{\bullet-}$ are dominant and at alkaline pH, HO^{\bullet} are controlling the oxidation efficacy, while at pH 7, both radicals participate equally in oxidation reactions (Liang and Su, 2009).

However, the overall extent of $SO_4^{\bullet-}$ generation depends on the type of activation used (Figure 1). The following paragraphs give an overview of different persulfate activation mechanisms with emphasis on the main advantages and disadvantages.

It should be added that the HO^{\bullet} -based processes, defined as advanced oxidation processes (AOPs), have been known since the end of 19th century, e.g. the Fenton reagent. In the last decades, these processes have been gradually, but increasingly substituted by $SO_4^{\bullet-}$ -based processes due to their higher selectivity towards the pollutants and wide application pH range (Tsitonaki et al., 2010). In addition, the less aggressive character of activated persulfate allows its application to various types of (waste)waters without carrying out any extra preventive measures, such as defoaming (Matzek and Carter, 2016). Moreover, compared to the HO^{\bullet} precursors, hydrogen peroxide and ozone, persulfate as $SO_4^{\bullet-}$ precursor has longer life span making it suitable for the elimination of recalcitrant organic pollutants.

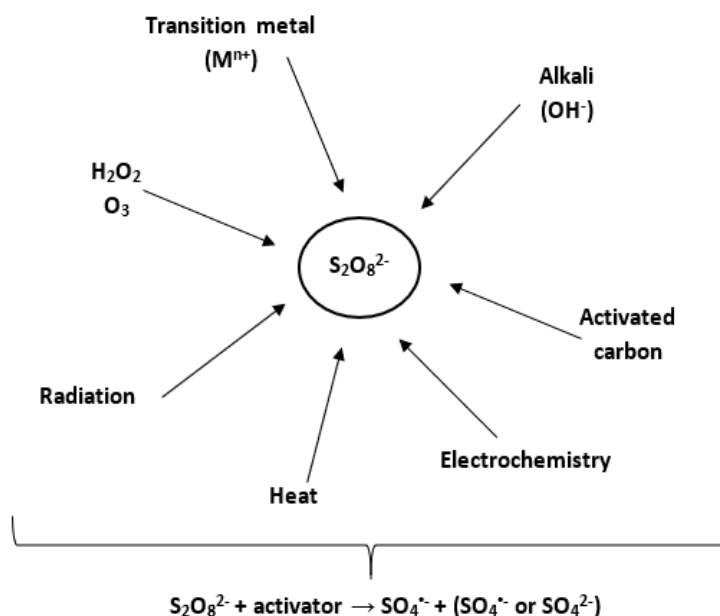


Figure 1. Different persulfate activation methods to generate sulfate radicals

The reaction mechanism for the oxidation of the studied recalcitrant pollutants by $SO_4^{\bullet -}$ is similar with HO^{\bullet} : hydrogen-atom abstraction, hydroxyl addition or electron transfer (Devi et al., 2016). The latter is more intrinsic to $SO_4^{\bullet -}$ and suggests that the characteristics of the contaminants helps to predict the transformation pathways.

1.2.1 Transition metal-activated persulfate

Activated persulfate treatment is used for *in situ* environmental applications and, thus, transition metals are the most suitable activation aids. The one-electron transfer from metal ion generates $SO_4^{\bullet -}$ without a need for special equipment or arrangements (Eqs. 3–5) (Zhang et al., 2015):



Fe(II), Fe(III), Mn(II), Ce(II), Co(II), Ru(III), V(III), Ag(II) and Ni(II) are amongst frequently studied metal activators (Anipsitakis and Dionysiou, 2004; Zhang et al., 2015; Devi et al., 2016; Waclawek et al., 2017). However, the toxic heavy metals presented in this list are undesirable to use, if not combined to a solid support material to avoid leaching and dissolving into the treated aqueous matrices (the heterogeneous activation of persulfate will be further discussed in section 1.2.2).

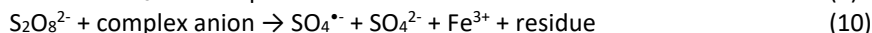
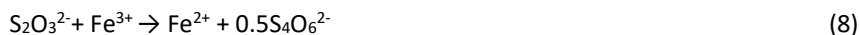
The non-toxic nature and good availability makes persulfate activation by iron one of the most applied options to produce $SO_4^{\bullet -}$. Such generation type of $SO_4^{\bullet -}$ has some limitations since the fast conversion of Fe(II) into Fe(III) (Eq. 6) occurs, and the excessive Fe(II) scavenges $SO_4^{\bullet -}$ (Eqs. 4 and 7), and thereby the efficacy of the pollutant degradation is reduced (Buxton et al., 1997).



The reaction given in Eq. 7 may be controlled by choosing the most suitable Fe(II) dose for persulfate activation or adding it in a stepwise mode.

Chelated transition metals, especially Fe(II), have appeared to be an effective alternative to decrease the metal concentrations required for persulfate activation at neutral pH (Liang et al., 2004b). Ethylenedinitrilotetraacetic acid (EDTA), ethylenediaminedisuccinate (EDDS), sodium polyphosphates, citric acid (CA), oxalic acid, tartaric acid, nitrilotriacetate and N-(2-hydroxyethyl) iminodiacetate are among most commonly used chelating agents (Liang et al., 2004b; Rastogi et al., 2009; Tsitonaki et al., 2010; Han et al., 2015). EDTA forms strong Fe(II) complexes and CA is favored for its biodegradability and overall feasibility (Liang et al., 2004b), being therefore often preferred chelating agents. It should be taken into consideration that some organic chelating agents, e.g. EDDS, might interfere with the pollutant degradation as a secondary contaminant (Yan and Lo, 2013).

The addition of reducing agent, thiosulfate ($\text{S}_2\text{O}_3^{2-}$), could facilitate the regeneration of a metal activator (Liang et al., 2004a) to endorse the $\text{SO}_4^{\bullet-}$ production extent. The mechanism of persulfate-thiosulfate interaction activated by a complex anion containing Fe(II) to produce the $\text{SO}_4^{\bullet-}$ is proposed as follows (Eqs. 8–10) (Liang et al., 2004a):



1.2.2 Heterogeneous metal-bearing species-activated persulfate

Heterogeneous activation of persulfate is an alternative to homogeneous transition metals to avoid the formation of metal hydroxide sludge. It must be noted that the quantity of the latter strongly depends how well are the treatment conditions optimized or controlled.

Zero-valent iron (ZVI, Fe(0)) as a solid iron source gradually releases Fe(II) into the solution via the reaction with persulfate (Eq. 11) or via acid corrosion (Eq. 12) that ensures the generation of $\text{SO}_4^{\bullet-}$ during longer period as described in Eq. 6 (Oh et al., 2009; Rodriquez et al., 2014).



However, this mechanism involves aqueous Fe(II), which means that the activation type is not heterogeneous. Oh et al. (2010) proposed the direct electron transfer from ZVI (Eq. 13) or surface-bound Fe(II) (Eq. 14) heterogeneously activating persulfate. Also, it is assumed that on the surface of ZVI, the recycling of Fe(III) can regenerate Fe(II) (Eq. 15). The generation of $\text{SO}_4^{\bullet-}$ is controlled by changing the particle size of ZVI: finer (from mm to nm) particle provides higher specific surface area, which enhances the generation of oxidative species (Li et al., 2014).



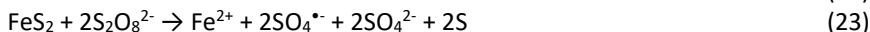
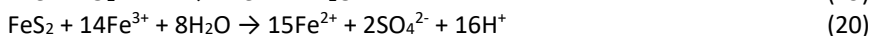
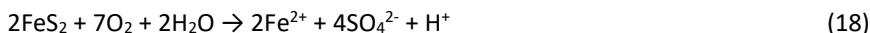
The rise in pH value promotes formation of iron hydroxide on ZVI, which may accumulate in a layer on the surface, and thereby inhibit the reactivity of ZVI (Rodriquez et al., 2014).

Persulfate treatment is commonly implemented for field applications and therefore, the natural soil constituents could be considered as potential activators of persulfate. The abundance of iron in soil provides numerous naturally occurring iron-containing species, of which ferrihydrite ($\text{Fe}_5\text{HO}_8 \cdot 4\text{H}_2\text{O}$), goethite ($\alpha\text{-FeO(OH)}$) and hematite (Fe_2O_3) (Ahmad et al., 2010), magnetite (Fe_3O_4) (Sabri et al., 2012), pyrite (FeS_2) (Zhang et al., 2017), and very recently, pyrrhotite (Fe_{1-x}S) (Xia et al., 2017), have been studied for persulfate activation. General activation mechanism for solid Fe(III)-containing minerals could be as follows (Eqs. 16–17) (Liu et al., 2014):



The regeneration of $\equiv\text{Fe}^{3+}$ together with the production of $\text{SO}_4^{\bullet-}$ should take place quite fast by persulfate (Eq. 17), after the surface metal is reduced via Eq. 16.

Fe(II)-containing pyrite is the most prevalent metal sulfide in soil and can activate persulfate under aerobic or anaerobic conditions. The mechanism is mainly based on the metal leaching from the mineral surface with the suggested following principal reactions (Eqs. 18–23) (Zhang et al., 2017):



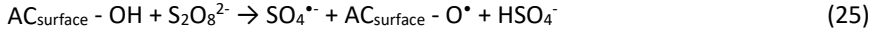
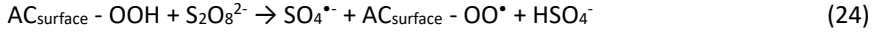
However, in the case of pyrrhotite, the main radical forming reactions are suggested to be initiated by the heterogeneous $\equiv\text{Fe(II)}$ on its surface and by homogeneous leached Fe(II) in the solution (Xia et al., 2017).

Other soil (transition metal) minerals, e.g. manganese- and copper-based ones, have similarities with iron-bearing species persulfate activating mechanisms, but their available environmental concentrations are too low to adequately activate persulfate. The availability of these species depends on the pH range and the presence of scavenging species on the surface of minerals (Ahmad et al., 2010; Teel et al., 2011).

1.2.3 Carbon-activated persulfate

Different modifications of carbon have been reported to successfully activate persulfate. These could be classified as a type of heterogeneous activators showing a certain advantage in being non-metallic species free from metal leaching problems. Carbon materials like nanodiamonds, graphene and carbon nanotubes (CNTs) have high chemical and thermal stability, ultrahigh pore volume and large specific surface area

believed to alleviate the issues related to the use of toxic metal activators (Duan et al., 2015). The first studies were implemented with the simplest form – activated carbon – a processed carbon with low-volume pores. The activation of persulfate by granulated activated carbon (GAC) could most likely proceed on the surface of GAC during the radical propagation mechanism (Eqs. 24–25) (Liang et al., 2009):

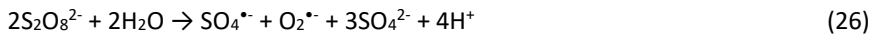


Further process in water treatment relies on the oxidative nature of $SO_4^{\bullet-}$ as well as the adsorptive properties of GAC (Matzek and Carter, 2016).

More detailed studies about CNTs, which are becoming more attractive to be used in water treatment, are accompanied by controversies whether the persulfate activation mechanism by CNTs is radical or non-radical. Duan et al. (2015) speculated that the active sites of carbon matrix can function as an electron mediator to propagate the peroxide bond weakening followed by the oxidation of adsorbed water or hydroxyl groups to generate HO^{\bullet} rather than $SO_4^{\bullet-}$. Sun et al. (2014) proposed that $SO_4^{\bullet-}$ were generated by electron transfer from CNTs. However, more recent studies from Lee et al. (2015) and Guan et al. (2017) about the activating properties of CNTs suggest that the interactions between persulfate and active sites of the solid catalyst initiate the formation of non-radical reactive complexes concurrently with the slow production of sulfate ions that are further responsible for the selected pollutants degradation.

1.2.4 Alkali-activated persulfate

This type of persulfate activation has been applied for *in situ* groundwater remediation by adding sodium or potassium hydroxide to raise the pH value above 11 (Furman et al., 2010). $SO_4^{\bullet-}$ are produced through the hydroperoxide (HO_2^{\bullet}) intermediate which is formed in the alkali-catalyzed hydrolysis of a persulfate molecule and which reacts with another persulfate molecule (Eq. 26). Also, HO^{\bullet} are generated as illustrated with Eq. 2.



If used on site, the pH value after the reaction should be near neutral, thus, it is suggested to follow the alkali to persulfate molar ratio 2:1 (Furman et al., 2011). The buffering properties of water and soil, or sulfuric acid formed in persulfate reactions may require additional alkalinity to keep the elevated pH value (Tsitonaki et al., 2010). This is a possible source to negative impact: high alkali concentrations may affect the soil natural properties (Tsitonaki et al., 2010; Furman et al., 2011).

1.2.5 Oxidant-activated persulfate

Persulfate is often used jointly with other oxidants, mostly in field applications (Tsitonaki et al., 2010), where the nature of soil and contaminant plays an important role in the treatment efficacy. H_2O_2 activation of persulfate has been applied for soil remediation (Tsitonaki et al., 2010) and landfill leachate treatment (Hilles et al., 2016). The knowledge about the interaction between two oxidants is still scarce, but it is

proposed that H₂O₂ is decomposed into HO[•], which are then activating persulfate to generate SO₄^{•-} (Eq. 27) (Lominchar et al., 2018). Another suggestion is that the exothermic reactions of H₂O₂ propagate SO₄^{•-} formation by heat (Tsao and Wilmarth, 1960). In turn, SO₄^{•-} can increase the formation of HO[•], which results in a multiradical system (Eqs. 28–29) (Lominchar et al., 2018).



A similar mechanism is involved when persulfate is indirectly activated by ozone (O₃) (Eqs. 30–41, 27 and 29) (Yang et al., 2016):



The indirect activation by ozone is common when working at pH values above 8.0 (Chiang et al., 2006). It is suggested that under acidic condition, a few HO[•] are generated, but more SO₄^{•-} could be formed via the asymmetric break of peroxide bond when persulfate is activated by acid (Yang et al., 2016). Neutral conditions favor O₃ direct reactions with the target pollutant with a decrease in the radical species generation.

1.2.6 Thermally-activated persulfate

According to Kolthoff and Miller (1951), persulfate exposure with sufficient heat energy produces two sulfate radicals (Eq. 35), but the reaction is pH-sensitive. At basic pH, further formation of HO[•] will occur (Eq. 2).



The required average energy to break the peroxide bond (O-O) in persulfate is different at neutral, basic and acidic pH with 119–129 kJ/mol, 134–139 kJ/mol and 100–116 kJ/mol, respectively (House, 1962). The most often used temperature range for thermal activation of persulfate is 40–70 °C (Ghauch et al., 2012; Zhang et al., 2015), but regarding the structural properties of the organic contaminants, temperatures higher than 100 °C might be needed to apply (Matzek and Carter, 2016). On the other hand, temperature is usually optimized to avoid formation of potential scavengers, chloride and bicarbonate ions, that affects pollutant degradation efficacy (Drzewicz et al., 2012), and to achieve cost-effectiveness.

Thermal activation of persulfate can be implemented via conventional or microwave heating, of which the latter is believed to activate persulfate more intensively (Qi et al., 2015). This prevails even when heat has been used simultaneously with iron indicating that heat energy is a more effective activator of persulfate (Oh et al., 2009). Yet, none of them is used to treat groundwater in real-scale due to the need for high-energy output and other related costs.

1.2.7 Radiation-activated persulfate

This activation type is similar to heat-activated persulfate, when UV radiation (Eq. 36), gamma-radiation (Eq. 37) or pulse radiolysis (Eq. 37) induces the cleavage of peroxide bond generating a pair of sulfate radicals (Tsitonaki et al., 2010; Criquet and Karpel Vel Leitner, 2011):



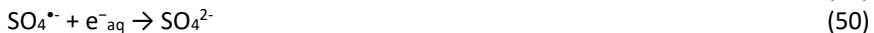
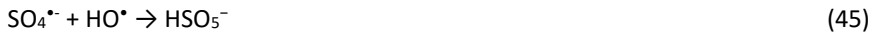
UV radiation activation of persulfate is typically implemented at wavelength of 254 nm mainly due to the diapason high energy and $\text{SO}_4^{\bullet-}$ absorptivity and maximum quantum yield (Hori et al., 2005; Wang and Wang, 2018). The activation of persulfate by UV-light may involve second mechanism according to the reaction given in Eq. 36: an electron can be produced from water exposure to UV, and persulfate is then activated by electron transfer (Eqs. 38–39):



Consequentially, persulfate activation with longer wavelength (365 nm) needs extended exposure period or additional activator (Matzek and Carter, 2016).

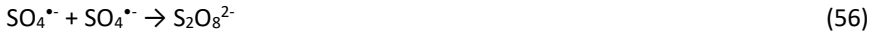
Quite often, UV-radiation is paired with Fe(II) to overcome the shortcomings of iron precipitation. The photo-reduction of ferric iron Fe(III) induces the generation of HO^{\bullet} and thereby provides steady concentration of reactive species (Pouran et al., 2015).

The gamma-irradiation and persulfate combination in water produces simultaneously reducing (hydrated electrons, e^-_{aq}) and oxidizing ($\text{SO}_4^{\bullet-}$) species. It is proposed that the target pollutant degradation is first initiated by water radiolysis products (e^-_{aq} , HO^{\bullet} , H^{\bullet}), which subsequently activate persulfate (Eqs. 37, 39–40), even though gamma rays alone possess sufficient activation energy (Criquet and Karpel Vel Leitner, 2011; Wang and Wang, 2018). Criquet and Karpel Vel Leitner (2011) have compiled principle side-reactions in water radiolysis with persulfate addition (Eqs. 41–52):



The fundamental study of Alkhurajji and Ajlouni (2017) led to the conclusion that the increased persulfate concentration reduces the irradiation dose necessary to generate $\text{SO}_4^{\bullet-}$. The pH value in the gamma-irradiated persulfate systems is proved to decrease owing to the acidity of persulfate and the formation of H^+ during water radiolysis as well the acidic by-products (Alkhurajji et al., 2017).

The sonication of persulfate in water produces $\text{SO}_4^{\bullet-}$ and HO^{\bullet} among other reactive species through the reactions given in Eqs. 53–63 (Darsinou et al., 2015; Wang and Zhou, 2016):



The sonochemical reaction should typically involve two main stages: radical generation from persulfate and water, following the degradation of organic pollutants by the formed reactive species, which performance is primarily controlled by the initial pH value of the aqueous solution (Darsinou et al., 2015)

Sonication implementation in water rapidly rises local temperature and pressure smoothly developing into a heat-activated process (Hoffmann et al., 1996). Thus, in some studies, persulfate sonication is referred as a type of heat activation.

1.2.8 Electrochemically-activated persulfate

Persulfate activation by iron electrode-involving system in aqueous environment consists of simple chain reactions. First, the process is initiated with the production of Fe(II) by anodic corrosion (Eq. 64), which activates persulfate (Eq. 6) and can be regenerated on a cathode (Eq. 65) (Yuan et al., 2014). The latter is suggested to be an opportunity to solve the issues related with total iron accumulation in the activated persulfate system. In addition, water electrolysis occurs on the cathode forming OH^- (Eq. 66) that may contribute to the pH value normalization.



It has been proposed that not only Fe(II), but also persulfate could be regenerated on the cathode from the sulfate ions formed after persulfate consumption (Eq. 67) (Matzek and Carter, 2016).



This type of activation allows effective control over the persulfate oxidation system through the current settings of iron electrode.

Persulfate can be activated by several methods, out of what the Fe(II)-based types could be preferred over the others mainly due to the environmental safety considerations. When aiming for the higher efficacies, the radiation-based activation is used. The most suitable activator should be selected towards the expected outcome of the persulfate process: whether the parameters of the treated water are in correspondence with given legislation, or there is a pre-treated wastewater going to the subsequent treatment phase. The applications of selected activators are presented in the following paragraph.

1.3 Activated persulfate treatment for natural water and high-strength wastewater

Persulfate was used in field applications for soil and groundwater remediation already in the beginning of 2000's. These studies focused mainly on similar type of chlorinated compounds and some main type of activators (Tsitonaki et al., 2010). However, regardless the development of the environmental technology, the variety and altering nature of the organic pollutants in the environmental compartments yet remains challenging in finding optimum treatment conditions to achieve the highest efficacy. Also, the composition of water matrix and the type of contaminant play a considerable role in overall efficiency of the process. Thus, fundamental lab-scale studies with real water matrices are still topical to improve activated persulfate processes implementation for the treatment of waters and wastewaters. In addition, the literature about the research conducted with real wastewaters and with practicable sulfate radical-based advanced oxidation technologies ($\text{SO}_4^{\bullet-}$ -AOTs) is still rather scarce.

1.3.1 Groundwater and other natural waters

Various organic substances, such as agrochemicals, pharmaceuticals, compounds of personal care products are among the most frequently detected groundwater pollutants along with nitrates, phosphates, heavy metals and radionuclides. However, the several possibilities to activate persulfate promote the application of this process for the degradation of diverse classes of pollutants.

Theoretically, groundwater remediation by activated persulfate treatment may be initiated by the presence of natural iron leached from soil. Iron in aquifer is in dissolved form, Fe(II), but is oxidized to Fe(III) when in contact with oxygen in air, or due the action of iron bacteria. The growth of the latter is greatly contributed by the dissolved iron in water (Ityel, 2011). When iron is insoluble form, the target contaminant elimination would be most likely hindered. Therefore, additional iron is used. Also, various groundwater constituents, mainly chloride (Cl^-), carbonate (CO_3^{2-}) and bicarbonate (HCO_3^-) ions and dissolved organic carbon may scavenge $\text{SO}_4^{\bullet-}$ producing less reactive radical species that suppresses the direct reactions with organic contaminants. The level of these components could be much higher in contaminated groundwater, subjected to the strength of pollution.

Liang et al. (2004a) artificially polluted soil samples with 0.45 mM of trichloroethylene, a potential groundwater contaminant, and conducted experiments in soil slurry. Their results indicated that the persulfate/Fe(II) system was efficiency increased with the oxidant/activator molar ratio until its certain value, but further increase did not provide any enhancement. Based on that, they suggested a stepwise addition of Fe(II) or even the use of reductive properties of sodium thiosulfate to make more Fe(II) available to activate persulfate. The combination of chelating agents, especially tartaric acid and citric acid, and Fe(II)-activated persulfate for the degradation on 0.5 mM of aniline also indicated improved efficacy (Han et al., 2015). The application of CA-chelated Fe(II)-activated persulfate system was performed in a soil tank model for the degradation of chlorobenzene: 36 h treatment resulted in 82.4% destruction of the studied contaminant (Wang et al., 2016).

Chen et al. (2016) applied heat-activated persulfate for the degradation of diclofenac at its initial concentration of 0.047 mM in polluted groundwater. Temperature of 50–70 °C or acidic pH improved the target compound degradation, but the presence of common groundwater ions, Cl^- and HCO_3^- , hindered the process efficacy at higher concentrations to a different extent. They also supported the findings of other studies (Liang et al., 2006; Bennedsen, et al., 2012) that Cl^- may have a positive influence on process efficacy. Similar findings were reported in the treatment of herbicide atrazine: 0.05 mM of the target pollutant was degraded in 120 min with 1 mM of persulfate under 60 °C (Ji et al., 2015). Further increase in the persulfate concentration or temperature improved the process efficacy, and low concentrations of Cl^- and HCO_3^- (5 mM) had insignificant effect to the overall treatment.

Simulated groundwater contaminated with benzene was treated with heterogeneous persulfate oxidation activated by three Fe(III)- and Mn(IV)-containing natural minerals: ferrihydrite, goethite and pyrolusite (Li et al., 2017). The findings of this study confirmed that high carbonate alkalinity obstructs the contaminant removal, but the effect of Cl^- remained negligible.

In river water, the UVC/ $\text{S}_2\text{O}_8^{2-}$ treatment ($[\text{S}_2\text{O}_8^{2-}]_0 = 0.5 \text{ mM}$) of different model water pollutants was promising: low levels of HCO_3^- ($\sim 2 \text{ mM}$) and Cl^- ($\sim 1 \text{ mM}$) did not decrease the process efficacy (Lutze et al., 2015). However, Cl^- is suggested to be the main scavenger of $\text{SO}_4^{\bullet-}$, forming at $\text{pH} > 5$ chloride radicals reacting with water producing HO^{\bullet} , and thus, sustaining the process efficacy. This study also proved that $\text{SO}_4^{\bullet-}$ react with fulvic acids representing the dissolved organic carbon less actively compared to HO^{\bullet} (Méndez-Díaz et al., 2010) and hence, the selectivity of $\text{SO}_4^{\bullet-}$ -AOTs will greatly contribute for its application for natural waters.

The effective removal of diuron (0.1 mM) and arsenic (6.6 μM) by Fe(II)/ $\text{S}_2\text{O}_8^{2-}$ treatment ($[\text{S}_2\text{O}_8^{2-}]_0 = 20 \mu\text{M}$, $[\text{Fe(II)}]_0 = 0.1\text{--}20 \mu\text{M}$) was studied by Zhou et al. (2013) showing the possibility of *in situ* remediation of groundwater.

1.3.2 Drinking water

Drinking water or potable water usually is chemically treated providing quality suitable for human consumption. In majority of water treatment facilities, chlorination is the most widely used disinfection process with a risk of generating toxic disinfection by-products (DBPs), particularly when the concentrations of organic pollutants are significant. The DBPs formation is excluded with the usage of $\text{SO}_4^{\bullet-}$ -AOTs, inducing the development of these processes for drinking water purification.

Tap water was used to study the mechanism of simultaneous heat energy, UVC irradiation, Fe(II), and H₂O₂ activation of persulfate for the degradation of 0.06 mM of carbamazepine, an antiepileptic drug (Monteagudo et al., 2015). The combination of SO₄^{•-} and HO[•] resulted in 99% total organic carbon (TOC) removal in 90 min contact time. Moreover, the TOC removal did not exceed 75% at 28.6 mM of Cl⁻ (1000 mg/L) in the studied solution.

Sonication-activated persulfate system was practicable to degrade tetracycline, a broad-spectrum antibiotic, in a tap water with a concentration of 0.052–0.156 mM (Nasseri et al., 2017). The results indicated 96.5% of target compound degradation with 61.2% of TOC removal after 120 min treatment time at [S₂O₈²⁻]₀ = 4 mM, pH 10 and ultrasound frequency 35 kHz. The presence of humic acid reduced the treatment efficacy, which, however, may be compensated by the higher concentration of persulfate.

UVC/S₂O₈²⁻ system was successfully studied for the degradation of iodoacids, i.e. iodinated disinfection by-products, in drinking water: a 1.5 μM solution of iodoacetic acid, the compound refractory to photodegradation, was degraded in 6 min at the contaminant/S₂O₈²⁻ molar ratio of 1/40. TOC was removed for 90% in 30 min (Xiao et al., 2016).

1.3.3 Secondarily treated wastewater

Conventional wastewater treatment processes often have limited capability to eliminate organic (micro)pollutants with high chemical stability and recalcitrant to biodegradation (Barbosa et al., 2016). The concentration of several ions, mainly chloride, (bi)carbonate, phosphate, nitrate and sulphate, and organic load, may be still rather high. This causes directly the pollution spreading to surface water and eventually even groundwater (Tijani et al., 2013). Therefore, the secondarily treated wastewater needs further purification; the research on SO₄^{•-}-AOTs has proved that its application brought several advantages.

Nasseri et al. (2017) also applied sonication-activated persulfate system for secondarily treated wastewater purification: 70% of 0.104 mM tetracycline initial concentration was degraded in 120 min. The organic matter and the elevated presence of carbonate and chloride significantly decreased the purification efficacy by scavenging reactive species. Thus, further modifications of this type of activated persulfate process may appear feasible.

Natural mineral pyrrhotite (1 g/L) was used as a persulfate (0.5 mM) activator to control the microbial water contamination by *Escherichia coli* K-12 bacteria: low performance of the treatment was reported owing to the nitrogen-containing organic matter in wastewater effluent that actively reacts with SO₄^{•-} (Xia et al., 2017).

ZVI/S₂O₈²⁻ system in wastewater effluent showed significant simultaneous removal of bisphenol A and phosphate: 74% of 22 μM bisphenol A and 91% of 5 mg/L phosphate were removed by applying 1 mM of persulfate and 0.5 g/L of ZVI at pH 7.5 (Zhao et al., 2016).

The simulated conditions of treated wastewater effluent were set up to study the aqueous matrix effect to the degradation of oxytetracycline by simulated solar light/Fe(II)/S₂O₈²⁻ system (Bi et al., 2016). The results indicated 86% of the target contaminant (0.04 mM) removal after applying 60 min of illumination with Fe(II)/S₂O₈²⁻ mass ratio of 1/4. They proved that it is essential to find the inhibiting concentration of various anions to adjust the activated persulfate system conditions.

1.3.4 Landfill leachate

The content of diverse classes of pollutants makes landfill leachate an emerging environmental concern. The properties of leachate are derived from the types of wastes and vary during the waste deposition period and seasons. The major constituents are dissolved organic matter, ammonium nitrogen, heavy metals, xenobiotic organic compounds and numerous emerging micropollutants. Thus, the purification of landfill leachate should most likely consist of separate or combined steps, including chemical and biological treatment. The author failed to find literature on the Fe(II)-activated persulfate process applied to the treatment of landfill leachate.

Deng and Ezyse (2011) carried out thermal activation of persulfate at 27, 40 and 50 °C in a landfill leachate with chemical oxygen demand (COD) of 1.2 g/L, ammonium nitrogen of 2 g/L, alkalinity of 4.9 g CaCO₃/L and pH of 8.3. They applied S₂O₈²⁻/12COD mass ratio of 0.25–2.0 at various pH values. The results of their study indicated high simultaneous removal efficacies of COD and ammonia nitrogen at S₂O₈²⁻/12COD > 0.5 under at least 40 °C. Also, acidic pH from 3.0 to 4.0 assures the invariable treatment efficacy of thermal-activated persulfate.

Microwave-activation of persulfate at 85 °C was studied for the purification of heavy-metal containing (ng/L) landfill leachate by Chou et al. (2015). Their findings proved suitability of this process for the landfill leachate pre-treatment followed by biological treatment: COD and TOC were removed for more than 70 and 90%, respectively, in 120 min of oxidation time; the most suitable pH values appeared to be 5.0 and 7.0; however, the process efficacy remained high also at pH 3.0 and 9.0.

Fe(II)-loaded GAC heterogeneous activation of persulfate was performed in a mature municipal landfill leachate (Li et al., 2016). They reached to a maximum of 88% COD removal from the initial 9 g O₂/L by 125 mg/L of Fe(II) and 0.5 M of persulfate at pH 3.0 in 30 min oxidation time. The authors also calcinated the catalyst in N₂ atmosphere at 550 °C; the regenerated catalyst was used up to three times with 50% of the initial COD removal efficacy.

Ozone-activation of persulfate was studied for the purification of semi-aerobic stabilized landfill leachate collected from aeration pond (Abu Amr et al., 2013). The leachate was characterized with high COD (2.5 g O₂/L) and low biodegradability (BOD₇/COD = 0.038) as well as high ammonia content (0.8 g NH₃-N/L). The application of different activator doses (30-80 g/m³) and persulfate concentrations (COD/S₂O₈²⁻ mass ratios of 1/1–1/7) showed promising results for the removal of COD (70%) and ammonium (80%) at pH 6.5 or 10.0 within 210 min.

1.3.5 Industrial wastewaters

Similarly to landfill leachate, the variety of industries and their specialization greatly dictates the composition of process effluents. For example, the food industry effluents could contain elevated levels of organics, whereas the process waters from metallurgy are rich in heavy metal concentrations.

Wastewater containing dinitrotoluenes from military ammunition plant was treated with electro-activated persulfate process (Chen et al., 2014). Strongly acidic pH (0.5) and persulfate anion concentration of 1.7 wt% almost completely degraded (initial TOC = 300 mg/L) the target pollutants after 8-h oxidation. This proves the applicability of SO₄^{•-}-AOTs for the highly-strength wastewater.

Moussavi et al. (2016) applied UVC activation of persulfate for the purification of chromium electroplating wastewater with a goal to degrade cyanide. They reported a complete degradation of 50 mg/L of cyanide to less toxic by-products in 50 min at $[S_2O_8^{2-}]_0 = 0.8$ g/L.

Solar light activation of persulfate was studied for the purification of winery wastewater (Rodríguez-Chueca et al., 2017). This type of wastewater is typically relatively acidic and contains elevated amounts of dissolved organic matter with composition varying between seasons. Up to 60% of COD removal from initial 5 g O₂/L and 40% removal of TOC from initial 1.7 g/L at pH 4.5 and 7.0 was achieved.

Based on these examples, the general trend is that the higher is the pollution level, the more energy-demanding persulfate activation methods are used. This approach could be justified since the heat or radiation activation provide high energy output sometimes for only a period of a few minutes. When the contamination is high at the organic content measured in g/L, this short activation may not be sufficient to degrade the target pollutants, and the treatment time is prolonged. Thus, the importance of adjusting the treatment parameters according to the nature of the target pollutants should not be neglected. The available literature also proved that the application of activated persulfate treatment for high-strength wastewaters was sufficiently studied.

1.4 Aim of the study

Even though different persulfate activation possibilities have been extensively studied for over a decade, there are still uncertainties related to the application in aqueous matrices containing diverse types of contaminants. In natural or processed waters, the synergistic effects of water matrix, persulfate and its activators, and the organic pollutant are of particular interest.

The aim of the current doctoral thesis was to assess the most viable persulfate activation options in water and in wastewater with different pollution levels and, thereby, to extend the justification for full-scale applications of SO₄^{•-}-AOTs. Newly observed classes of emerging micropollutants (artificial sweetener and non-steroidal anti-inflammatory drug) were chosen in this research with the intention to prove activated persulfate treatment efficacy degrading various organic contaminants at various initial concentrations. The addition of chelating agents was studied with further intention to conduct the activated persulfate treatment *in situ*.

The following principal objectives raised from aim were set as follows:

- to observe the practicability of Fe(II)-activation in high-strength wastewaters (pyrolysis wastewater and landfill leachate) with the intention to assess the changes in wastewater parameters (COD, BOD₇, BOD₇/COD) after the treatment;
- to evaluate the efficacy of the Fe(II)/chelating agent or Fe(II)/reducing agent activation in ultrapure water or landfill leachate;
- to investigate the UVA/Fe(II) activation in ultrapure water, groundwater and secondarily treated wastewater for the degradation and mineralization of artificial sweetener ACE;
- to study the H₂O₂ and H₂O₂/Fe(II) activation in ultrapure water for the degradation and mineralization of non-steroidal anti-inflammatory drug NPX;
- to evaluate the effect of persulfate concentration and different activators' importance, pH and treatment time to the SO₄^{•-}-AOTs efficacy.

2 MATERIALS AND METHODS

2.1 Chemicals and materials

All reagents were of analytical grade and used as received without further purification. Stock solutions were prepared in ultrapure water (Millipore Simplicity® UV System, Merck, Germany). Sodium hydroxide, sulfuric acid or phosphate buffering aqueous solutions were used to adjust pH.

Pyrolysis wastewater sample was obtained from an oil shale thermal treatment plant in Ida-Viru County, Estonia. The main specific properties of the sample are listed in *Paper I, Table 1*. Landfill leachate was collected from a municipal non-hazardous waste landfill in Harju County, Estonia; the main specific properties are listed in *Paper II, Table 1*. Secondarily treated wastewater sample was collected from a local municipal wastewater treatment plant in Tallinn city, and groundwater sample was collected from a 19-m deep borehole in Harju County. All untreated samples were stored at 4 °C. The chemical composition and main parameters of the water matrices are presented in Table 1.

Table 1. The chemical composition and main parameters of water matrices

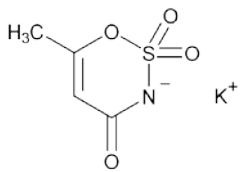
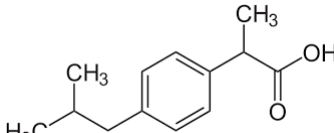
Parameter	Pyrolysis wastewater	Landfill leachate L1	Landfill leachate L2	Ground-water	Secondarily treated waste-water
COD, mg/L	39700±1700	9700±381	21153±877	-	-
TOC, mg/L	-	-	-	4.3	13.2
DOC, mg/L	9010±25	2740±11	6185±175	-	-
BOD ₇ , mg/L	5500±390	2480±122	9428±381	-	-
BOD ₇ /COD	0.14	0.26	0.45	-	-
Total phenols, mg/L	730±15	24±1	87	-	-
Fe(II), mg/L	-	-	-	0.03	0
Total Fe, mg/L	2.86±0.11	-	-	0.1	0
pH	8.88	7.84	7.03	7.75	7.20
Alkalinity, mgCaCO ₃ /L	-	9520±80	8500±375	650±0	370±15
Conductivity, µS/cm	10430	22.1	15.8	617±1	1022±1
F ⁻ , mg/L	-	-	-	0.2	<LOQ*
Cl ⁻ , mg/L	-	-	-	87	450
NO ₃ ⁻ , mg/L	-	-	-	<LOQ	64
PO ₄ ³⁻ , mg/L	-	-	-	<LOQ	12
SO ₄ ²⁻ , mg/L	-	-	-	41	75

*- – not measured

*<LOQ – below limit of quantification

Artificially contaminated solutions of analytically pure ($\geq 98\%$) ACE and NPX were prepared by dissolving each studied compound in ultrapure water (*Papers III, IV*) or in secondarily treated wastewater and groundwater (*Paper III*) to achieve the pollutant concentration of $75 \mu\text{M}$. The structure and main properties of the studied micropollutants are given in Table 2.

Table 2. The properties of ACE and NPX (Zorita et al., 2009; Lange et al., 2012)

Properties	Acesulfame (ACE)	Naproxen (NPX)
Molecular structure		
Classification	Artificial sweetener	Non-steroidal anti-inflammatory drug
CAS nr	55589-62-3	22204-53-1
Chemical formula	$\text{C}_4\text{H}_4\text{KNO}_4\text{S}$	$\text{C}_{14}\text{H}_{14}\text{O}_3$
Molecular weight, g/mol	201.24	230.26
Solubility in water, g/L	270 (20 °C)	0.0159 (25 °C)
pKa	2.0	4.45

2.2 Experimental procedure

Papers I, II

Fe(II)-activated persulfate experiments were carried out in a batch mode and in non-buffered solutions at ambient room temperature. Wastewater samples (0.5 L) were treated in a 1-L cylindrical glass reactor with a permanent agitation speed (400 rpm) for a maximum of 24 h oxidation period. The pH of the wastewater samples was adjusted to 3.0 (*Paper II*), if not specified otherwise (*Paper I*). The activator ($\text{FeSO}_4 \cdot 7\text{H}_2\text{O}$) was dissolved in the sample followed by the persulfate addition to initiate oxidation. In *Paper I*, stepwise addition of activator, oxidant and activator/oxidant after 0.0, 30.0 and 60.0 min reaction were studied. The oxidant dose was determined as the persulfate/COD weight (g/g O_2) (*Paper I*) or molar (mol/mol O_2) ratio (*Paper II*). In *Paper II*, sodium thiosulfate ($\text{S}_2\text{O}_3^{2-}$), the reductant of Fe(III), was added simultaneously with persulfate (reductant/Fe(II) mol/mol of 0.1/1 to 1/1). The oxidation was terminated by the addition of NaOH (10 M) to adjust pH value to 8.5; the settling period of ferric hydroxy complexes was 19–24 h. Finally, the supernatant was collected for further analysis. The experiments with non-activated persulfate oxidation were performed in identical reactor under respective activated persulfate treatment conditions. All experiments were duplicated, and the data of the initial parameters of wastewater samples were verified with at least three replicates. The results of the analyses are presented as the mean with a standard deviation of at least three parallel replicates.

UVA-activated persulfate (*Paper III*) and Fe(II)- or H₂O₂-activated persulfate (*Paper IV*) experiments were conducted in a batch mode and in non-buffered (*Paper IV*) or buffered (*Paper III*) solutions at ambient room temperature. ACE solutions (0.8 L) or NPX solutions (0.4 L) were treated in a cylindrical glass reactor with a permanent agitation speed of 400 rpm for 120 min (*Paper III*) or 180 min (*Paper IV*) of oxidation period. The pH of the solutions was adjusted to 3.0 (*Papers III, IV*), 5.0 (*Paper IV*), 5.8 (*Paper III*), 7.0 (*Paper IV*), 7.4 (*Paper III*) or 9.0 (*Paper IV*), if not specified otherwise. The activator (ferrous iron source) (*Papers III, IV*) or activator/chelating agent (C₆H₈O₇·H₂O, CA) (*Paper IV*) was dissolved in the sample followed by the persulfate addition to initiate oxidation. In *Paper IV*, both oxidants were added simultaneously in the case of combined H₂O₂/S₂O₈²⁻ system.

In *Paper III*, a low-pressure mercury lamp (11 W OSRAM Dulux S BLUE) located in a quartz tube inside the reactor, was immediately inserted into the solution after the addition of oxidant. The lamp was previously warmed up outside the reactor at least 5 min before the trial to provide constant output. The average irradiance entering the solution in the reactor measured by Ocean Optics USB2000+ spectrometer equipped with SpectraSuite software was 2.2 mW/cm². The temperature in the reactor was kept constant by using a water cooling jacket.

Sample aliquots were withdrawn at pre-determined time intervals. The oxidation was terminated by the addition of ethanol (EtOH) (sample/EtOH volume ratio of 10/1) (*Paper III*), Na₂SO₃ at a [oxidant]₀/SO₃²⁻ mol/mol of 1/10 (*Papers III, IV*) or by the addition of NaOH 1-M solution to adjust pH to 9.0 (*Paper IV*). To identify the radicals formed in the activated persulfate systems, radical scavengers EtOH and *tert*-Butanol (*t*-BuOH), were spiked into the reaction solutions prior to the addition of Fe(II) or Fe(II)/CA and persulfate at a ACE or NPX/[scavenger]₀ mol/mol of 1/500. The experiments on NPX oxidation with non-activated persulfate were conducted in identical reactors and treatment conditions for the respective activated oxidation trials (*Paper IV*). All experiments were duplicated; the results of the analysis are presented as the mean with a standard deviation of at least three parallel replicates less than 5%.

2.3 Analytical methods

An overview of the principal analytical methods used in the study is collected in Table 3. The methods listed were used to analyze the different water parameters before or after the application of respective activated persulfate treatment.

The quantification of ACE concentration (*Paper III*) during the applied activated persulfate treatment was carried out by using high-performance liquid chromatograph (HPLC, YL-Instrument 9300, China). The HPLC was equipped with a Waters Bridge C18 (150 x 3.0 mm inner diameter, 3.5 μm particle size) column and UV/Vis detector. The analysis was performed using isocratic method with a mobile phase mixture of 10% acetonitrile and 90% of 0.1% acetic acid aqueous solution. Samples (20 μL) were analyzed at the flow rate of 200 μL/min at wavelength of 230 nm. In the case of trials with groundwater and secondarily treated wastewater, samples were filtered through 0.45-μm Whatman® Puradisc AQUA cellulose acetate syringe filters. The concentration of ACE was determined by using the standard multipoint calibration.

The quantification of NPX concentration (*Paper IV*) was carried out by a HPLC combined with diode array detector (HPLC-PDA, Prominence SPD-M20A, Shimadzu)

equipped with a Phenomenex Gemini (150 × 2.0 mm inner diameter, 1.7 μm particle size) NX-C18 (110 Å, 5 μm) column. The analysis was performed using isocratic method with a mobile phase mixture of 40% acetonitrile and 60% of 0.1% formic acid aqueous solution. The flow rate was kept at 200 μL/min. Samples (30 μL) were scanned at 190-800 nm and analyzed at wavelength of 232 nm. The concentration of NPX was determined by using the standard multipoint calibration. The by-products formed during activated persulfate treatment of NPX were identified by the HPLC combined with mass spectrometer (HPLC-MS, Shimadzu LC-MS 2020). Phenomenex Gemini-NX 5u C18 (110A 150 × 2.0 mm inner diameter, 1.7 μm particle size) column was used with isocratic mobile phase mixture, 0.3% formic acid aqueous solution (60%) and acetonitrile (40%), and total flow rate of 200 μL/min. Mass spectra was acquired in full-scan mode, scanning in the range 50–500 m/z. The instrument was operated in positive ESI mode and the results obtained with MS detector were handled using Shimadzu LabSolutions software.

Table 3. Analytical methods applied for the analysis of water matrices

Parameter/Analysis	Analytical instrument/Method	Paper
Chemical oxygen demand (COD)	Closed reflux colorimetric method (APHA, 2012)	I, II
Biochemical oxygen demand (BOD ₇)	7-day biochemical oxygen demand, oxygen analyzer (APHA, 2012)	I, II
Total organic carbon (TOC)	TOC/TN analyzer	I-III
Dissolved organic carbon (DOC)	TOC/TN analyzer	I, II
Non-purgeable organic carbon (NPOC)	TOC/TN analyzer	IV
Dissolved nitrogen (DN)	TOC/TN analyzer	II
Total solids (TS)	APHA, 2012	I, II
Total suspended solids (TSS)	APHA, 2012	I, II
Total fixed solids (TFS)	APHA, 2012	I, II
Fe(II)	Spectrophotometric method (Merck, 1994)	I, III, IV
Total Fe	Spectrophotometric method (Merck, 1994)	I, III
Residual persulfate	Spectrophotometric method (Sof'ina et al., 2003)	I, II, IV
	Spectrophotometric method (Liang et al., 2008)	III
Total phenols	HACH-Lange cuvette test LCK 345	I, II
Alkalinity	Titrimetric method (APHA, 2012)	II, III
pH	Digital pH-meter	I-IV
Conductivity	Digital conductivity meter	I-III
Anions	Ion chromatograph with chemical suppression	III

3 RESULTS AND DISCUSSION

Activated persulfate treatment was carried out in different water matrices with different type of activation (Table 4).

Table 4. Types of persulfate activation and water matrices used in the current study

Matrix	Type of persulfate activation	Paper
Pyrolysis wastewater	Fe(II)	I
Landfill leachate	Fe(II), Fe(II)/S ₂ O ₈ ²⁻	II
Secondarily treated wastewater	UVA, UVA/Fe(II)	III
Groundwater	UVA, UVA/Fe(II)	III
Ultrapure water	UVA, UVA/Fe(II), Fe(II), H ₂ O ₂ , H ₂ O ₂ /Fe(II), Fe(II)/CA, H ₂ O ₂ /Fe(II)/CA	III, IV

The evaluation of applicability of these systems was done by comparing the changes in organic load (*Papers I–IV*), biodegradability (roughly estimated by the value of BOD₇/COD ratio) (*Paper I*), acute toxicity (*Paper I*), target compound concentration (*Papers III, IV*) as well as persulfate concentration (*Papers I–IV*) and pH (*Papers I–IV*).

3.1 Fe(II)-activated persulfate treatment

Fe(II) activation of persulfate was applied for the purification of high-strength pyrolysis wastewater (*Paper I*), landfill leachate of different seasons (*Paper II*) and for the degradation of NPX in ultrapure water (*Paper IV*).

Pyrolysis wastewater used in this study could be characterized as highly polluted industrial effluent with relatively high COD and total phenols contents, and low biodegradability (Table 1; *Paper I, Table 1*). Thus, COD/S₂O₈²⁻/Fe(II) g O₂/g/g of 1/0.4/0.04, 1/0.4/0.08, 1/0.4/0.16 and 1/0.8/0.16 were applied with 47%, 50%, 52% and 60% of COD removal after 24 h treatment period, respectively (*Paper I, Figure 2 and Table 2*). The maximum mineralization extent (39%) was achieved with the highest chemical doses used (COD/S₂O₈²⁻/Fe(II) g O₂/g/g of 1/0.8/0.16). The latter was unfavorable for biodegradability with slightly decreased BOD₇/COD ratio (0.15) than compared to untreated wastewater (0.19) (*Paper I, Figure 2*). Nevertheless, the residual concentration of persulfate after the treatment at all the studied COD/S₂O₈²⁻/Fe(II) ratios was negligible, as well as the residual iron concentration ranging below 2 mg/L. The trial with non-activated persulfate at COD/S₂O₈²⁻ g O₂/g of 1/0.4 showed moderate COD removal (47%), but significantly lower mineralization (11%) of organic load, which confirms the necessity to activate persulfate (Figure 2).

The pH of wastewater was not adjusted prior to oxidation, but after 24 h of treatment time the pH values were below 2.4 in all the trials. The more suitable initial pH value of 3.0 for Fe(II) activating properties was also tested, but no changes in the treatment efficacies were noticed. This suggests that the Fe(II) activation of persulfate at alkaline pH at 9.0 took place with high efficacies proving its applicability to wastewater treatment.

Fe(II) activation of persulfate is known to have an important disadvantage, the rapid conversion of Fe(II) to Fe(III). To alleviate this unwanted reaction, the gradual addition of

Fe(II), $S_2O_8^{2-}$, or Fe(II) and $S_2O_8^{2-}$ was conducted with COD/ $S_2O_8^{2-}$ /Fe(II) g O₂/g/g of 1/0.4/0.08 with the chemical(s) added in three equal portions (Figure 2; Paper I, Figure 3). As a result of stepwise chemicals addition, a 4–6% of improved dissolved organic carbon (DOC) removal was noticed. The COD removal improved for 1–2% with slightly lowered or stationary biodegradability.

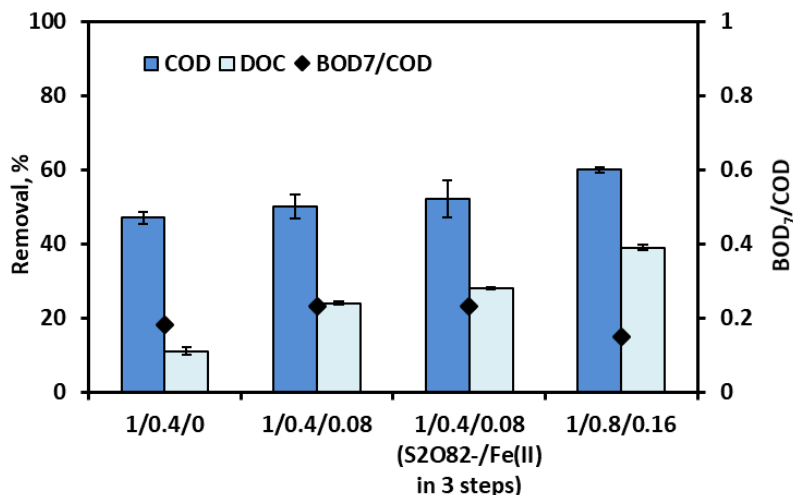


Figure 2. COD, DOC removal and the BOD₇/COD ratio as a function of different COD/ $S_2O_8^{2-}$ /Fe(II) ratios, g/g/g

Based on the respective results, somewhat promising increase in treatment efficacies led to a suggestion that the sequential addition of activator and oxidant chemicals could result in improved final parameters. In general, relatively modest improvement could be explained by insufficient chemical doses of stepwise addition, and this possibly indicates that the overall elevated concentrations of chemicals could be used in gradual addition.

Regarding the properties of pyrolysis wastewater, the acute toxicity with *Daphnia magna* 24 h tests was assessed after the activated persulfate treatment (Paper I, Table 3). The results were similar regardless of the chemical doses applied: at COD/ $S_2O_8^{2-}$ /Fe(II) g O₂/g/g of 1/0.4/0.16 (EC₅₀ = 1.12%) and COD/ $S_2O_8^{2-}$ /Fe(II) g O₂/g/g of 1/0.8/0.16 (EC₅₀ = 1.09%). Compared to the initial EC₅₀ value (0.34%), the acute toxicity was reduced during the applied process. This, along with the other parameters studied in this research, endorses the Fe(II) activation of persulfate to high-strength wastewater as a pre-treatment step.

Landfill leachate samples in this study were collected from a municipal landfill in summer (L1) and in late autumn (L2) (Table 1; Paper II, Table 1). This way it was possible to evaluate the Fe(II)-activated persulfate treatment efficacy in respect to the leachate of the same origin, although at slightly different strength of wastewater. Majority of the experiments were conducted with L1 to set the main process conditions that could be later transmitted to L2 treatment.

The oxidant dose was determined as the $S_2O_8^{2-}$ /COD mol/mol O₂ with the equivalent weight ratio of $S_2O_8^{2-}$ to O₂ as 12. Thus, to indicate the $S_2O_8^{2-}$ dose, the weight ratio of $S_2O_8^{2-}$ /12COD was used in this study. Accordingly, at the $S_2O_8^{2-}$ /12COD weight ratio of 1, the $S_2O_8^{2-}$ /COD molar ratio is 1/1. The $S_2O_8^{2-}$ /Fe²⁺ mol/mol varied in the range of 50/1 to 1/1.

Different activator concentrations were studied at $S_2O_8^{2-}/Fe^{2+}$ mol/mol of 50/1, 25/1, 10/1, 5/1 and 1/1 ($S_2O_8^{2-}/COD$ mol/mol O_2 was fixed at 0.25/1). The results showed nearly 3-fold decrease in COD, DOC and DN values when increasing the activator's concentration with $S_2O_8^{2-}/Fe^{2+}$ ratio (mol/mol) reduced from 50/1 (13%, 37% and 9%, respectively) to 1/1 (13%, 34% and 19%, respectively) (Figure 3a).

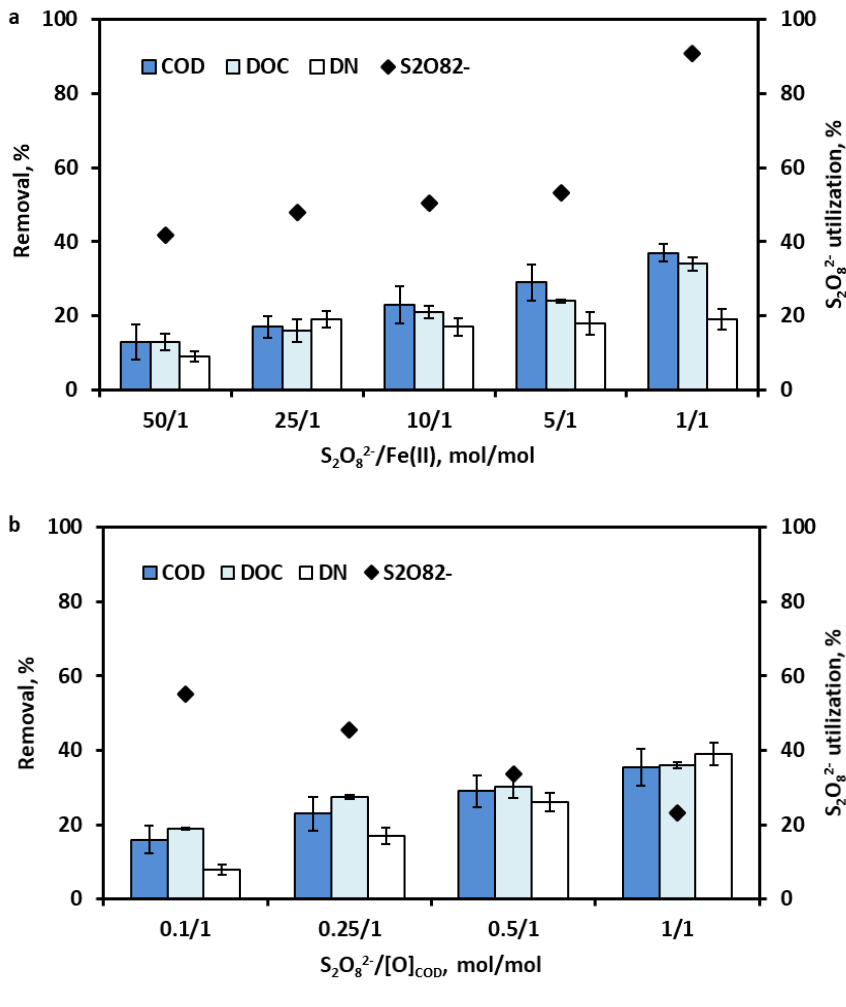


Figure 3. COD, DOC and DN removal and $S_2O_8^{2-}$ utilization versus $S_2O_8^{2-}/Fe(II)$ mol/mol (a) ($S_2O_8^{2-}/[O]_{COD}$ mol/mol $O_2 = 0.25/1$) and $S_2O_8^{2-}/[O]_{COD}$ mol/mol O_2 (b) ($S_2O_8^{2-}/Fe(II)$ mol/mol = 10/1)

The total phenols removal was consistently high exceeding 90%. The highest Fe(II) dose used also resulted in the highest, 91%, persulfate consumption. $S_2O_8^{2-}/COD$ mol/mol O_2 of 0.25/1 and $S_2O_8^{2-}/Fe^{2+}$ mol/mol of 5/1 were used for the sample L2 with the similar treatment efficacy as was achieved with $S_2O_8^{2-}/Fe^{2+}$ mol/mol of 1/1 for the sample L1: 30% of COD and 24% of DOC removal along with 95% of total phenols removal, and 29% of DN removal.

The activation potential of Fe(II) was also studied with variable persulfate concentrations. The activator dose was kept constant at $S_2O_8^{2-}/Fe^{2+}$ mol/mol of 10/1 with the $S_2O_8^{2-}/COD$ mol/mol O_2 of 0.1/1, 0.25/1, 0.5/1 and 1/1. The results showed an improvement in COD, DOC and DN removal with every increase in oxidant dose with the maximum efficacy of nearly 40% in respect to all wastewater parameters (Figure 3b). In general, a 10-fold oxidant concentration increase from $S_2O_8^{2-}/COD$ mol/mol O_2 of 0.1/1 to 1/1 resulted in nearly two-fold improvement in COD removal, from 19% to 36%. At $S_2O_8^{2-}/COD$ mol/mol O_2 of 1/1, the DOC removal was also 36%. The phenolic contents were also reduced for more than 87% with all persulfate doses. Unfortunately, the residual oxidant concentration was increasing from 45% to 77% with the increase of $S_2O_8^{2-}/COD$ mol/mol O_2 implying to the constantly increasing Fe(II) concentration that could have possibly been decreased or kept constant for high-yield oxidant use.

Relatively promising efficacy of the DN removal by the Fe(II)-activated persulfate treatment likely favors the application of a biological post-treatment to achieve additional removal in COD, if necessary. The DN removal by this system is initiated by the ammonia and ammonium (reductive ammonium nitrogen) that donate electrons to $SO_4^{\bullet-}$, and thereby, the nitrogen is oxidized to a higher valence state, like N_2 (Deng and Ezyse, 2011).

The known stability of persulfate, selective reactivity of $SO_4^{\bullet-}$ and higher content of organics in sample L2 created suitable background to evaluate different oxidation period durations of Fe(II)-activated persulfate. The experiments were carried out with 1, 2, 4, 6, and 24 h oxidation time at $S_2O_8^{2-}/COD$ mol/mol O_2 of 0.25/1 and $S_2O_8^{2-}/Fe^{2+}$ mol/mol of 5/1. It was proved that the process could be conducted in less than 24 h, since the maximum removal of COD (30%) and DOC (24%) was already reached in 6 h of oxidation (Paper II, Figure 4). Moreover, the DN removal was similar (~30%) after all the oxidation periods studied, and more than 90% of total phenols was removed already in 1 h of oxidation.

The rapid conversion of Fe(II) to Fe(III) in Fe(II) activation of persulfate can occur not only in higher pH range, but when there are complex water matrices to be treated. Thus, the $S_2O_3^{2-}$ addition to the $S_2O_8^{2-}/Fe^{2+}$ system in sample L1 was considered, and the results are presented in Paper II, Figure 5. The COD, DOC and DN removal efficacies were evaluated at a $S_2O_8^{2-}/Fe^{2+}/S_2O_3^{2-}$ molar ratio of 10/1/0.1, 10/1/0.5 and 10/1/1 (fixed $S_2O_8^{2-}/COD$ mol/mol O_2 of 0.5/1). Every increase in reducing agent concentration improved the Fe(II)-activated persulfate process efficacy with the maximum improvement of 15% in COD and 5% in DN removal at $S_2O_8^{2-}/Fe^{2+}/S_2O_3^{2-}$ molar ratio of 10/1/1. The DOC removal was not improved indicating the presence of recalcitrant organics that are not subjected to mineralization.

It should be noted that after the oxidation step of landfill leachate treatment the pH of the samples were around 2 at all the applied oxidant/activator ratios. This pH region can only induce the decomposition of persulfate without the generation of radical species (Tsitonaki et al., 2010). However, this needs further study related to the water matrix and contaminant-specific properties.

Artificially NPX-contaminated ultrapure water was used to evaluate the Fe(II) activation of persulfate (Paper IV). The blank experiments with non-activated persulfate showed negligible NPX degradation, thus, the subsequent application of Fe(II) activation was justified. The Fe(II) activation of persulfate was conducted with pH adjusted to 3.0. The NPX/ $S_2O_8^{2-}/Fe(II)$ molar ratio of 1/10/0.5, 1/10/1 and 1/10/2 (corresponding to a $[S_2O_8^{2-}]_0$ 750 μM and $[Fe(II)]_0$ 37.5, 75 and 150 μM , respectively) were applied to evaluate

the changes in NPX concentration and NPOC content. The lowest studied dose of Fe(II) indicated more than 99% of NPX degradation in 180 min, whereas at the four-fold higher Fe(II) concentration the same result was achieved in 60 min (Figure 4a).

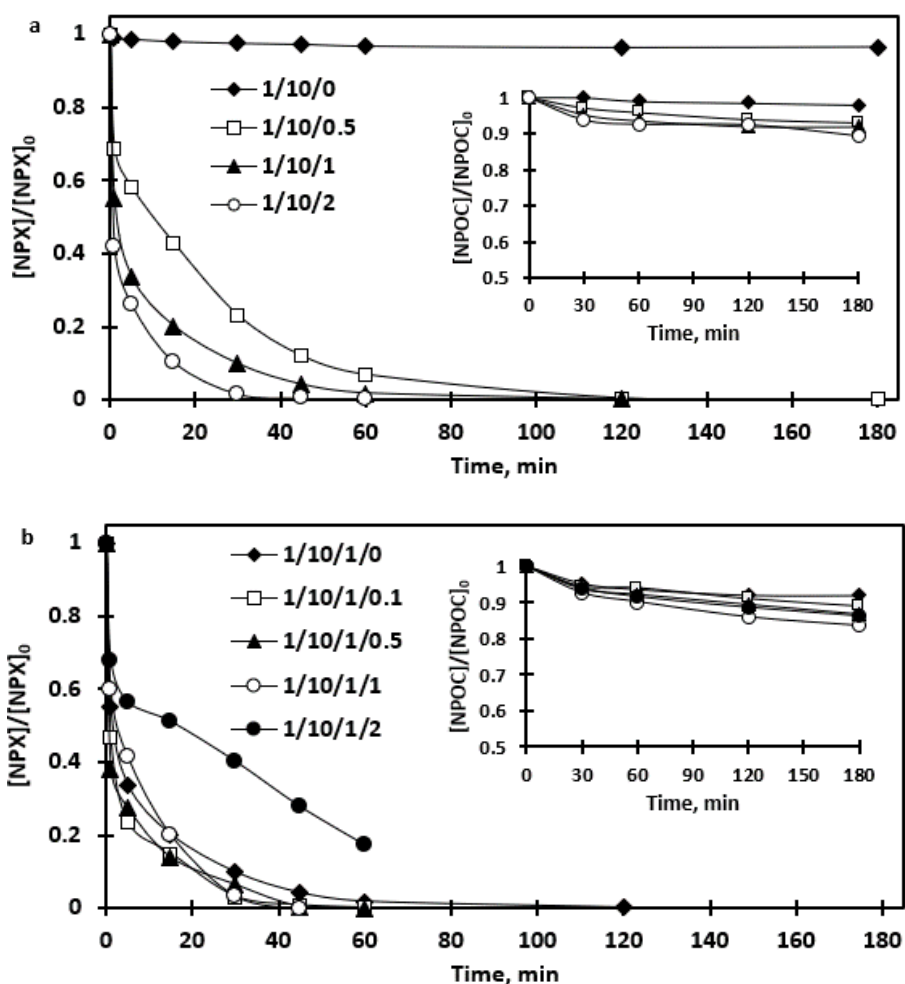


Figure 4. Naproxen degradation and NPOC reduction by the $S_2O_8^{2-}/Fe(II)$ process (NPX/ $S_2O_8^{2-}/Fe(II)$ mol/mol/mol) at different Fe(II) (a) and CA (b) initial concentrations (pH 3)

The increase in Fe(II) dose simultaneously increased the oxidant consumption from 15.2% up to 33.1%. NPX mineralization was considerably lower than the compound degradation: the highest NPOC removal was 11% at NPX/ $S_2O_8^{2-}/Fe(II)$ molar ratio of 1/10/2. This low removal is most likely caused by the accumulation of NPX transformation products competing for $SO_4^{\cdot-}$, as a result deteriorating the process efficacy. The observations of the NPX oxidation profile suggest the fast degradation phase (around 50%) during the first minute followed by the steady degradation during the rest of 180 min of total treatment period. This is presumably induced by the fast generation of radical species from activated persulfate; Fe(II) conversion to Fe(III) proceeded with slow reduction reactions with organic radicals.

The evaluation of increased initial pH values of 5.0, 7.0 and 9.0 showed NPX treatment efficacies similar to the ones at strongly acidic pH (*Paper IV, Figure 3b*).

The availability of Fe(II) at elevated pH to activate persulfate may be limited due to the chemical properties of ferrous ion forming poorly soluble hydroxides at high pH. Hence, the environmental-friendly chelating agent, CA, was used to evaluate its influence on the Fe(II)-activated system. The target compound degradation was evaluated after applying the following CA doses with fixed activator and oxidant dose: NPX/S₂O₈²⁻/Fe(II)/CA molar ratio of 1/10/1/0.1, 1/10/1/0.5, 1/10/1/1 and 1/10/1/2 (corresponding to CA concentrations of 7.5, 37.5, 75 and 150 μM). The NPOC content in these systems must be accounted as NPOC of NPX and NPOC of CA. The results indicated that the persulfate activation was enhanced at Fe(II)/CA mol/mol of 1/0.5 and 1/1, then compared to the treatment without chelating agent, with almost complete degradation of NPX in 60 and 45 min of treatment, respectively (*Figure 4b*). Moreover, more than 50% of oxidant consumption in chelated iron activation was achieved (*Paper IV, Table 2*). The effect of CA addition was also assessed with the initial pH increased to 5.0, 7.0 and 9.0. At elevated pH values, the role of CA becomes more significant when it is responsible to prevent the precipitation of iron as Fe(III). At pH 5.0, the application of different CA concentrations showed an enhanced target compound degradation and oxidant consumption (*Paper IV, Table 2 and Figure 5b*). Further increase of pH values to 7.0 and 9.0 at a Fe(II)/CA mol/mol of 1/1 indicated NPX degradation and mineralization similar to the one shown at pH 5.0 (*Paper IV, Figure 6b*).

The oxidant activation of persulfate is discussed in section 3.3, but the addition of CA to the H₂O₂/S₂O₈²⁻/Fe(II) system is intended to directly influence the availability of Fe(II) for both oxidants. The same Fe(II)/CA ratios, mol/mol, were applied as in Fe(II) activation of persulfate: 1/0.1, 1/0.5, 1/1 and 1/2 (*Paper IV, Figure 4c*). Some improvement was noticed in the NPX degradation as a result of CA-chelation, but the simultaneous presence of two oxidants that may have competitive reactions with Fe(II), decrease the overall system efficacy. The concentration of activator or oxidant(s) alone did not exhibit inhibiting properties to target compound elimination. The use of Fe(II)/CA mol/mol at 1/2 revealed notably lower NPX degradation and mineralization in conjunction with the increased residual concentration of H₂O₂ or S₂O₈²⁻; that could refer to the full complexation of Fe(II) with subsequent lack of its availability for oxidants. Another limitation may be the various predominant form of CA-Fe(II) complexes that are sensitive to the matrix pH. The dual-oxidant chelated iron system showed improved NPX degradation similarly to the S₂O₈²⁻/Fe(II)/CA system at pH 5.0, but remained similar at further pH rise up to 7.0 and 9.0 (*Paper IV, Figure 6c*). This could be explained by the pH-sensitivity of different predominant iron chelate forms. Also, at near neutral pH values, the availability of Fe(II) may be reduced due to the HO• domination over SO₄⁻ that provokes the formation of mixed chelated iron complexes.

The study about the principal radicals both in the chelated and non-chelated Fe(II) activation systems was conducted. The proportion of SO₄⁻ and HO• was investigated at pH 3.0 and 7.0 by introducing excess volumes of alcohol scavengers: EtOH that scavenges both radicals, and *t*-BuOH that is more selective towards the scavenging of HO•. The results of these experiments are presented in *Paper IV, Table 3* indicating the higher scavenging effect of these alcohols to the chelated systems. This proves that more radicals are generated arising from the enhanced availability of Fe(II). Nevertheless, the overall findings suggested that HO• were the main oxidative species in the Fe(II)-activated persulfate systems applied for NPX degradation.

This finding allowed to speculate the probable transformation pathway of NPX in the $S_2O_8^{2-}/Fe(II)/CA$ and $H_2O_2/S_2O_8^{2-}/Fe(II)/CA$ systems. The attack of $HO^*/SO_4^{\bullet-}$ to aromatic molecule causes hydroxylation (TP1a and TP1b) followed by the decarboxylation (TP2–TP4) or demethoxylation (TP5) (Figure 5).

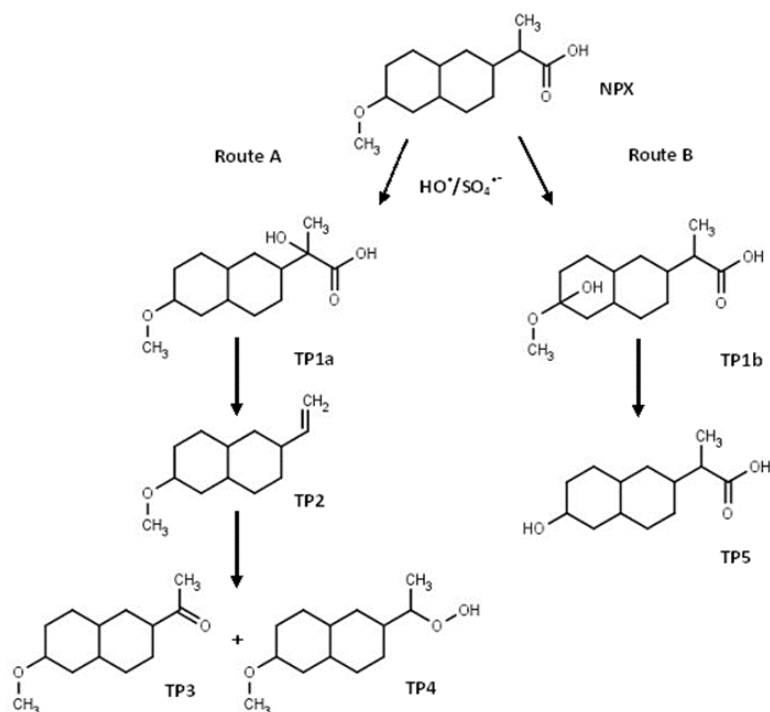


Figure 5. Possible degradation pathways for the degradation of NPX by the $S_2O_8^{2-}/Fe(II)/CA$ and $H_2O_2/S_2O_8^{2-}/Fe(II)/CA$ systems

3.2 UVA/Fe(II)-activated persulfate treatment

UVA and UVA/Fe(II) activation of persulfate were applied for the degradation of ACE in ultrapure water, groundwater and secondarily treated wastewater (*Paper III*). Ultrapure water was used to find the most viable $S_2O_8^{2-}/Fe(II)$ molar ratios for the following trials in natural matrices. pH at the trials was adjusted to 3.0 to assure the solubility of Fe(II). According to calculations based on the assumption that ACE would be completely oxidized, the stoichiometric value of ACE/ $S_2O_8^{2-}$, mol/mol, was 10.5. First, persulfate (ACE/ $S_2O_8^{2-}$ mol/mol of 1/10) was activated solely with UVA irradiation. This trial resulted in 60.7% of ACE degradation and negligible mineralization in 2 h of treatment time. Based on this modest efficacy, further treatment was carried out with UVA/Fe(II) activation of persulfate.

The effect of Fe(II) addition was evaluated by using $S_2O_8^{2-}/Fe(II)$ mol/mol of 10/0.2, 10/0.5, 10/1 and 10/2 corresponding to Fe(II) initial concentration of 15, 37.5, 75 and 150 μ M. Persulfate concentration of 750 μ M was derived from ACE/ $S_2O_8^{2-}$ mol/mol of 1/10, and was kept constant. It was observed that the degradation time of ACE reduced noticeably from 90 to 15 min when increasing ACE/ $S_2O_8^{2-}/Fe(II)$ molar ratio from 1/10/0.2

to 1/10/1 (Figure 6a). Further increased Fe(II) dose of ACE/S₂O₈²⁻/Fe(II) molar ratio of 1/10/2 indicated no changes in ACE removal time. This phenomenon was predictable as excess Fe(II) is known to scavenge SO₄^{•-} proceeding to the generation of less reactive species that are not so effective to degrade the target organic pollutant (Matzek and Carter, 2016). The data about mineralization is in correlation with the observations of target compound degradation reaching to lowest residual TOC value of 19.7% at ACE/S₂O₈²⁻/Fe(II) molar ratio of 1/10/1 (Figure 6a).

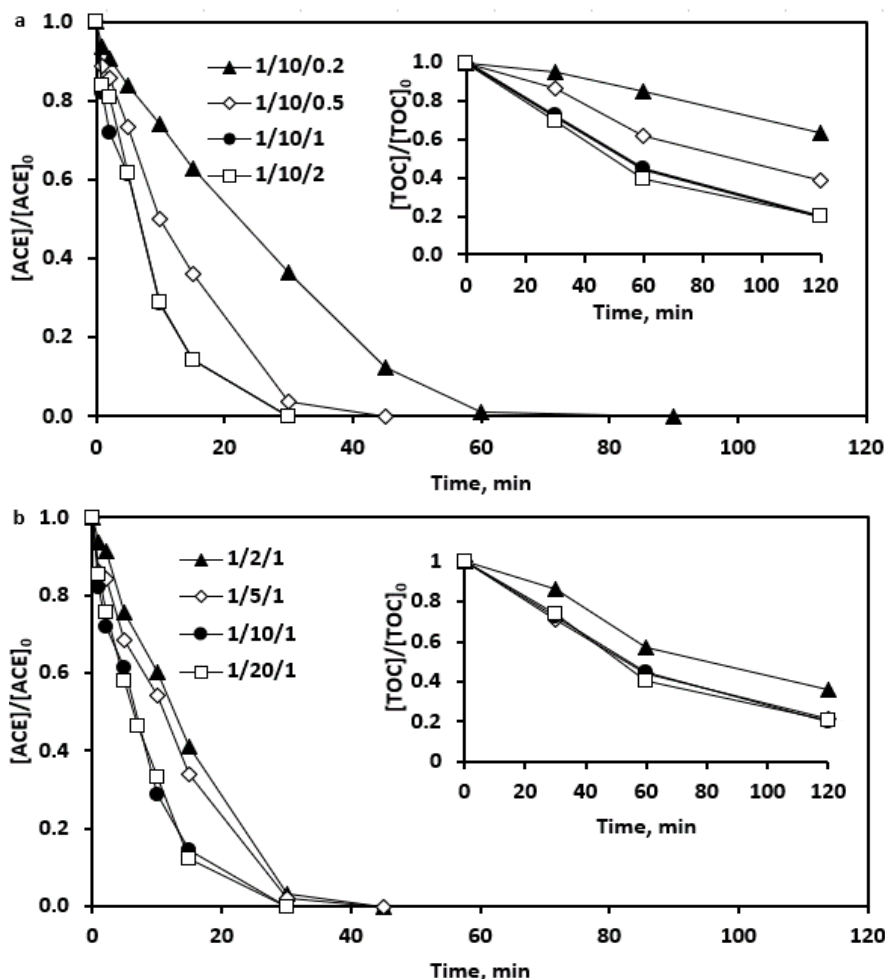


Figure 6. Acesulfame degradation and TOC reduction by the S₂O₈²⁻/Fe(II) process (ACE/S₂O₈²⁻/Fe(II) mol/mol/mol) at different Fe(II) (a) and S₂O₈²⁻ (b) initial concentrations (pH 3.0) ([ACE]₀ = 75 μM)

At a ACE/Fe(II) mol/mol 1/1, the effect of persulfate concentration with the following ACE/S₂O₈²⁻/Fe(II) molar ratio was studied: 1/2/1, 1/5/1, 1/10/1 and 1/20/1. Similar pattern was again observed: ACE degradation shortened from 45 to 30 min by applying ACE/S₂O₈²⁻/Fe(II) molar ratio of 1/10/1 and remained stable at ACE/S₂O₈²⁻/Fe(II) molar ratio of 1/20/1 (Figure 6b). The consumption of persulfate decreased with the increased dose of S₂O₈²⁻ or Fe(II), and was nearly 60% at ACE/S₂O₈²⁻/Fe(II) molar ratio of 1/10/1. Most likely, the increase in persulfate dose already exceeded the optimal Fe(II) activating

capability under the respective treatment conditions, and the disproportionate amount of oxidant probably scavenged $\text{SO}_4^{\bullet-}$. Thus, the $\text{ACE}/\text{S}_2\text{O}_8^{2-}/\text{Fe(II)}$ molar ratio of 1/10/1 was considered to be used in further experiments with groundwater and secondarily treated wastewater.

Besides pH 3.0, $\text{ACE}/\text{S}_2\text{O}_8^{2-}/\text{Fe(II)}$ molar ratio of 1/10/1 was applied in ultrapure water at pH 5.8 (initial pH of ACE solution) and at 5.8 and 7.4 (the average pH value of natural or processed water samples) in buffered solutions. Expectedly, ACE degradation was inhibited in buffered solution (*Paper III, Figure 4b*). While pH 3 favors the Fe(II) not Fe(III) activation of persulfate, then the non-buffered pH 5.8 contributes to the same conditions: the fast pH drop due to the acidity of Fe(II) and persulfate to below 4 in the first minute creates basically similar terms. However, at higher pH values, the coexistence of $\text{SO}_4^{\bullet-}$ and HO^{\bullet} is proposed to improve the activated persulfate treatment efficacy. The proportion of these reactive species was investigated at pH 3.0 and 5.8 by introducing excess volumes of radical scavengers into the $\text{UVA}/\text{S}_2\text{O}_8^{2-}/\text{Fe}^{2+}$ system (*Paper III, Table 2*). The addition of *t*-BuOH decreased the treatment efficacy at pH 3 by about 60% and the addition of EtOH by more than 80%. At pH 5.8, the corresponding results were more than 30% (*t*-BuOH) and 45% (EtOH). These results suggest that in the UVA/Fe(II)-activated persulfate system both HO^{\bullet} and $\text{SO}_4^{\bullet-}$ were involved in the degradation of ACE, but the HO^{\bullet} proved to be principal.

The UVA/Fe(II) activation of persulfate in groundwater and secondarily treated wastewater was studied by applying $\text{ACE}/\text{S}_2\text{O}_8^{2-}/\text{Fe(II)}$ molar ratio of 1/10/1 at pH adjusted to 3.0 and unadjusted pH values of the chosen matrices (*Paper III, Table 3*). The measured parameters of these water matrices (Table 1) allowed speculating that the treatment will have some decrease in the efficacy. ACE degradation in groundwater occurred faster (60 min) at pH 3.0 compared to the initial pH 7.75, where only about 5% of ACE was degraded in 120 min treatment time. Also, a complete degradation of ACE was achieved in the secondarily treated wastewater at pH 3.0 within 120 min. A modest (less than 5%) target compound degradation was noticed at initial pH 7.20 in 120 min treatment. Regarding the ACE degradation efficacy at unadjusted initial pH, a negligible oxidant consumption was observed in both matrices. At pH 3.0, somewhat lower residual persulfate concentration (~50%) was found in secondarily treated wastewater trials. This may be observed due to the higher organic matter and chloride ions content scavenging more of $\text{SO}_4^{\bullet-}$. The TOC values decreased for around 30% in both water matrices at pH 3.0, remaining unchanged, however, at initial pH values. Besides ACE mineralization, the reduced TOC content is derived from the oxidation of organic matter in water matrix. These findings suggest that in such type of water matrices, the molar ratio of persulfate/activator may be increased towards the enhanced consumption of persulfate and activator, or the prolongation of oxidation period need be considered.

During the experimental data processing, the order of ACE degradation kinetics was also estimated. It was suggested that the compound degradation was following not clearly defined reaction order, and, if any should be proposed, the reaction proceeds between the pseudo-first and -second orders: the degradation of ACE was observed taking place via distinct stages of different rate.

The dominance of HO^{\bullet} in the UVA/Fe(II)-activated persulfate system helps to propose the potential transformation pathways of ACE. The symbiosis of irradiation and transition metal probably attack the C=C bond (TP1) proceeding with $\text{HO}^{\bullet}/\text{SO}_4^{\bullet-}$ oxidation ring opening ending up with the formation of tartronic (TP3b), formic (TP3c) and acetic (TP3d) acids (Figure 7) (Punturat and Huang, 2017).

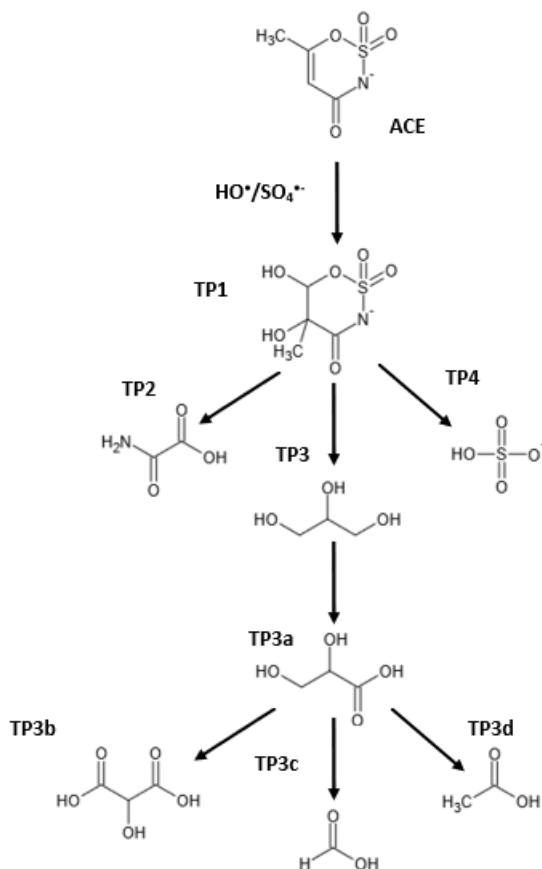


Figure 7. Possible degradation pathways for the degradation of ACE by the UVA/ $\text{S}_2\text{O}_8^{2-}$ /Fe(II) system

3.3 H_2O_2 -activated persulfate treatment

H_2O_2 and $\text{H}_2\text{O}_2/\text{Fe(II)}$ activations of persulfate were applied for the degradation of NPX in ultrapure water (*Paper IV*). The experiments were mainly carried out at pH 3.0, but the effect of pH values of 5.0, 7.0 and 9.0 was also studied.

The peroxide-activated persulfate process was conducted at a NPX/ $\text{H}_2\text{O}_2/\text{S}_2\text{O}_8^{2-}$ molar ratio of 1/10/10 (pH 3.0), which indicated less than 4% NPX degradation and a negligible NPOC reduction in 180 min of treatment (*Paper IV, Figure 2c*). However, two-stage NPX degradation was noticed: the fast decrease of NPX in the first minute followed by a gradual target compound oxidation during the remained treatment period. The measurements of H_2O_2 showed 97.9% of residual oxidant-activator (*Paper IV, Table 1*). Residual persulfate could not be detected due to interference with H_2O_2 in the samples. These findings clearly show that under these reaction conditions, H_2O_2 activation of persulfate has low potential. Thus, the system was combined with Fe(II) with the intention to initiate the concurrent reactions of the oxidants with the activator. The application of NPX/ $\text{H}_2\text{O}_2/\text{S}_2\text{O}_8^{2-}/\text{Fe(II)}$ molar ratio of 1/10/10/1 (pH 3.0) resulted in NPX degradation within 120 min; further two-fold increase in Fe(II) concentration shortened the degradation time to 30 min (*Paper IV, Figure 2c*). The removal of NPOC after 180-min

treatment resulted comprised 21% or 39% at $\text{NPX}/\text{H}_2\text{O}_2/\text{S}_2\text{O}_8^{2-}/\text{Fe(II)}$ molar ratio of 1/10/10/1 or 1/10/10/2, respectively.

The effect of initial pH to NPX degradation in $\text{NPX}/\text{H}_2\text{O}_2/\text{S}_2\text{O}_8^{2-}/\text{Fe(II)}$ system was also evaluated. The target compound degradation and mineralization decreased notably when pH value was raised to 5.0, 7.0 and 9.0 (*Paper IV, Figure 3c*). The most probable cause is Fe(II) sensitivity to pH above 3, making the activator to co-precipitate with ferric oxyhydroxides. A viable solution to avoid this disadvantage, especially when implementing in natural or processed water matrices, is to use iron-chelating agents. This promising approach was discussed in paragraph 3.1.

The study about principal reactive species in the $\text{H}_2\text{O}_2/\text{S}_2\text{O}_8^{2-}/\text{Fe(II)}$ process at pH 3.0 and 7.0 suggested that similarly to ACE degradation (paragraph 3.2), HO^\bullet and $\text{SO}_4^{\bullet-}$ were involved in the degradation of NPX, but the HO^\bullet proved to be principal oxidative species (*Paper IV, Table 3*). This was estimated based on the reduced efficacies of NPX removals compared to the mixtures containing no radical scavengers: at pH 3.0, the NPX degradation efficacy was reduced for 65% with *t*-BuOH, whereas EtOH reduced the oxidation efficacy for as much as 80%. The corresponding numbers at pH 7.0 comprised for more than 50% with *t*-BuOH and nearly 70% with EtOH.

CONCLUSIONS

Different persulfate activation types were studied for the treatment of real water and wastewater samples. The novelty of the studies consists of the activation of persulfate by Fe(II) implemented for the first time in pyrolysis wastewater and landfill leachate. Also, the combined activated persulfate system was used for the first time to treat naproxen, as well as the UVA/Fe(II) activation of persulfate – for the degradation of acesulfame.

Fe(II)-activated persulfate treatment appeared feasible for reduced organic load and acute toxicity, as well as improved biodegradability of the heavily contaminated industrial wastewater and landfill leachate. In the case of the latter, addition of thiosulfate, an iron reducing agent, showed significant improvement in COD and DN removal referring to its potential applications in municipal wastewater treatment.

UVA/Fe(II)-activated persulfate system was promising in degradation of micropollutant acesulfame in groundwater and secondarily treated wastewater at pre-acidified pH. The use of UVA part of the sunlight in persulfate activation contributes to the sustainable water treatment technology along with the iron constituent of natural minerals.

The Fe(II)/CA-activated persulfate and combined peroxide/persulfate oxidation are effective in degradation of micropollutant naproxen in aqueous solution at a wide range of pH suggesting the practicability of their *in situ* application.

Based on the principal radical species proposed in the acesulfame and naproxen degradation, HO[•] and SO₄^{•-} were involved in the target compound degradation with the HO[•] prevalence, the transformation pathways of the parent compounds were proposed.

The results of this study provide valuable information for further *in situ* full-scale applications of activated persulfate processes for the purification of water or high-strength wastewater at various pollution levels with the most effective concentrations of reagents used.

REFERENCES

- Abu Amr, S.S., Aziz, H.A., Adlan, M.N. Optimization of stabilized leachate treatment using ozone/persulfate in the advanced oxidation process. – *Waste Management*, 2013, 13, 1434–1441.
- Anipsitakis, G.P., Dionysiou, D.D. Radical generation by the interaction of transition metals with common oxidants. – *Environmental Science and Technology*, 2004, 38, 3705–3712.
- APHA (American Public Health Association). Standard methods for the examination of water and wastewater. 22nd ed. Washington DC: American Water Works Association, Water Environment Federation, 2012.
- Ahmad, M., Teel, A.L., Watts, R.J. Persulfate activation by subsurface minerals. – *Journal of Contaminant Hydrology*, 2010, 115, 34–45.
- Alkhouraiji, T.S., Ajlouni, A.-W. Destruction of amphetamine in aqueous solution using gamma irradiation. – *Radiation Physics and Chemistry*, 2017, 139, 17–21.
- Alkhouraiji, T.S., Boukari, S.O.B., Alfadhl, F.S. Gamma irradiation-induced complete degradation and mineralization of phenol in aqueous solution: effects of reagent. – *Journal of Hazardous Materials*, 2017, 328, 29–36.
- Barbosa, M.O., Moreira, N.F.F., Ribeiro, A.R., Pereira, M.F.R., Silva, A.M.T. Occurrence and removal of organic micropollutants: an overview of the watch list of EU Decision 2015/495. – *Water Research*, 2016, 94, 257–279.
- Behrman, E.J., Dean, D.H. Sodium peroxydisulfate is a stable and cheap substitute for ammonium peroxydisulfate (persulfate) in polyacrylamide gel electrophoresis. – *Journal of Chromatography B: Biomedical Sciences and Applications*, 1999, 723, 325–326.
- Bennedsen, L.R., Muff, J., Sjøgaard, E.G. Influence of chloride and carbonates on the reactivity of activated persulfate. – *Chemosphere*, 2012, 86, 1092–1097.
- Bi, W., Wu, Y., Wang, X., Zhai, P., Dong, W. Degradation of oxytetracycline with $\text{SO}_4^{\bullet-}$ under simulated solar light. – *Chemical Engineering Journal*, 2016, 302, 811–818.
- Buxton, G.V., Malon, T.N., Salmon, G.A. Reaction of $\text{SO}_4^{\bullet-}$ with Fe^{2+} , Mn^{2+} and Cu^{2+} in aqueous solution. – *Journal of the Chemical Society, Faraday Transactions*, 1997, 93, 2893–2897.
- Chen, J., Qian, Y., Liu, H., Huang, T. Oxidative degradation of diclofenac by thermally activated persulfate: implication for ISCO. – *Environmental Science and Pollution Research*, 2016, 23, 3824–3833.
- Chen, W.-S., Jhou, Y.-C., Huang, C.-P. Mineralization of dinitrotoluenes in industrial wastewater by electro-activated persulfate oxidation. – *Chemical Engineering Journal*, 2014, 252, 166–172.
- Chiang, Y.-P., Liang, Y.-Y., Chang, C.-N., Chao, A.C. Differentiating ozone direct and indirect reactions on decomposition of humic substances. – *Chemosphere*, 2006, 65, 2395–2400.
- Chou, Y.-C., Lo, S.-L., Kuo, J., Yeh, C.-J. Microwave-enhanced persulfate oxidation to treat mature landfill leachate. – *Journal of Hazardous Materials*, 2015, 284, 83–91.
- Criquet, J., Karpel Vel Leitner, N. Electron beam irradiation of aqueous solution of persulfate ions. – *Chemical Engineering Journal*, 2011, 169, 258–262.
- Darsinou, B., Frontistis, Z., Antonopoulou, M., Konstantinou, I., Mantzavinos, D. Sono-activated persulfate oxidation of bisphenol A: kinetics, pathways and the controversial role of temperature. – *Chemical Engineering Journal*, 2015, 280, 623–633.

Deng Y., Ezyske C.M. Sulfate radical-advanced oxidation process (SR-AOP) for simultaneous removal of refractory organic contaminants and ammonia in landfill leachate. – *Water Research*, 2011, 45, 6189–6194.

Devi, P., Das, U., Dalai, A.K. *In-situ* chemical oxidation: Principle and applications of peroxide and persulfate treatments in wastewater systems. – *Science of The Total Environment*, 2016, 571, 643–657.

Drzewicz, P., Perez-Estrada, L., Alpatova, A., Martin, J.W., El-Din, M.G. Impact of peroxydisulfate in the presence of zero valent iron on the oxidation of cyclohexanic acid and naphthenic acids from oil sands process-affected water. – *Environmental Science and Technology*, 2012, 46, 8984–8991.

Duan, X., Sun, H., Kang, J., Wang, Y., Indrawirawan, S., Wang, S. Insights into heterogeneous catalysis of persulfate activation on dimensional-structured nanocarbons. – *ACS Catalysis*, 2015, 5, 4629–4636.

Furman, O.S., Teel, A.L., Watts, R.J. Mechanism of base activation of persulfate. – *Environmental Science and Technology*, 2010, 44, 6423–6428.

Furman, O.S., Teel, A.L., Ahmad, M., Merker, M.C., Watts, R.J. Effect of basicity on persulfate reactivity. – *Journal of Environmental Engineering*, 2011, 137(4), 241–247.

Ghauch, A., Tuqan, A.M., Kibbi, N. Ibuprofen removal by heated persulfate in aqueous solution: a kinetics study. – *Chemical Engineering Journal*, 2012, 197, 483–492.

Guan, C., Jiang, J., Luo, C., Pang, S., Jiang, C., Ma, J., Jin, Y., Li, J. Transformation of iodide by carbon nanotube activated peroxydisulfate and formation of iodoorganic compounds in the presence of natural organic matter. – *Environmental Science and Technology*, 2017, 51, 479–487.

Han, D., Wan, J., Ma, Y., Wang, Y., Li, Y., Li, D., Guan, Z. New insights into the role of organic chelating agents in Fe(II) activated persulfate processes. – *Chemical Engineering Journal*, 2015, 269, 425–433.

Hayon, E., Treinin, A., Wilf, J. Electronic spectra, photochemistry, and autoxidation mechanism of the sulfite-bisulfite-pyrosulfite systems. SO_2^- , SO_3^- , SO_4^- , and SO_5^- radicals. – *Journal of The American Chemical Society*, 1972, 94, 47–57.

Hilles, A.H., Abu Amr, S.S., Hussein, R.A., El-Sebaie, O.D., Arafa, A.I. Performance of combined sodium persulfate/ H_2O_2 based advanced oxidation process in stabilized landfill leachate treatment. – *Journal of Environmental Management*, 2016, 166, 493–498.

Hoffmann, M.R., Hua, I., Hochemer, R.H. Application of ultrasonic irradiation for the degradation of chemical contaminants in water. – *Ultrasonics Sonochemistry*, 1996, 3, S163–S172.

Hori, H., Yamamoto, A., Hayakawa, E., Taniyasu, S., Yamashita, N., Kutsuna, S. Efficient decomposition of environmentally persistent perfluorocarboxylic acids by use of persulfate as a photochemical oxidant. – *Environmental Science and Technology*, 2005, 39, 2383–2388.

House, D.A. Kinetics and mechanism of oxidations by peroxydisulfate. – *Chemical Reviews*, 1962, 62, 185–203.

Ityel, D. Ground water: dealing with iron contamination. – *Filtration & Separation*, 2011, 48, 26–28.

Ji, Y., Dong, C., Kong, D., Lu, J., Zhou, Q. Heat-activated persulfate oxidation of atrazine: implications for remediation of groundwater contaminated by herbicides. – *Chemical Engineering Journal*, 2015, 263, 45–54.

Kolthoff, I.M., Miller, I.K. The chemistry of persulfate. I. The kinetics and mechanism of the decomposition of the persulfate ion in aqueous medium. – *Journal of the American Chemical Society*, 1951, 73, 3055–3059.

Lange, F.T., Scheurer, M., Brauch, H.-J. Artificial sweeteners – a recently recognized class of emerging environmental contaminants: a review. – *Analytical and Bioanalytical Chemistry*, 2012, 403, 2503–2518.

Lee, H., Lee, H.-J., Jeong, J., Lee, J., Park, N.-B., Lee, C. Activation of persulfates by carbon nanotubes: oxidation of organic compounds by nonradical mechanism. – *Chemical Engineering Journal*, 2015, 266, 28–33.

Li, H., Wan, J., Ma, Y., Wang, Y., Huang, M. Influence of particle size of zero-valent iron and dissolved silica on the reactivity of activated persulfate for degradation of acid orange 7. – *Chemical Engineering Journal*, 2014, 237, 487–496.

Li, W., Orozco, R., Camargos, N., Liu, H. Mechanisms on the impacts of alkalinity, pH, and chloride on persulfate-based groundwater remediation. – *Environmental Science and Technology*, 2017, 51, 3948–3959.

Li, Z., Yang, Q., Zhong, Y., Li, X., Zhou, L., Li, X., Zeng, G. Granular activated carbon supported iron as a heterogeneous persulfate catalyst for the pretreatment of mature landfill leachate. – *Royal Society of Chemistry Advances*, 2016, 6, 987–994.

Liang, C., Bruell, C.J., Marley, M.C., Sperry, K.L. Persulfate oxidation for *in situ* remediation of TCE. I. Activated by ferrous ion with and without a persulfate-thiosulfate redox couple. – *Chemosphere*, 2004a, 55, 1213–1223.

Liang, C., Bruell, C.J., Marley, M.C., Sperry, K.L. Persulfate oxidation for *in situ* remediation of TCE. II. Activated by chelated ferrous ion. – *Chemosphere*, 2004b, 55, 1225–1233.

Liang, C., Wang, Z.S., Mohanty, N. Influences of carbonate and chloride ions on persulfate oxidation of trichloroethylene at 20 °C. – *Science of The Total Environment*, 2006, 370, 271–277.

Liang, C., Huang, C.-F., Mohanty, N., Kurakalva, R.M. A rapid spectrophotometric determination of persulfate anion in ISCO. – *Chemosphere*, 2008, 73, 1540–1543.

Liang, C., Lin, Y.-T., Shih, W.-H. Treatment of trichloroethylene by adsorption and persulfate oxidation in batch studies. – *Industrial & Engineering Chemistry Research*, 2009, 48, 8373–8380.

Liang, C., Su, H.W. Identification of sulfate and hydroxyl radicals in thermally activated persulfate. – *Industrial & Engineering Chemistry Research*, 2009, 48, 5558–5562.

Liu, H., Bruton, T.A., Doyle, F.M., Sedlak, D.L. *In situ* chemical oxidation of contaminated groundwater by persulfate: decomposition by Fe(III)- and Mn(IV)-containing oxides and aquifer materials. – *Environmental Science and Technology*, 2014, 48, 10330–10336.

Lominchar, M.A., Rodríguez, S., Lorenzo, D., Santos, N., Romero, A., Santos, A. Phenol abatement using persulfate activated by nZVI, H₂O₂ and NaOH and development of a kinetic model for alkaline activation. – *Environmental Technology*, 2018, 39, 35–43.

Lutze, H.V., Kerlin, N., Schmidt, T.C. Sulfate radical-based water treatment in presence of chloride: formation of chlorate, inter-conversion of sulfate radicals into hydroxyl radicals and influence of bicarbonate. – *Water Research*, 2015, 72, 349–360.

Méndez-Díaz, J., Sánchez-Polo, M., Rivera-Utrilla, J., Canonica, S., von Gunten, U. Advanced oxidation of the surfactant SDBS by means of hydroxyl and sulphate radicals. – *Chemical Engineering Journal*, 2010, 163, 300–306.

Merck, E. The testing of water. 9th edition. Darmstadt: Merck, 1994.

Monteagudo, J.M., Durán, A., González, R., Expósito, A.J. *In situ* chemical oxidation of carbamazepine solutions using persulfate simultaneously activated by heat energy, UV light, Fe²⁺ ions, and H₂O₂. – *Applied Catalysis B: Environmental*, 2015, 176–177, 120–129.

Moussavi, G., Pourakbar, M., Aghayani, E., Mahdavianpour, M., Shekoohyian, S. Comparing the efficacy of VUV and UVC/S₂O₈²⁻ advanced oxidation processes for degradation and mineralization of cyanide in wastewater. – *Chemical Engineering Journal*, 2016, 294, 273–280.

Nasseri, S., Mahvi, A.H., Seyedsalehi, M., Yaghmaeian, K., Nabizadeh, R., Alimohammadi, M., Safari, G.H. Degradation kinetics of tetracycline in aqueous solutions using peroxydisulfate activated by ultrasound irradiation: effect of radical scavenger and water matrix. – *Journal of Molecular Liquids*, 2017, 241, 704–714.

Oh, S.-Y., Kim, H.-W., Park, J.-M., Park, H.-S., Yoon, C. Oxidation of polyvinyl alcohol by persulfate activated with heat, Fe²⁺, and zero-valent iron. – *Journal of Hazardous Materials*, 2009, 168, 346–351.

Oh, S.-Y., Kang, S.-G., Chiu, P.C. Degradation of 2,4-dinitrotoluene by persulfate activated with zero-valent iron. – *Science of The Total Environment*, 2010, 408, 3464–3468.

Pouran, S.R., Aziz, A.R.A., Daud, W.M.A.W. Review on the main advances in photo-Fenton oxidation system for recalcitrant wastewaters. – *Journal of Industrial Engineering and Chemistry*, 2015, 21, 53–69.

Punturat, V., Huang, K.-L. Degradation pathways and organic matter transformation of acesulfame potassium electro-oxidation in real water matrices. – *Journal of the Taiwan Institute of Chemical Engineers*, 2017, 80, 222–230.

Qi, C., Liu, X., Zhao, W., Lin, C., Ma, J., Shi, W., Sun, Q., Xiao, H. Degradation and dechlorination of pentachlorophenol by microwave-activated persulfate. – *Environmental Science and Pollution Research*, 2015, 22, 4670–4679.

Rastogi, A., Al-Abed, S.R., Dionysiou, D.D. Effect of inorganic, synthetic and naturally occurring chelating agents on Fe(II) mediated advanced oxidation of chlorophenols. – *Water Research*, 2009, 43, 684–694.

Rodriguez, S., Vasquez, L., Costa, D., Romero, A., Santos, A. Oxidation of Orange G by persulfate activated by Fe(II), Fe(III) and zero valent iron (ZVI). – *Chemosphere*, 2014, 101, 86–92.

Rodríguez-Chueca, J., Amor, C., Mota, J., Lucas, M.S., Peres, J.A. Oxidation of winery wastewater by sulphate radicals: catalytic and solar photocatalytic activations. – *Environmental Science and Pollution Research*, 2017, 24, 22414–22426.

Sabri, N., Hanna, K., Yargeau, V. Chemical oxidation of ibuprofen in the presence of iron species at near neutral pH. – *Science of The Total Environment*, 2012, 427–428, 382–389.

Sof'ina, N.A., Beklemishev, M.K., Kapanadze, A.L., Dolmanova, I.F. Sorptioncatalytic method for the chromium determination. – *Moscow University Chemistry Bulletin*, 2003, 44, 189–198 (in Russian).

Sun, H., Kwan, C., Suvorova, A., Ang, H.M., Tadó, M.O., Wang, S. Catalytic oxidation of organic pollutants on pristine and surface nitrogen-modified carbon nanotubes with sulfate radicals. – *Applied Catalysis B: Environmental*, 2014, 154–155, 134–141.

Teel, A.L., Ahmad, M., Watts, R.J. Persulfate activation by naturally occurring trace minerals. – *Journal of Hazardous Materials*, 2011, 196, 153–159.

Tijani, J., Fatoba, O., Petrik, L.F. A Review of pharmaceuticals and endocrine-disrupting compounds: sources, effects, removal, and detections. – *Water, Air & Soil Pollution*, 2013, 224, 1–29.

Tsao, M.-S., Wilmarth, W.K. II(a). Oxidation-reduction reactions involving inorganic substrates. Aqueous chemistry of inorganic free radicals. Part 3. The kinetics and mechanism of the reaction of peroxydisulfate ion and hydrogen peroxide. – *Discussions of the Faraday Society*, 1960, 29, 137–145.

Tsitonaki, A., Petri, B., Crimi, M., Mosabaek, H., Siegrist, R.L., Bjerg, P.L. *In situ* chemical oxidation of contaminated soil and groundwater using persulfate: a review. – *Critical Reviews in Environmental Science and Technology*, 2010, 40, 55–91.

Waclawek, S., Lutze, H.V., Grübel, K., Padil, V.V.T., Černík, M., Dionysiou, D.D. Chemistry of persulfates in water and wastewater treatment: A review. – *Chemical Engineering Journal*, 2017, 330, 44–62.

Wang, J., Wang, S. Activation of persulfate (PS) and peroxymonosulfate (PMS) and application for the degradation of emerging contaminants. – *Chemical Engineering Journal*, 2018, 334, 1502–1517.

Wang, J., Yu, M., Cai, X., Yang, Y., Li, D. Sodium persulfate activation by Fe²⁺ for the *in situ* remediation of chlorobenzene-contaminated groundwater. – *Chinese Journal of Environmental Engineering*, 2016, 10, 1276–1280.

Wang, S., Zhou, N. Removal of carbamazepine from aqueous solution using sono-activated persulfate process. – *Ultrasonics Sonochemistry*, 2016, 29, 156–162.

Xia, D., Yin, R., Sun, J., An, T., Li, G., Wang, W., Zhao, H., Keung Wong, P. Natural magnetic pyrrhotite as a high-efficient persulfate activator for micropollutants degradation: radicals identification and toxicity evaluation. – *Journal of Hazardous Materials*, 2017, 340, 435–444.

Xiao, Y., Zhang, L., Zhang, W., Lim, K.-Y., Webster, R.D., Lim, T.-T. Comparative evaluation of iodoacids removal by UV/persulfate and UV/H₂O₂ processes. – *Water Research*, 2016, 102, 629–639.

Yan, D.Y., Lo, I.M. Removal effectiveness and mechanisms of naphthalene and heavy metals from artificially contaminated soil by iron chelate-activated persulfate. – *Environmental Pollution*, 2013, 178, 15–22.

Yang, Y., Guo, H., Zhang, Y., Deng, Q., Zhang, J. Degradation of bisphenol A using ozone/persulfate process: kinetics and mechanism. – *Water, Air & Soil Pollution*, 2016, 227, 1–12.

Yuan, S., Liao, P., Alshawabkeh, A.N. Electrolytic manipulation of persulfate reactivity by iron electrodes for trichloroethylene degradation in groundwater. – *Environmental Science and Technology*, 2014, 48, 656–663.

Zhang, B.-T., Zhang, Y., Teng, Y., Fan, M. Sulfate radical and its application in decontamination technologies. – *Critical Reviews in Environmental Science and Technology*, 2015, 45, 1756–1800.

Zhang, Y., Tran, H.P., Du, X., Hussain, I., Huang, S., Zhou, S., Wen, W. Efficient pyrite activating persulfate process for degradation of p-chloroaniline in aqueous systems: A mechanistic study. – *Chemical Engineering Journal*, 2017, 308, 1112–1119.

Zhao, L., Ji, Y., Kong, D., Lu, J., Zhou, Q., Yin, X. Simultaneous removal of bisphenol A and phosphate in zero-valent iron activated persulfate oxidation process. – *Chemical Engineering Journal*, 2016, 303, 458–466.

Zhou, L., Zheng, W., Ji, Y., Zhang, J., Zeng, C., Zhang, Y., Wang, Q., Yang, X. Ferrous-activated persulfate oxidation of arsenic(III) and diuron in aquatic system. – *Journal of Hazardous Materials*, 2013, 263, 422–430.

Zorita, S., Mårtensson, L., Mathiasson, L. Occurrence and removal of pharmaceuticals in a municipal sewage treatment system in the south of Sweden. – *Science of The Total Environment*, 2009, 407, 2760–2770.

ACKNOWLEDGEMENTS

I sincerely appreciate the support and motivation of my dear supervisors Dr. Niina Dulova and Prof. Marina Trapido throughout the years of my PhD study. Dr. Dulova's valuable guidance and numerous encouraging discussions gave me several opportunities to attend conferences, special courses and other meetings related to my PhD research area. This was very inspiring and knowledge-growing experience that improved my competence and gave me new connections in the field of my research. These four years would not have been that much enjoyable and fruitful without her thoughtful supervision and amazing energy. I am also sincerely grateful to Prof. Trapido for the possibility to carry out this PhD research and for useful remarks and discussions throughout these years. I am thankful for all my colleagues in the Laboratory of Environmental Technology (and all the colleagues in the former Department of Chemical Engineering).

The most important supportive force was my loving family: fiancé, father, mother, brothers, sister-in-laws, nephews and nieces. They saw all my positive and negative periods and continued to "cheer" this journey towards a "victorious end". I am also grateful to my amazing friends for their patience and sense of humor during this intensive period.

I would like to acknowledge the Estonian Ministry of Education and Research (IUT1-7), Archimedes Foundation (AR12017; Kristjan Jaak scholarship), Estonian Research Council (ETF7812), European Regional Development Fund (Dora plus program), European Cooperation in Science and Technology (COST) program, Association for Chemistry and the Environment (ACE), and UTs and TTÜs graduate school "Functional materials and technologies" for the financial support.

ABSTRACT

Application of Activated Persulfate Processes for the Treatment of Water and High-Strength Wastewater

Suitable treatment methods for purification of water should be chosen based on the character and strength of pollution, taking into account the aqueous matrix. Such approach provides the highest efficacy of the applied processes. However, traditional water and wastewater treatment technologies are often not designed to remove organic pollutants of low (ng/L–µg/L) or high (g/L) concentrations. These pollutants may be removed by the promising radical-based advanced oxidation technologies based on the strong oxidative properties of hydroxyl and/or sulfate radicals.

Sulfate radicals generated in the activated persulfate processes selectively oxidize various organic pollutants, e.g. pharmaceuticals, dyes, agrochemicals, and personal care product components. The activation of persulfate may be implemented in several ways, e.g. reaction with metals, application of heat, radiation, peroxide, or alkali, which generally needs careful adjustment to achieve high efficacy in water purification. Even though different persulfate activation possibilities have been extensively studied for over a decade, there are still many uncertainties related to the application in aqueous matrices containing diverse types of contaminants. It should be emphasized that real aqueous matrices are not very often used in lab-scale experiments, not to mention full-scale application of activated persulfate.

Accordingly, the aim of this research was to assess the most feasible persulfate activation options in water and wastewater treatment containing different pollutants at various pollution levels, and thereby extend the background for full-scale applications of $\text{SO}_4^{\bullet-}$ -AOTs. The aqueous matrices of wide variation were used to study the potential of activated persulfate processes. New classes of emerging micropollutants, artificial sweetener acesulfame and non-steroidal anti-inflammatory drug naproxen were chosen for studies with the intention to prove activated persulfate treatment efficacy degrading organic contaminants at different initial concentrations. The most viable activators, i.e. ferrous iron/chelated ferrous iron and UV light were used aiming to implement these *in situ*. The efficacy of the applied oxidative systems was evaluated by the changes in chemical and biological oxygen demand, total organic carbon and BOD_7/COD ratio, as well as the changes in initial pollutant concentration.

In this thesis, pyrolysis wastewater and landfill leachate treatment by Fe(II)-activated persulfate was investigated for the first time. Similarly, the acesulfame and naproxen degradation by the UVA/Fe(II) or chelated combined persulfate system was not previously studied. The results of these experiments extend the knowledge of the activated persulfate systems approximating their full-scale application in various aqueous matrices. In addition, the use of UVA fraction of the sunlight may contribute to the sustainable water treatment technology along with application of iron, a typical constituent of natural minerals.

All the studied activated persulfate systems indicated promising efficacies in purification of the selected water matrices with different contamination degree. In the case of pyrolysis wastewater and landfill leachate, the persulfate oxidative system could be implemented as an effective pre-treatment step.

Acesulfame and naproxen were approached as emerging micropollutants, and the experimental data indicated that these substances could be degraded, although not

mineralized at the chosen conditions. Identification of radicals responsible for the target compounds oxidation in the activated persulfate systems allowed proposing possible transformation pathways for these micropollutants.

Based on the obtained results, the pollution level and characteristics of water are the conditions of high importance when choosing the effective activated persulfate treatment. The findings allow future applications of the studied persulfate systems for the full-scale purification of contaminated waters at a full-scale.

LÜHIKOKKUVÕTE

Aktiveeritud persulfaadi protsesside kasutamine vee ja raskesti saastatud reovee puhastamiseks

Inimtegevuse tagajärjel tekkinud vee saastumine omab keskkonnale pikaajalist mõju ja seega on tõhusate veetöötlusmeetodite leidmine väga olulise tähtsusega. Sobilike puhastusprotsesside valik sõltub vesikeskkonnas leiduvate saasteainete väga erinevast päritolust ning vee saastatuse astmest. See tagab kõrgeima võimaliku puhastusefektiivsuse. Paljud püsivad orgaanilised saasteained esinevad vees aga mikrokontsentratsioonides, mida tavaliste (reo)veepuhastusprotsesside käigus ei ole võimalik eemaldada. Sellisel juhul võib rakendada tõhusaid süvaoksüdatsiooniprotsesse, mis põhinevad hüdroksüül- või sulfaatradikaalide tugeval oksüdeerimisvõimel.

Tugeva ja stabiilse oksüdeerija, persulfaadi, aktiveerimisel tekkinud sulfaatradikaalid on võimelised lagundama erinevaid orgaanilisi saasteaineid nagu näiteks ravimid, värvained, põllumajanduses kasutatavate kemikaalide komponendid, isiklike hügieenivahendite koostisosad. Persulfaati saab aktiveerida mitmel viisil (näiteks metallide, soojuse, kiirituse, peroksiidi või aluse toimel), kuid tõhusa veepuhastuse jaoks vajab see hoolikat reguleerimist. Erinevaid persulfaadi aktiveerimisvõimalusi on põhjalikumalt uuritud juba üle kümne aasta, kuid sellegipoolest on nende rakendamisega erinevate saasteainete lagundamiseks seotud mitmeid vastamata küsimusi. Muuhulgas on uuringutes väga vähe kasutatud reaalsete vett/reovett rääkimata aktiveeritud persulfaadi protsesside rakendamisest (reo)veepuhastusjaamades.

Eelpool toodust lähtuvalt oli käesoleva doktoritöö peamiseks eesmärgiks hinnata kõige tõhusamate persulfaadi aktiveerimisvõimaluste rakendamist erineva saastatusega vees ja reovees seeläbi täiustada olemasolevaid teadmisi sulfaatradikaalidel põhinevatest süvaoksüdatsiooniprotsessidest. Töös kasutati väga erinevate näitajatega vett/reovett, mis võimaldas hästi uurida aktiveeritud persulfaadi protsesside laialdast tõhusust. Antud uurimistöös kasutati uute esilekerkivate mikrosaasteainete hulka kuuluvaid ühendeid (kunstlik magusaine atsesulfaam, mittesteroidne põletikuvastane ravim naprokseen) eesmärgiga tõestada kasutatud protsesside rakendatavust erinevate omaduste ja kontsentratsioonidega orgaaniliste ühendite lagundamiseks. Töös valiti uuritavad persulfaadi aktivaatorid põhimõttel, mis võimaldaks tulevikus nende *in situ* (kohapeal) kasutamist. Kasutatud süsteemide efektiivsust hinnati keemilise ja bioloogilise hapnikutarve, üldorgaanilise süsiniku ja hinnangulise biolagundatavuse väärtuste ning saasteainete algkontsentratsiooni (atsesulfaam, naprokseen) muutuste põhjal.

Antud doktoritöös uuriti esmakordselt kahevalentse rauaga aktiveeritud persulfaadi rakendamist pürolüüsivee ja prügila nõrgvee töötlemiseks. Samuti polnud varem uuritud ultraviolet A/kahevalentse raua või kelateeritud kombineeritud (peroksiid/persulfaat/kahevalentne raud) süsteemi rakendamist atsesulfaami/naprokseeni lagundamiseks. Saadud tulemused laiendavad aktiveeritud persulfaadi protsesside rakendusala erinevate saastunud vete puhastamiseks. Lisaks saab antud tehnoloogiaid nimetada jätkusuutlikeks, sest ultraviolet A kiirgus sisaldub teatud määral ka päikesevalguses ning raua (tavaliselt kolmevalentsena) leidub ulatuslikult ka looduslikes mineraalides.

Kõik uuritud aktiveeritud persulfaadi süsteemid näitasid paljulubavat tõhusust valitud erineva saastatusega vete puhastamisel. Pürolüüsivee ja prügila nõrgveega teostatud

eksperimentid näitasid, et selliste reovete puhul sobib aktiveeritud persulfaadi töötlus hästi kasutamiseks eelpuhastusastmena.

Atsesulfaami ja naprokseeni kasutati antud töös (esilekerkivate) mikrosaasteainetena ning eksperimentide põhjal saadud tulemused näitasid, et antud ühendeid on võimalik lagundada, kui mitte täielikult eemaldada (mineraliseerida). Uuritud ainete jaoks pakuti radikaalipüüdjate kasutamise abil välja ka võimalikud lagunemise skeemid.

Saadud tulemuste põhjal saab väita, et vee saastatuse aste ja vee näitajad on aktiveeritud persulfaadi protsesside sobivaimate rakendamistingimuste valikul äärmiselt olulise tähtsusega. Sellest hoolimata on võimalik uuritud persulfaadi süsteemide edaspidine kasutamine vee/reovee töötlemiseks (reo)veepuhastusjaamades.

APPENDIX

PAPER I

Kattel, E., Dulova, N., Viisimaa, M., Tenno, T., Trapido, M. Treatment of high-strength wastewater by Fe²⁺-activated persulfate and hydrogen peroxide. – *Environmental Technology*, 2016, 37 (3), 352–359.

Reproduced with the permission of Taylor & Francis.

Treatment of high-strength wastewater by Fe²⁺-activated persulphate and hydrogen peroxide

E. Kattel^a, N. Dulova^{a*}, M. Viisimaa^a, T. Tenno^b and M. Trapido^a

^aDepartment of Chemical Engineering, Tallinn University of Technology, Ehitajate tee 5, Tallinn 19086, Estonia; ^bDepartment of Chemistry, University of Tartu, Ravila 14a, Tartu 50411, Estonia

(Received 2 March 2015; accepted 26 June 2015)

Ferrous ion-activated persulphate and hydrogen peroxide were studied for the treatment of real high-strength industrial effluent. The Fenton process demonstrated greater organic load removal, biodegradability improvement and toxicity reduction as well as lower treatment cost than the activated persulphate system. However, the use of an activated persulphate process was more favourable due to the exothermic effect intrinsic to the Fenton reaction, which resulted in a rapid increase in the temperature of the high-strength wastewater along with excessive foam formation. Overall, for the H₂O₂/Fe²⁺ and S₂O₈²⁻/Fe²⁺ processes, the application of a chemical oxygen demand (COD)/oxidant/Fe²⁺ weight ratio of 1/0.4/0.075 resulted in a COD removal of 58 and 50%, a 7-day biochemical oxygen demand/COD ratio increase from 0.14 to 0.3 and 0.23, and an increase in the EC₅₀ (*Daphnia magna*) by 6.5-fold and 2.9-fold, respectively. The stepwise addition of the oxidant and activator was favourable for the Fenton process and resulted in negligible improvement in the wastewater treatment efficacy in the activated persulphate system.

Keywords: acute toxicity; Fenton process; ferrous ion-activated persulphate; sulphate radical; wastewater treatment

1. Introduction

The application of advanced oxidation technologies (AOTs) is a viable solution for the destruction of virtually all persistent organic pollutants that exist in highly loaded industrial wastewater.[1–6] The strength of AOTs relies on the generation of highly reactive hydroxyl radicals (HO•) that are believed to react fast and non-selectively with a majority of the organic contaminants. The oxidation of organic pollutants by persulphate (S₂O₈²⁻) has been studied as an alternative to conventional HO•-based AOTs.[7–11] The sodium persulphate is characterized by high solubility at ambient temperature, and the sulphate ions, which are the major product of persulphate reduction, are relatively harmless and considered to be environmentally friendly.[12] The decomposition of persulphate via heat, ultrasound or UV light activation, transition metal activation, alkaline activation (pH > 10) or peroxide activation proceeds with the generation of more powerful sulphate-free radicals (SO₄^{•-}).[7,12] In contrast to hydroxyl radicals, sulphate radicals are more selective for the oxidation of unsaturated bonds and aromatic constituents.[13]

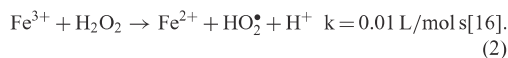
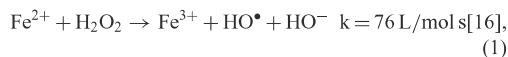
Oil shale is an immature source rock that contains relatively large amounts of organic matter with an elemental composition that primarily includes carbon, hydrogen, oxygen and small amounts of sulphur and nitrogen. During

the thermal processing of oil shale using a hot recycled solids technology, this material is heated to 500–550°C to yield shale oil by pyrolysis. The by-products of this process are gas, process water and solid residue. The phenolic wastewater, which is formed from the condensation of vapour, was used in this study as a real high-strength wastewater sample to assess the potential of HO•- and SO₄^{•-}-based AOTs to treat complex and heavily contaminated oil-in-water emulsions.

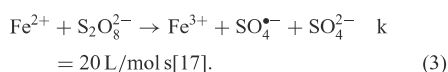
In this study, the efficacies of the Fenton process and the S₂O₈²⁻/Fe²⁺ system for the advanced chemical treatment of high-strength wastewater were investigated and compared. The objective was to reduce the organic content, increase the biodegradability and reduce the toxicity to make the subsequent biological treatment more practical. The Fenton process is one of the most attractive wastewater treatment methods among the conventional AOTs due to its high efficacy for organic contaminant removal and harmless reagents (Equations (1) and (2)) used to generate HO•.[2,14,15] However, the Fenton treatment imposes a few restrictions during its application for highly loaded wastewater purification, including the use of elevated temperatures due to the exothermic nature of the Fenton reaction (Equation (1)) and the production of excessive foam through CO₂ and O₂ evolution, the latter being due to the

*Corresponding author. Email: niina.dulova@ttu.ee

thermal decomposition of H_2O_2 . [14]



The application of treatment methods based on similarly powerful but less aggressive $\text{S}_2\text{O}_8^{2-}/\text{SO}_4^{\cdot-}$ may help to overcome the above-mentioned problems. The reaction of $\text{S}_2\text{O}_8^{2-}$ with Fe^{2+} to generate sulphate-free radicals (Equation (3)) is similar to the Fenton reaction (Equation (1)) and is probably the most favourable for environmental protection application compared to other activation techniques. [12]



The results obtained within this study expand the knowledge of ferrous ion-activated persulphate and hydrogen peroxide applicability to treat real high-strength industrial wastewaters along with complex and heavily contaminated oil-in-water emulsions. The efficacy of different treatment schemes is assessed by taking into account both the treatment performance and cost-effectiveness. There are no previously published studies evaluating and comparing the potential of ferrous ion-activated persulphate and hydrogen peroxide for phenolic high-strength industrial wastewater treatment. In general, the available literature concerning such types of wastewater treatment is very limited.

2. Experimental protocols

2.1. Chemicals and materials

Hydrogen peroxide (PERDROGENTTM, $\geq 30\%$), sodium persulphate ($\text{Na}_2\text{S}_2\text{O}_8$, $\geq 99\%$) and ferrous sulphate heptahydrate ($\text{FeSO}_4 \cdot 7\text{H}_2\text{O}$, $\geq 99\%$) were purchased from Sigma-Aldrich. All the other chemicals were of reagent grade and used without further purification. Ultrapure water (Millipore Simplicity[®] UV System) was used to prepare the stock solutions.

The studied effluent was a phenolic wastewater formed during condensation of vapour from an oil shale thermal process, and was obtained from an oil shale thermal treatment plant (the wastewater is rich in phenols, such as phenol, *p*-cresol, dimethylphenols, resorcinol, 5-methylresorcinol and 2,5-dimethylresorcinol). The main properties of the wastewater sample after removal of the shale oil layer are listed in Table 1.

2.2. Experimental procedure

All of the Fenton and persulphate oxidation trials were performed in batch mode and in non-buffered solutions

Table 1. Main wastewater parameters.

Parameter	Unit	Value
COD	mg/L	39700 ± 1700
DOC	mg/L	9010 ± 25
BOD ₇	mg/L	5500 ± 390
Biodegradability, BOD ₇ /COD	–	0.14
Total phenols	mg/L	730 ± 15
Total Fe	mg/L	2.86 ± 0.11
pH	–	8.88 ± 0.04
Conductivity	mS/cm	10.43 ± 0.09
TS (105°C)	mg/L	448 ± 42
TFS (600°C)	mg/L	335 ± 16
Acute toxicity to <i>D. magna</i> , EC ₅₀	%	0.34 ± 0.03
Inhibition of oxygen consumption, IC ₅₀	%	1.7
Inhibition of nitrification, IC ₅₀	%	0.35

at ambient room temperature ($21 \pm 1^\circ\text{C}$). Wastewater samples (0.5 L) were treated in a 1 L cylindrical glass reactor with a constant agitation speed (400 rpm) for 24 h. First, the activator ($\text{FeSO}_4 \cdot 7\text{H}_2\text{O}$) was added, and after its complete dissolution, oxidation was initiated by immediately adding H_2O_2 or $\text{S}_2\text{O}_8^{2-}$. The effect of a stepwise addition of the activator, oxidant (H_2O_2 or $\text{S}_2\text{O}_8^{2-}$) and activator/oxidant after 0, 30 and 60 min of oxidation was also investigated. The pH of the wastewater samples was not adjusted in the subsequent treatment, unless otherwise specified. The oxidation was terminated by addition of NaOH (10 M) to adjust the pH of the treated samples to ~ 8.5 . This process was followed by a settling period of 24 h. Lastly, the supernatant was collected for further analysis. The wastewater oxidation experiments with non-activated hydrogen peroxide and persulphate were conducted in identical reactors under the same treatment conditions for the respective activated oxidation trials. All of the experiments were performed in duplicate, and the results of the analysis are presented as the mean with a standard deviation.

2.3. Analytical methods

The chemical oxygen demand (COD) was determined using a closed reflux colorimetric method. [18] The correction for the hydrogen peroxide interference of the COD test was performed using the correlation equation reported by Kang et al. [19] The total solids (TS), total fixed solids (TFS) and the 7-day biochemical oxygen demand (BOD₇) were determined according to APHA (American Public Health Association). [18] The activated sludge used as a seed source in the BOD₇ test was obtained from a municipal wastewater treatment plant (WWTP) in Tallinn, Estonia, and was not acclimated before BOD₇ measurements. The electrical conductivity was measured using a digital EC meter (HANNA Instruments HI9032), and the pH was measured using a digital pH meter (Schott CG-840). The

total iron concentrations in the initial and treated samples were measured using a phenanthroline method.[18] The residual hydrogen peroxide concentration in the treated samples was measured using a spectrophotometric method with Ti^{4+} [20] by a Helios- β UV/VIS spectrophotometer (Thermo Electron Corporation). The residual persulphate concentration in the treated samples was measured spectrophotometrically at 446 nm with *o*-dianisidine.[21] The total phenols were measured spectrophotometrically with aminoantipyrine according to ISO 6439.[22] The dissolved organic carbon (DOC) was measured in filtered (Puradisc Aqua, 0.45 μ m, cellulose acetate membrane) wastewater samples using a Total organic carbon analyzer multi N/C[®] 3100 (Analytik Jena). The acute toxicities to *Daphnia magna* (*Cladocera*, *Crustacea*) of the initial and treated samples were measured with DAPHTOXKIT FTM MAGNA (MicroBioTest Inc.) in a 24-h toxicity test according to ISO 6341.[23] The measurements on inhibition of oxygen consumption by activated sludge and nitrification efficiency were performed according to ISO 8192 [24] and ISO 9509,[25] respectively. The activated sludge used in inhibition tests originated from a municipal WWTP in Tartu, Estonia.

3. Results and discussion

3.1. Advanced chemical treatment

During the iron-activated hydrogen peroxide or persulphate treatment of the wastewater samples, both the oxidation and coagulation of the ferric-hydroxy complexes contributed to the removal of organic contaminants. The main limitation in the application of these processes

is the formation of a large amount of ferric sludge in the coagulation stage, which requires further processing. Therefore, the optimization of both processes is required to attain better utilization of the oxidant and activator to reduce sludge production. In this study, all the measurements of the observed parameters were performed after 24 h of oxidation followed by 24 h of sedimentation.

The optimization of the oxidant to contaminant ratio is an essential step for improving the Fenton-based oxidation treatment efficacy. The results of the wastewater treatment with different COD/H₂O₂ weight ratios are shown in Figure 1 and Table 2. In these trials, the weight ratio of H₂O₂/Fe²⁺ was maintained at 5:1, which is optimal for highly loaded wastewater treatment.[2] An increase in the H₂O₂/COD ratio led to an improvement in the organic load removal (COD, DOC) and biodegradability (the BOD₇/COD ratio was used as a rough indicator) of the treated wastewater samples. Irrespective of the applied hydrogen peroxide concentration, the mineralization was lower than the COD removal. Therefore, at a COD/H₂O₂/Fe²⁺ w/w/w of 1/0.4/0.08 ([H₂O₂]₀ = 16 g/L, [Fe²⁺]₀ = 3.2 g/L), the reduction in DOC was two times less effective (28%) than the COD removal (58%). For higher H₂O₂/COD ratios, the mineralization extent was more substantial but with a similar difference in COD and DOC removal. Therefore, the treatment at a COD/H₂O₂/Fe²⁺ w/w/w of 1/1.2/0.24 ([H₂O₂]₀ = 48 g/L, [Fe²⁺]₀ = 9.6 g/L) resulted in 51% and 22% residual DOC and COD, respectively. No traces of residual hydrogen peroxide were detected in the treated wastewater samples, indicating the complete utilization of H₂O₂ under the treatment conditions. The residual iron concentrations

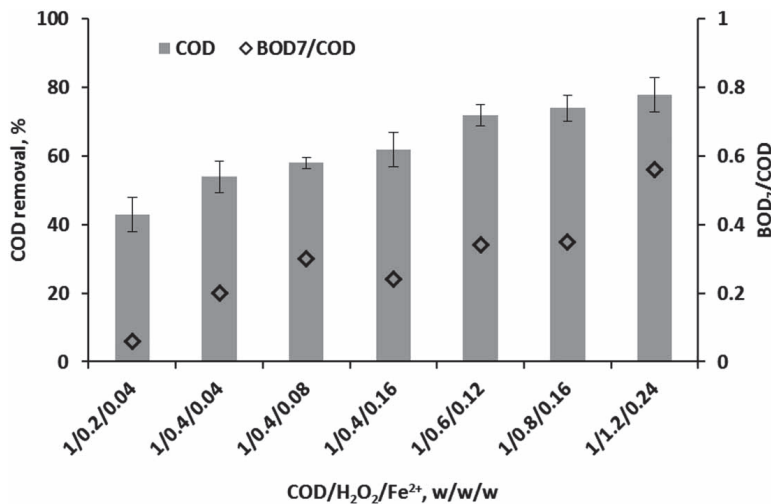


Figure 1. COD removal and the BOD₇/COD ratio as a function of the COD/H₂O₂/Fe²⁺ weight ratio in the Fenton treatment ([COD]₀ = 40 g/L).

Table 2. COD, BOD₇ and DOC removal after treatment at different COD/oxidant/Fe²⁺ weight ratios.

COD/oxidant/Fe ²⁺ , w/w/w	COD, g/L	COD removal, %	BOD ₇ , g/L	BOD ₇ removal, %	DOC, g/L	DOC removal, %
initial	40	—	5.5	—	9	—
H ₂ O ₂						
1/0.4/0.08	16.8	58	4.95	10	6.5	28
1/0.4/0.08 ^a	13.1	67	4.2	24	6	33
1/0.6/0.12	11.2	72	3.8	31	5.85	35
1/0.8/0.16	10.4	74	3.6	34.5	5.2	42
S ₂ O ₈ ²⁻						
1/0.4/0	21.2	47	3.8	31	8	11
1/0.4/0.08	20	50	4.6	16.5	6.85	24
1/0.4/0.08 ^b	19.2	52	4.4	20	6.5	28
1/0.8/0.16	16	60	2.4	56	5.5	39

^aOxidant/Fe²⁺ addition in three steps.

were lower than 1.5 mg/L in all the Fenton treatment trials. The non-activated hydrogen peroxide oxidation at a COD/H₂O₂ w/w of 1/0.4 ([H₂O₂]₀ = 16 g/L) resulted in no organic load reduction and more than 85% of unused H₂O₂ in the wastewater sample after 24 h of treatment.

In general, an initial pH between 2 and 4 favours the Fenton reaction (Equation (1)). However, at the beginning of the oxidation without pH adjustment, a fast decrease in the pH of the reaction mixture was observed in all the trials, except for the treatment at a COD/H₂O₂/Fe²⁺ w/w/w of 1/0.2/0.04 ([H₂O₂]₀ = 8 g/L, [Fe²⁺]₀ = 1.6 g/L), which resulted in a pH of 7.55 after 24 h of oxidation. This decrease was primarily due to the acidity of the added Fe²⁺ salt and the formation of acidic by-products. Therefore, the pH values were lower than 2.7 in the oxidation systems when the H₂O₂/COD w/w was higher than 0.4/1 (24 h of oxidation at a COD/H₂O₂/Fe²⁺ w/w/w of 1/0.4/0.08 resulted in a pH of 4.22). Insufficient treatment efficacy at lower H₂O₂ concentrations may be due to the need for pH adjustment prior to the Fenton reaction initialization. The adjustment of the pH to ~3 prior to the addition of the reagents in the Fenton treatment at a COD/H₂O₂/Fe²⁺ w/w/w of 1/0.4/0.08 resulted in COD and DOC removal enhancement up to 11% and 5%, respectively.

The effect of the H₂O₂/Fe²⁺ weight ratio was studied to determine the potential for reducing the final ferric sludge amount (Figure 1). Both a two-fold increase and decrease in the Fe²⁺-activator amount resulted in less than a 5% change in the COD reduction and negligible changes in the mineralization extent but lowered the BOD₇/COD ratio, which indicated that a H₂O₂/Fe²⁺ weight ratio of 5:1 was reasonable.

The main challenge in the application of the H₂O₂/Fe²⁺ process is the temperature increase and foam formation immediately after initialization of the Fenton oxidation. A temperature increase of 10°C and foam formation of as much as 25% of the initial sample volume were observed during wastewater treatment at a COD/H₂O₂/Fe²⁺ w/w/w of 1/0.4/0.08. Such a moderate increase in temperature

actually favours the Fenton treatment efficacy. However, a further increase in the H₂O₂ concentration resulted in a severe temperature increase and more aggressive foam formation. Therefore, a temperature increase of more than 50°C and foam formation as large as 300% of the initial sample volume were observed during oxidation at a COD/H₂O₂/Fe²⁺ w/w/w of 1/1.2/0.24. Therefore, for full-scale phenolic wastewater treatment using the Fenton process, the addition of a defoaming agent as well as temperature monitoring may be required to control the foam production and exothermic reaction. To overcome this problem, persulphate as an alternative oxidant to treat the phenolic wastewater.

The iron-activated persulphate treatment of the wastewater resulted in lower organic load removal and biodegradability improvement than the Fenton process (Figures 1 and 2; Table 2). However, the complete exclusion of foam formation and only negligible increase in temperature (2–4°C) during oxidation makes the S₂O₈²⁻/Fe²⁺ process a viable solution for the treatment of highly contaminated phenolic wastewater. To optimize the Fe²⁺-activated persulphate oxidation, the effect of different oxidant and activator concentrations (Figure 2 and Table 2) as well as pH adjustment to acidic values were studied. The COD removal and mineralization remained nearly identical in the trials with a COD/S₂O₈²⁻ w/w of 1/0.4 ([S₂O₈²⁻]₀ = 16 g/L) irrespective of the S₂O₈²⁻/Fe²⁺ w/w applied. A two-fold increase in the S₂O₈²⁻ concentration up to a COD/S₂O₈²⁻ w/w of 1/0.8 ([S₂O₈²⁻]₀ = 32 g/L) resulted in an additional 10% COD removal. Unexpectedly, the results of the non-activated persulphate treatment at a COD/S₂O₈²⁻ weight ratio of 1/0.4 resulted in considerable COD removal (47%). However, the mineralization was higher for the activated persulphate treatment at 11%, 24% and 39% with a COD/S₂O₈²⁻/Fe²⁺ w/w/w of 1/0.4/0, 1/0.4/0.08 ([S₂O₈²⁻]₀ = 16 g/L, [Fe²⁺]₀ = 3.2 g/L) and 1/0.8/0.16 ([S₂O₈²⁻]₀ = 32 g/L, [Fe²⁺]₀ = 6.4 g/L), respectively. The BOD₇ removal was enhanced

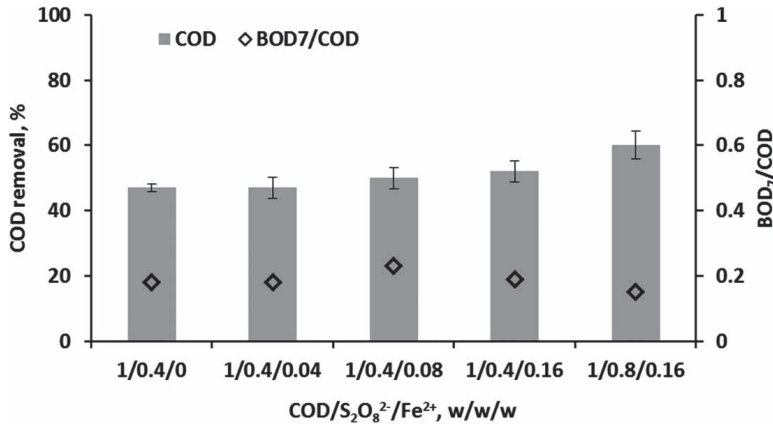
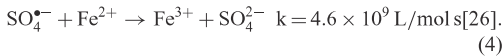


Figure 2. COD removal and the BOD₇/COD ratio as a function of the COD/S₂O₈²⁻/Fe²⁺ weight ratio in the persulphate treatment ([COD]₀ = 40 g/L).

by application of a higher persulphate concentration, resulting in a lower BOD₇/COD ratio after treatment at a COD/S₂O₈²⁻/Fe²⁺ w/w/w of 1/0.8/0.16. Only traces of S₂O₈²⁻ and more than 25% of unreacted S₂O₈²⁻ were detected in the treated wastewater after application of the activated and non-activated persulphate, respectively. The residual iron concentrations were lower than 2 mg/L in all the activated persulphate trials. Similar to the Fenton treatment experiments, at the beginning of the activated/non-activated persulphate oxidation without pH adjustment, a fast decrease in the pH of the reaction mixture was observed and resulted in the final pH values lower than 2.4 in all the trials. The adjustment of the pH to ~3 was assumed to improve the treatment efficacy due to ensured presence of the ferrous form of iron at the beginning of oxidation. However, the results exhibited negligible improvement in the COD, DOC and BOD₇ removal.

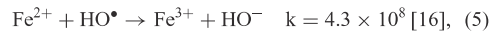
The lower treatment efficacy of the iron-activated persulphate compared to the Fenton process may be due to a lack of direct reduction of Fe³⁺ to Fe²⁺ by the oxidant, as given in Equation (2) for the Fenton systems. In addition, the sulphate radical also reacts with Fe²⁺ and rapidly converts it to Fe³⁺ via the process shown in Equation (4).



Therefore, the oxidation of Fe²⁺ to Fe³⁺ occurs not only during the generation of SO₄^{•-} but also in the conversion of SO₄^{•-} to SO₄²⁻. The newly generated SO₄^{•-} immediately reacts through a competitive reaction (Equations (3) and (4)) with the contaminant and excess Fe²⁺ resulting in a lower treatment efficiency. To control the reaction shown in Equation (4), the stepwise addition of S₂O₈²⁻, Fe²⁺ and S₂O₈²⁻/Fe²⁺ was studied (Figure 3 and Table 2). All the steps contained equal portions of the reagents that result in

the total amount of chemicals used. The results indicated a negligible additional COD removal as well as up to 4–6% of additional mineralization in all the systems. The BOD₇ removal in the stepwise addition systems was higher and resulted in lower biodegradability of the treated samples compared to the trial with all the reagents added at the same time.

The stepwise addition may also improve the Fenton treatment by controlling the HO• scavenging effect essential to systems with excess Fe²⁺ (Equation (5)) or H₂O₂ (Equation (6)). [15] Similar to the activated persulphate system, the optimization of the oxidation process was performed by stepwise addition of H₂O₂, Fe²⁺ and H₂O₂/Fe²⁺ Figure (3).



The wastewater treatment with H₂O₂ and H₂O₂/Fe²⁺ added in three steps with a COD/H₂O₂/Fe²⁺ w/w/w of 1/0.4/0.08 resulted in an additional 9% and 5% COD and DOC removal, respectively, along with an improvement in biodegradability of 10%. In addition, a considerable decrease in the increase in temperature (more than 40%) and foam formation (up to 50%) was observed during wastewater oxidation with the stepwise addition of reagents. The Fe²⁺ addition, which was divided into three steps, proved ineffective for improving the wastewater treatment efficacy, which is primarily due to the lower pH reduction at the very beginning of oxidation and scavenging of the HO• by the excess H₂O₂.

3.2. Acute toxicity and inhibition effect

The direct application of a conventional activated sludge treatment to the studied wastewater was limited due to

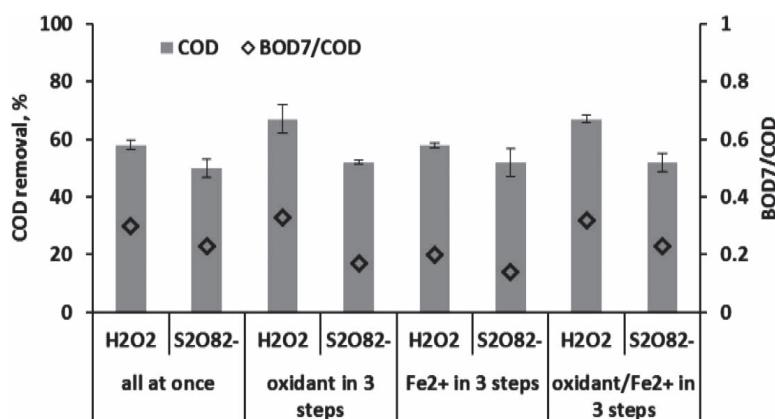


Figure 3. COD removal and the BOD₇/COD ratio as a function of the method of reagent addition at a COD/oxidant/Fe²⁺ weight ratio of 1/0.4/0.08 ([oxidant]₀ = 16 g/L, [Fe²⁺]₀ = 3.2 g/L) in the Fenton and activated persulphate treatments.

the high level of pollution and toxicity, as indicated in Table 1. To assess the options available for subsequent biological treatment of the chemically pre-treated wastewater, the acute toxicity to *D. magna* along with the inhibition of oxygen consumption by activated sludge and nitrification efficacy were evaluated.

The results of the acute toxicity to *D. magna*, which are shown in Table 3, indicated the relationship between the toxicity reductions in the Fenton pre-treated wastewater samples and the concentration of the applied reagents. Therefore, the extent of detoxification improved with an increase in H₂O₂/COD and decrease in H₂O₂/Fe²⁺ w/w ratio. Irrespective of the COD/S₂O₈²⁻/Fe²⁺ w/w/w applied, the toxicity reduction was similar in the treated samples and typically lower than in the Fenton pre-treated samples. The most feasible and reasonable treatment of the phenolic wastewater occurred with the Fenton treatment at a COD/H₂O₂/Fe²⁺ w/w/w of 1/0.4/0.08 (the stepwise Fenton reagent addition), which resulted in more than 67% COD removal, a BOD₇/COD ratio of 0.32, a moderate temperature increase and foam formation, and a more than 12-fold decrease in acute toxicity. The evaluation of inhibition of oxygen consumption by activated sludge and nitrification efficiency of this chemically pre-treated sample indicated 5-fold and 24-fold increase in IC₅₀, respectively.

Although the acute toxicity and inhibition effect was significantly reduced after the advanced chemical treatment, the treated wastewater remained rather toxic. Therefore, the application of a properly optimized Fe²⁺-activated hydrogen peroxide or persulphate can be recommended for practical use as an oxidation step prior to biological treatment of the effluent mixed with domestic/municipal wastewater by a conventional activated sludge system.

Table 3. Acute toxicity to *D. magna* (EC₅₀, %).

COD/oxidant/Fe ²⁺ , w/w/w [COD] ₀ = 40 g/L	EC ₅₀ , %	
	H ₂ O ₂	S ₂ O ₈ ²⁻
initial	0.34 ± 0.03	—
1/0.2/0.04	0.58 ± 0.05	—
1/0.4/0	—	0.51 ± 0.04
1/0.4/0.04	1.02 ± 0.1	1.32 ± 0.09
1/0.4/0.08	2.21 ± 0.2	0.97 ± 0.07
1/0.4/0.08, oxidant/ Fe ²⁺ in 3 steps	4.24 ± 0.3	1.14 ± 0.1
1/0.4/0.16	4.86 ± 0.48	1.12 ± 0.11
1/0.6/0.12	3.41 ± 0.33	—
1/0.8/0.16	4.83 ± 0.43	1.09 ± 0.09
1/1.2/0.24	5.93 ± 0.48	—

3.3. Evaluation of operational costs

To evaluate the economic feasibility of the H₂O₂/Fe²⁺ and S₂O₈²⁻/Fe²⁺ systems for high-strength wastewater treatment, the operational costs were calculated. The cost estimation and methodology were based on the calculations performed by Dulov et al.[15] The data obtained from the laboratory trials allowed for approximate calculations of the operating costs comprising only chemicals (H₂O₂, Na₂S₂O₈, FeSO₄·7H₂O and NaOH) used for the Fenton and ferrous ion-activated persulphate treatment. All of the calculations were performed in units per m³ of treated wastewater. The costs of H₂O₂ (50%), Na₂S₂O₈, FeSO₄·7H₂O and NaOH were estimated as 1, 2.2, 0.35 and 0.4 €/kg, respectively. Energy consumption in the studied advanced oxidation processes was not taken into consideration, as it would be small and highly dependent on the exact equipment used. Treatment cost estimates in €/m³ can be seen in Table 4.

Table 4. Operational costs of wastewater treatment at different COD/oxidant/Fe²⁺ weight ratios.

COD/oxidant/Fe ²⁺ , w/w/w [COD] ₀ = 40 g/L	H ₂ O ₂ (50%), kg/m ³	Na ₂ S ₂ O ₈ , kg/m ³	FeSO ₄ ·7H ₂ O, kg/m ³	NaOH ^a , kg/m ³	COD removal, %	Treatment cost, €/m ³
H ₂ O ₂						
1/0.2/0.04	16	–	7.94	1.4	43	19.34
1/0.4/0.08	32	–	15.89	2.5	58/67 ^b	38.56
1/0.6/0.12	48	–	23.83	6.5	72	58.94
1/0.8/0.16	64	–	31.77	8.1	74	78.36
1/1.2/0.24	96	–	47.66	12.2	78	117.56
S ₂ O ₈ ²⁻						
1/0.4/0	–	19.83	–	7.5	47	46.63
1/0.4/0.08	–	19.83	15.89	5.1	50/52 ^b	51.23
1/0.8/0.16	–	39.67	31.77	11.3	60	102.91

^aFor pH adjustment to ~8.5.

^bOxidant/Fe²⁺ addition in three steps.

The results indicate that the Fenton treatment proved to be more efficient in terms of both treatment efficacy and cost than the ferrous ion-activated persulphate process. Accordingly, the application of a COD/oxidant/Fe²⁺ w/w/w of 1/0.4/0.08 with the stepwise reagents addition resulted in a COD removal of 67% and treatment cost of 38.6 €/m³ for the Fenton treatment compared to respective 52% and 51.2 €/m³ for the activated persulphate process. Moreover, the operating costs of the Fenton treatment could be substantially reduced by reuse of iron-containing sludge as a coagulant for influent pre-treatment prior to the Fenton process, resulting in up to 50% reduction in the required coagulant [27] or as an effective activator for the Fenton-based process.[28]

4. Conclusions

The result of this study indicated the feasibility of both activated oxidants to reduce the organic load and acute toxicity as well as to improve the biodegradability of the heavily contaminated industrial wastewater. In general, the Fenton process demonstrated a higher treatment efficacy and lower treatment cost than the Fe²⁺-activated persulphate system. Thus, the application of H₂O₂/Fe²⁺ and S₂O₈²⁻/Fe²⁺ processes at a COD/oxidant/Fe²⁺ w/w/w of 1/0.4/0.08 resulted in a COD removal of 58% and 50%, DOC removal of 29% and 24%, and treatment cost of 38.6 and 51.2 €/m³, respectively. Conversely, the Fenton process was characterized by a temperature increase and excessive foam formation. As a result, the persulphate proved to be a feasible alternative oxidant due to the reasonable treatment conditions and sustainable treatment of the wastewater. The presence of ferrous ions for the activation of persulphate improved the mineralization of the organic contaminant and toxicity reduction but resulted in similar to non-activated persulphate efficacy in COD removal and biodegradability. The stepwise addition of the reagents was favourable for the Fenton treatment of highly loaded wastewater. In general, the application of advanced chemical pre-treatment proved

to be an effective option that improved the overall wastewater quality and increased the possibility of subsequent biological treatment of the effluent, preferably diluted by less polluted domestic/municipal wastewater. The results of this study are unique and may provide important insights for further implementation in treatment of heavily contaminated industrial wastewaters and complex oil-in-water emulsions.

Acknowledgments

The authors thank Mr. Alar Saluste for his assistance in the sample collection and Ms. Piret Mäestu for her assistance with the experiments.

Disclosure statement

No potential conflict of interest was reported by the authors.

Funding

This research was supported by institutional research funding IUT (1–7) of the Estonian Ministry of Education and Research and the European Union through the European Regional Development Fund project CHEMBIO (code 3.2.0802.11–0043).

References

- [1] Klavarioti M, Mantzavinos D, Kassinos D. Removal of residual pharmaceuticals from aqueous systems by advanced oxidation processes. *Environ Intern.* 2009;35:402–417.
- [2] Dulova N, Trapido M. Application of Fenton's reaction for food-processing wastewater treatment. *J Adv Oxid Technol.* 2011;14:9–16.
- [3] Martins RC, Silva AMT, Castro-Silva S, Garção-Nunes P, Quinta-Ferreira RM. Advanced oxidation processes for treatment of effluents from a detergent industry. *Environ Technol.* 2011;32:1031–1041.
- [4] Oller I, Malato S, Sánchez-Pérez JA. Combination of advanced oxidation processes and biological treatments for wastewater decontamination – A review. *Sci Total Environ.* 2011;409:4141–4166.
- [5] Wang JL, Xu LJ. Advanced oxidation processes for wastewater treatment: formation of hydroxyl radical and

- application. *Crit Rev Environ Sci Technol.* 2012;42:251–325.
- [6] Dulov A, Dulova N, Trapido M. Photochemical degradation of nonylphenol in aqueous solution: the impact of pH and hydroxyl radical promoters. *J Environ Sci.* 2013;25:1326–1330.
- [7] Chen W-S, Su Y-C. Removal of dinitrotoluenes in wastewater by sono-activated persulfate, *Ultrason. Sonochem.* 2012;19:921–927.
- [8] Hussain I, Zhang Y, Huang S, Du X. Degradation of *p*-chloroaniline by persulfate activated with zero-valent iron. *Chem Eng J.* 2012;203:269–276.
- [9] Fang G-D, Dionysiou DD, Zhou D-M, et al. Transformation of polychlorinated biphenyls by persulfate at ambient temperature. *Chemosphere.* 2013;90:1573–1580.
- [10] Nachiappan S, Muthukumar K. Treatment of pharmaceutical effluent by ultrasound coupled with dual oxidant system. *Environ Technol.* 2013;34:209–217.
- [11] Moussa MA, Serge C. Solar photo-Fenton-like using persulfate for carbamazepine removal from domestic wastewater. *Water Res.* 2014;48:229–236.
- [12] Tsitonaki A, Petri B, Crimi M, Mosbaek H, Siegrist RL, Bjerg PL. In situ chemical oxidation of contaminated soil and groundwater using persulfate: A review. *Crit Rev Environ Sci Technol.* 2010;40:55–91.
- [13] Neta P, Madhavan V, Zemel H, Fessenden RW. Rate constants and mechanisms of reaction of $\text{SO}_4^{\bullet-}$ with aromatic compounds. *J Am Chem Soc.* 1977;99:163–164.
- [14] Bautista P, Mohedano AF, Casas JA, Zazo JA, Rodriguez JJ. An overview of the application of Fenton oxidation to industrial wastewaters treatment. *J Chem Technol Biotechnol.* 2008;83:1323–1338.
- [15] Dulov A, Dulova N, Trapido M. Combined physicochemical treatment of textile and mixed industrial wastewater. *Ozone Sci Eng.* 2011;33:285–293.
- [16] Chen R, Pignatello JJ. Role of quinone intermediates as electron shuttles in Fenton and photoassisted Fenton oxidations of aromatic compounds. *Environ Sci Technol.* 1997;31:2399–2406.
- [17] Travina OA, Kozlov YN, Purmal AP, Rodko IY. Synergism of the action of the sulfite oxidation initiators, iron and peroxydisulfate ions. *Russ J Phys Chem.* 1999;73:1215–1219.
- [18] APHA (American Public Health Association). Standard methods for the examination of water and wastewater. 22nd ed. Washington, DC: American Water Works Association, Water Environment Federation; 2012.
- [19] Kang YW, Cho M-J, Hwang K-Y. Correction of hydrogen peroxide interference on standard chemical oxygen demand test. *Water Res.* 1999;33:1247–1251.
- [20] Eisenberg GM. Colorimetric determination of hydrogen peroxide. *Ind Eng Chem Anal Ed.* 1943;15:327–328.
- [21] Sofina NA, Beklemishev MK, Kapanadze AL, Dolmanova IF. Sorption-catalytic method for the chromium determination. *Moscow Univ Chem Bull.* 2003;44:189–198 (in Russian).
- [22] ISO 6439. Water Quality – Determination of Phenol Index – 4-Aminoantipyrine Spectrometric Methods after Distillation. Geneva: International Organization for Standardization; 1990.
- [23] ISO 6341. Water Quality – Determination of the Inhibition of the Mobility of *Daphnia Magna* Straus (Cladocera, Crustacea) – Acute Toxicity Test. Geneva: International Organization for Standardization; 1996.
- [24] ISO 8192. Water Quality – Test for Inhibition of Oxygen Consumption by Activated Sludge for Carbonaceous and Ammonium Oxidation. Geneva: International Organization for Standardization; 2007.
- [25] ISO 9509. Water Quality – Method for Assessing the Inhibition of Nitrification of Activated Sludge Micro-organisms by Chemicals and Waste Waters. Geneva: International Organization for Standardization; 1989.
- [26] Buxton GV, Malone TN, Salmon GA. Reaction of $\text{SO}_4^{\bullet-}$ with Fe^{2+} , Mn^{2+} and Cu^{2+} in aqueous solution. *J Chem Soc Faraday Trans.* 1997;93:2893–2897.
- [27] Yoo H-C, Cho S-H, Ko S-O. Modification of coagulation and Fenton oxidation processes for cost-effective leachate treatment. *J Environ Sci Health A Tox Hazard Subst Environ Eng.* 2001;36:39–48.
- [28] Bolobajev J, Kattel E, Viisimaa M, et al. Reuse of ferric sludge as an iron source for the Fenton-based process in wastewater treatment. *Chem Eng J.* 2014;255:8–13.

PAPER II

Kattel, E., Dulova, N. Ferrous ion-activated persulphate process for landfill leachate treatment: removal of organic load, phenolic micropollutants and nitrogen. – *Environmental Technology*, 2017, 38 (10), 1223–1231.

Reproduced with the permission of Taylor & Francis.



Ferrous ion-activated persulphate process for landfill leachate treatment: removal of organic load, phenolic micropollutants and nitrogen

Eneliis Kattel and Niina Dulova

Department of Chemical Engineering, Tallinn University of Technology, Ehitajate tee 5, Tallinn, Estonia

ABSTRACT

The innovative $S_2O_8^{2-}/Fe^{2+}$ treatment technology based on sulphate radicals induced oxidation was applied for the treatment of landfill leachate. The performance of chemical oxygen demand (COD) and dissolved organic carbon (DOC) removal in the Fe^{2+} -activated persulphate system was moderate; however, the results of dissolved nitrogen (DN) and total phenols removal showed significant efficacy ($\leq 39\%$ and $\geq 87\%$, respectively). $S_2O_3^{2-}$ addition to the $S_2O_8^{2-}/Fe^{2+}$ system enhanced the treatment efficacy and resulted in supplementary 15% of COD and 5% of DN removal. Hydroxyl radical-based H_2O_2/Fe^{2+} treatment of the landfill leachate was performed as well; the results indicated higher removal efficacy of COD and DOC compared to the $S_2O_8^{2-}/Fe^{2+}$ system. However, practical application of the H_2O_2/Fe^{2+} system is considerably influenced by temperature rise and excessive foam formation. Generally, the ferrous ion-activated persulphate treatment could be a promising technology for *ex situ* as well as *in situ* landfill leachate treatment applications.

ARTICLE HISTORY

Received 15 October 2015
Accepted 2 August 2016

KEYWORDS

Activated persulphate;
Fenton process; landfill
leachate; sulphate radical;
reducing agent

1. Introduction

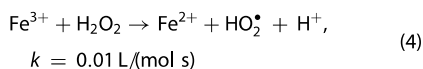
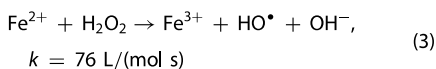
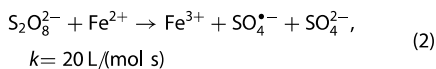
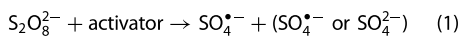
Municipal waste landfill leachate is a serious environmental concern as it contains diverse classes of pollutants, and the leachate from different solid wastes has different deposition period and moisture content.[1] In general, it is composed of dissolved organic matter, inorganic macrocomponents (mainly ammoniacal nitrogen in high concentrations), heavy metals, xenobiotic organic compounds and emerging micropollutants such as phenolic substances.[1] Thus, due to the hazardous nature of the leachate, there is a requirement for its appropriate collection and subsequent purification to prevent potential unwanted exposure to soil and groundwater. The treatment and post-treatment methods for landfill leachate can be classified into biological, chemical and physical. These methods can be applied individually or in combinations depending on the pollution strength.[2–5] The biological treatment of leachate in anaerobic or aerobic sludge reactors has proved to be a favourable method due to its simple and low cost of application. However, a high content of organic matter recalcitrant to biological degradation can hinder the effective application of this technique to mature landfill leachate.[2] Thus, a method or a sequence of methods for landfill leachate treatment despite stabilisation time or organic load strength has

a discernible advantage. For example, a combination of biological and physical or chemical processes, such as coagulation-flocculation, adsorption, flotation and chemical treatment (oxidation), has shown adequate results in the removal of refractory organics.[6–8]

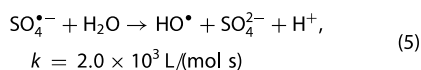
Chemical treatment methods, which include processes such as ozonation, electrochemical oxidation and different hydroxyl radical-based advanced oxidation technologies (HO^\bullet -AOTs), have been widely studied.[9–11] Among HO^\bullet -AOTs, the Fenton process has been proved to be effective for organic load removal and micropollutants decomposition in wastewater and landfill leachate.[12–16] The efficacy of this process results from the highly reactive hydroxyl radicals (HO^\bullet ; $E^0 = 2.70$ V[17]) formed from a combination of hydrogen peroxide and ferrous iron salts under strong acidic conditions.[17] The final rate of refractory organic matter reduction depends on the pH of the wastewater or landfill leachate, strength of contamination, activator and oxidant doses, and oxidation duration.[18] Conversely, similar to other HO^\bullet -AOTs, the Fenton treatment removes organic load effectively, but it is ineffective for the removal of ammoniacal nitrogen,[13,19,20] which is also one of the main municipal waste landfill leachate pollutants. Moravia et al. [21] suggested that the Fenton process in combination with the membrane

separation systems could increase the efficacy of landfill leachate treatment. Improvement in all the main parameters of the leachate was observed, except the content of ammonia.[21] Therefore, it is necessary to develop a new method for landfill leachate treatment that is practicable not only in the decomposition of organic compounds, but also in nitrogen removal. Recent applications of the activated persulphate treatment have shown promising results in both organic load and ammoniacal nitrogen removal from landfill leachate.[22,23] In addition, sulphate ions formed from the decomposition of persulphate have a harmless effect on the environment, and the elimination of biological treatment inhibitor, ammonia, predisposes subsequent biodegradation as post-treatment.

Persulphate is a novel oxidant used mainly for *in situ* groundwater and soil treatment.[24,25] The activation of persulphate ($S_2O_8^{2-}$, $E^0 = 2.01$ V[26]) by pH increase, heat, UV light, ultrasound, ozone, peroxide or transition metals (Equation 1) generates more powerful sulphate radicals ($SO_4^{\bullet-}$; $E^0 = 2.60$ V[26]).[26–29] In practical applications, mainly ferrous iron is used as persulphate activator in terms of its activating properties of $S_2O_8^{2-}$, environmental-friendly nature and cost-effectiveness. The main advantage of the $S_2O_8^{2-}/Fe^{2+}$ system (Equation 2) compared to the H_2O_2/Fe^{2+} system (Equations 3 and 4) is the relative stability of the formed $SO_4^{\bullet-}$. The oxidation of target contaminants, especially aromatic constituents or compounds with an unsaturated bond, is more selective.[24,30] In addition, the transition metal activation of persulphate generates and scavenges sulphate radicals since the excess of the activator reacts with the formed $SO_4^{\bullet-}$. [17,24]



The presence of $SO_4^{\bullet-}$ in the solution can initiate HO^{\bullet} generation by its interconversion according to Equation (5) [24,31]:



Therefore, the occurrence of both $SO_4^{\bullet-}$ and HO^{\bullet} in the $S_2O_8^{2-}/Fe^{2+}$ system indicates its potential to increase the contaminant degradation rate and the possibility to

destruct various organic and inorganic compounds.[31] Several studies have demonstrated the ability of $SO_4^{\bullet-}$ -AOTs to degrade a broad array of organic pollutants [16, 23] and micropollutants.[32] Romero et al. [27] successfully proved that activated persulphate appears to be an effective oxidising agent for the degradation of diuron, an herbicide found in surface water and effluents from wastewater treatment plants. Furthermore, Fe^{2+} -activated persulphate was applied to remove antibiotics as emerging micropollutants from water and groundwater.[32]

The main objective of this study was to evaluate the efficacy of the $S_2O_8^{2-}/Fe^{2+}$ system in the simultaneous removal of organic load, nitrogen and phenolic substances from landfill leachate and compare it with the performance of the H_2O_2/Fe^{2+} treatment. Nitrogen removal was observed as the elimination of dissolved nitrogen (DN), which comprised ammoniacal nitrogen, nitrate and nitrite. In general, the application of Fe^{2+} -activated persulphate and hydrogen peroxide has been studied for the degradation of different classes of organic contaminants in various aqueous matrixes. However, data on the use of the former processes for treating real wastewater samples have not been fully evaluated. Moreover, as ferrous ion-activated persulphate has been successfully used in *in situ* soil and groundwater remediation,[22,25,32] the results of this study could provide fundamental support for landfill leachate *in situ* treatment, given the risk of leachate leakage to soil. To the authors' best knowledge, this is the first study on the application of ferrous iron-activated persulphate in landfill leachate treatment.

2. Experimental protocols

2.1 Leachate characteristics and chemicals

Two leachate samples were obtained from a municipal non-hazardous waste landfill (Rebala village, Jõelähtme Parish, Harjumaa, Estonia), which has been operated over 10 years. The produced leachate rate varies in seasons and is 500–2500 m³ per month. The samples were collected manually in June and November 2014 and placed in 5 L containers. The samples were transported to the laboratory, and the initial parameters were measured. Then, the samples were stored at 4°C. The leachate samples were collected and stored according to the Standard Methods for the Examination of Water and Wastewater.[33] The main properties of the leachate samples used in this work are presented in Table 1. Irrespective of the different seasons when the

Table 1. Chemical composition and main properties of leachate samples.

Parameter	Unit	Leachate 1 (L1, June 2014)	Leachate 2 (L2, November 2014)
COD	mg/L	9700 ± 381	21,153 ± 877
BOD ₇	mg/L	2480 ± 122	9428 ± 381
BOD ₇ /COD		0.26	0.45
DOC	mg/L	2740 ± 11	6185 ± 175
DN	mg/L	1760 ± 18	1920 ± 10
TPh	mg/L	24 ± 1	87
Conductivity	µS/cm	22.1	15.8
pH	–	7.84	7.03
TS (105°C)	mg/L	13,973 ± 4	n/a ^a
TFS (600°C)	mg/L	9437 ± 16	17,031 ± 32
TSS (105°C)	mg/L	3370 ± 160	9593 ± 38
Alkalinity	mgCaCO ₃ /L	9520 ± 80	8500 ± 375

^a n/a – not analysed.

samples were taken, the leachate samples contained high concentrations of organics and DN.

Hydrogen peroxide (PERDROGEN™, ≥30%), sodium persulphate (Na₂S₂O₈, ≥99%), ferrous sulphate heptahydrate (FeSO₄·7H₂O, ≥99%) and sodium thiosulphate pentahydrate (Na₂S₂O₃·5H₂O, ≥99.5%) were purchased from Sigma–Aldrich Co. (U.S.A.). All the other chemicals were of analytical grade and used without further purification. Stock solutions were prepared in ultrapure water (Millipore Simplicity® UV System, Merck, Germany). Sulphuric acid and sodium hydroxide aqueous solutions were used to adjust the pH.

2.2 Chemical treatment

Fe²⁺-activated persulphate and hydrogen peroxide treatments were conducted in a batch mode and non-buffered solutions. Leachate samples of 0.5 L were treated in a 1 L cylindrical glass reactor with permanent magnetic stirring (400 rpm) for 1, 2, 4, 6 or 24 h (oxidation period). The pH of the wastewater samples was adjusted to 3 with H₂SO₄ (98 wt%) in the subsequent treatment, if not specified otherwise. The activator (FeSO₄·7H₂O) was added, and after its complete dissolution, the reaction was initiated by adding Na₂S₂O₈ or H₂O₂. The oxidant dose was determined as the S₂O₈²⁻/chemical oxygen demand (COD) or H₂O₂/COD molar ratio (m/m). The equivalent weight ratio of S₂O₈²⁻ and H₂O₂ to O₂ is 12 and 2.125, respectively. Thus, to indicate the S₂O₈²⁻ and H₂O₂ dose, the weight ratio of S₂O₈²⁻/12COD and H₂O₂/2.125COD, respectively, was used in this study. Accordingly, at the S₂O₈²⁻/12COD and H₂O₂/2.125COD weight ratios of 1, the S₂O₈²⁻/COD and H₂O₂/COD molar ratios are 1/1. The H₂O₂/Fe²⁺ m/m of 10/1 was considered optimal [34]; the S₂O₈²⁻/Fe²⁺ m/m varied in the range of 1/1–50/1. In the case of the S₂O₈²⁻/Fe²⁺/S₂O₃²⁻ systems, the reductant (S₂O₃²⁻/Fe²⁺ m/m of 0.1/1–1/1) was added

simultaneously with Na₂S₂O₈. Next, the coagulation step of ferric hydroxy complexes for 19–24 h was initiated by the addition of NaOH (10 M) to adjust the pH to 8.5. Finally, the unfiltered supernatant was collected for further analysis. The wastewater oxidation experiments with non-activated persulphate and hydrogen peroxide were conducted in identical reactors under respective activated oxidant treatment conditions.

All the experiments were duplicated, and data of the initial parameters of the leachate samples were verified with at least three replicates. The results of the analyses are presented as the mean with a standard deviation of at least three parallel replicates. The experiments were performed at an ambient room temperature (21 ± 1°C).

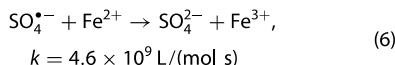
2.3 Analytical methods

COD was determined with a closed reflux colorimetric method.[33] Correction for hydrogen peroxide interference on the COD test was performed by the correlation equation, as described previously in Dulov et al. [35]. A seven-day biochemical oxygen demand (BOD₇), total suspended solids (TSS), total solids (TS), total fixed solids (TFS) and alkalinity were determined according to American Public Health Association.[33] pH was measured using a digital pH/Ion meter (Mettler Toledo S220, Switzerland), and electrical conductivity was measured using a digital EC meter (HQ 430d flexi, HACH Company, U.S.A.). The residual persulphate concentration in the treated samples was measured spectrophotometrically at λ = 446 nm with *o*-dianisidine by an *o*-dianisidine–peroxydisulphate complex formation (GENESYS 10S UV/Vis, Thermo Scientific, U.S.A).[36] The initial hydrogen peroxide concentration in the stock solutions was measured spectrophotometrically at λ = 254 nm. The residual hydrogen peroxide concentration in the treated samples was measured spectrophotometrically at λ = 410 nm with titanium sulphate by a hydrogen peroxide–Ti⁴⁺ complex formation.[37] The total iron concentration in the solution was measured at λ = 492 nm with a spectrophotometer (GENESYS 10S UV/Vis, Thermo Scientific, U.S.A) by using the *o*-phenanthroline method.[33] The concentration of total phenols (TPh, sum of mono- and diphenols) was measured by the 4-aminoantipyrine method using the HACH-Lange cuvette test LCK 345. Dissolved organic carbon (DOC) and DN were measured in filtered (Puradisc Aqua, 0.45 µm, CA, Whatman®, GE Healthcare, U.K) leachate samples by the TOC analyser Multi N/C® 3100 (Analytik Jena, Germany). Measurements of all studied parameters were performed immediately after the supernatant decantation.

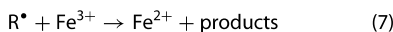
3. Results and discussion

3.1 Effect of the activator concentration

The role of ferrous iron as an initiator and its amount in the $S_2O_8^{2-}/Fe^{2+}$ system is important because it can act as a scavenger of $SO_4^{\bullet-}$ and advance Fe^{3+} and SO_4^{2-} formation (Equation 6) [27]:



Fe^{3+} does not activate persulphate decomposition, [38] and thus, the oxidation of target compounds is inhibited. Conversely, since Fe^{2+} activation occurs fast, other oxidative species might be present in the $S_2O_8^{2-}/Fe^{2+}$ system to generate $SO_4^{\bullet-}$. Wu et al. [38] indicated the simultaneous existence of the reactive oxygen species, $SO_4^{\bullet-}$ and HO^{\bullet} , in the $S_2O_8^{2-}/Fe^{2+}$ system at acidic/near to acidic pH values; the latter could promote continuous Fe^{3+} reduction. In addition, organic radicals (Equation (7)) can reduce ferric ions:



Five different $[Fe^{2+}]_0$, that is, 3, 6, 15, 30 and 150 mM with $[S_2O_8^{2-}]_0 = 150 \text{ mM}$ ($S_2O_8^{2-}/COD$ m/m of 0.25/1), were applied, corresponding to 50/1, 25/1, 10/1, 5/1 and 1/1 m/m of $S_2O_8^{2-}/Fe^{2+}$, respectively, to investigate the effect of activator initial concentration on landfill leachate treatment. Oxidant dose was selected towards efficient organic load reduction and maximum utilisation of persulphate in the treatment with a 24-h oxidation period; the perspective of cost-effectiveness was also taken into consideration. To find an optimal ferrous iron concentration, experiments were conducted on L1; L2 was treated with no additional activator dose variation. However, the control experiments with an optimal amount of activation reagent were carried out to analyse the COD impact as an organic substance concentration effect. The results demonstrated that the COD and DOC removal increased in conjunction with the increasing activator dose, from 13% ($[Fe^{2+}]_0 = 3 \text{ mM}$) to 37% ($[Fe^{2+}]_0 = 150 \text{ mM}$) and 13% ($[Fe^{2+}]_0 = 3 \text{ mM}$) to 34% ($[Fe^{2+}]_0 = 150 \text{ mM}$), respectively (Figure 1). A further increase in activator dose was not studied due to the ultimately increasing amount of residual ferric waste along with the cost of the treatment process.

The residual concentration of persulphate remained at around 47–58% of $[S_2O_8^{2-}]_0$ added in the $S_2O_8^{2-}/Fe^{2+}$ system with $[Fe^{2+}]_0$ from 3 to 30 mM. The residual oxidant content was 9% from initial only at the highest activator dose used ($[Fe^{2+}]_0 = 150 \text{ mM}$). The reduction in TPh concentration after the treatment at all studied conditions was $\geq 90\%$. The BOD_7 removal

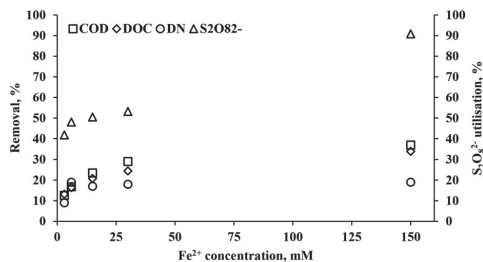


Figure 1. COD, DOC and DN removal and $S_2O_8^{2-}$ utilisation versus Fe^{2+} concentration by the Fe^{2+} -activated persulphate treatment of sample L1 ($[S_2O_8^{2-}]_0 = 150 \text{ mM}$; 24-h oxidation period).

was around 30% at all activator doses used. At the lowest ferrous iron concentration of 3 mM, the reduction in DN was 9%; conversely, a further increase in the activator dose up to 150 mM resulted in 19% of DN removal.

The results of sample L2 treatment at a $S_2O_8^{2-}/COD$ m/m of 0.25/1 ($[S_2O_8^{2-}]_0 = 330 \text{ mM}$) and $S_2O_8^{2-}/Fe^{2+}$ m/m of 5/1 ($[Fe^{2+}]_0 = 66 \text{ mM}$) with a 24-h oxidation period showed similar COD (30%) and DOC (24%) reduction as with sample L1. In addition, the removal of TPh and DN was 95% and 29%, respectively. Conversely, the amount of persulphate utilised was lower and comprised 32% from the initial concentration as compared to 53% observed in the case of sample L1. The latter observation could be explained by the differences in the chemical composition of the studied samples (Table 1), which most likely lead to variations in the readily available ferrous activator concentration during the ferrous ion-activated persulphate oxidation. Nevertheless, similar results obtained with L1 and L2 treatments indicate that the Fe^{2+} -activated persulphate process is suitable for a high-organic load and phenolic micropollutants removal in landfill leachate.

3.2 Effect of the oxidant concentration

The mechanism of the ferrous ion-activated persulphate process is similar to that of the Fenton process; however, different reactions are involved in the processes according to Equations (2) and (4). The Fe^{3+} that is formed in Equation (2) is more stable in the $S_2O_8^{2-}/Fe^{2+}$ system as compared to the H_2O_2/Fe^{2+} system, where Fe^{3+} is readily reduced to Fe^{2+} ; as a result, the subsequent activation of $S_2O_8^{2-}$ is inhibited.[39] Furthermore, the pH of the activated oxidative systems has an important effect on the target compounds' degradation. Kusic et al. [40] reported that the $S_2O_8^{2-}/Fe^{2+}$ system has an advantage over the H_2O_2/Fe^{2+} system due to a wider range of initial pH. However, the pH of the system is influenced by the formation of H^+ in the $S_2O_8^{2-}/Fe^{2+}$ system

according to Equation (5), resulting in a rapid decrease in the pH of the reaction mixture. Additionally, Romero et al. [27] found that diuron degradation by the Fe^{2+} -activated persulphate process was more efficient at acidic pH values ($\text{pH} \leq 3$). Thus, in this study, the pH value of the initial leachate sample was adjusted to 3 in both $\text{H}_2\text{O}_2/\text{Fe}^{2+}$ and $\text{S}_2\text{O}_8^{2-}/\text{Fe}^{2+}$ systems in order to provide the activator in its reduced state as Fe^{2+} and facilitate the comparison of the considered AOTs. Besides, Fe^{2+} activation of $\text{S}_2\text{O}_8^{2-}$ at acidic conditions was considered as more preferable because iron precipitates as ferric hydroxy complexes at $\text{pH} > 4$. [41] The effect of different oxidant doses was studied to optimise the ferrous iron-activated persulphate oxidation. Accordingly, the $\text{S}_2\text{O}_8^{2-}/\text{Fe}^{2+}$ m/m was 10/1 ($[\text{Fe}^{2+}]_0$ 6–60 mM), while the m/m of $\text{S}_2\text{O}_8^{2-}/\text{COD}$ varied from 0.1/1 to 1/1, corresponding to $[\text{S}_2\text{O}_8^{2-}]_0$ 60–600 mM, respectively. At all examined concentrations, COD, DOC and DN removal increased with the increase in the persulphate dose as presented in Figure 2. A 10-fold oxidant concentration increase from 60 to 600 mM resulted almost in a twofold rise in the COD removal efficacy, that is, from 19% to 36%. The mineralisation extent, given as DOC, was up to 1–3% higher, reaching its maximum (36%) at the highest oxidant concentration of 600 mM. The residual concentration of persulphate was 45–77% of $[\text{S}_2\text{O}_8^{2-}]_0 = 60 - 600$ mM.

At the lowest studied oxidant concentration, $[\text{S}_2\text{O}_8^{2-}]_0 = 60$ mM, the reduction of DN was modest and comprised only 8%; conversely, a fivefold higher removal of DN (39%) at a $[\text{S}_2\text{O}_8^{2-}]_0$ of 600 mM was achieved. The BOD_7 removal tended to increase simultaneously with the oxidant dose with a maximum removal rate of 46% at a $[\text{S}_2\text{O}_8^{2-}]_0$ of 600 mM, corresponding to 1/1 m/m of $\text{S}_2\text{O}_8^{2-}/\text{COD}$. The content of phenolic micropollutants was also measured; at least 87% of the initial concentration of 24 g/L was eliminated after different persulphate concentrations were applied.

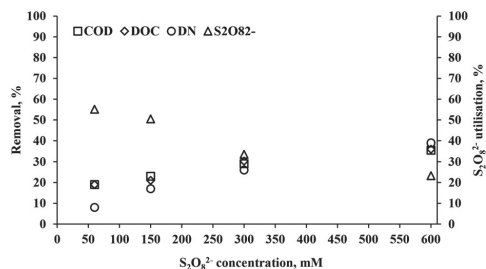


Figure 2. COD, DOC and DN removal and $\text{S}_2\text{O}_8^{2-}$ utilisation versus $\text{S}_2\text{O}_8^{2-}$ concentration by the Fe^{2+} -activated persulphate treatment of sample L1 ($[\text{Fe}^{2+}]_0 = 6-60$ mM at a fixed $\text{S}_2\text{O}_8^{2-}/\text{Fe}^{2+}$ molar ratio of 10/1; 24-h oxidation period).

In this study, the Fenton treatment of landfill leachate was carried out with the goal of comparison. In general, the mechanisms of the activated persulphate oxidation, as well as the application of this process for aqueous matrices treatment, are scarcely studied as compared to the published literature on the Fenton system. Thus, in the case of landfill leachate samples, the optimal treatment conditions for the Fenton process are reported in several studies. [12,14,34]

Similar to the $\text{S}_2\text{O}_8^{2-}/\text{Fe}^{2+}$ system, the effect of oxidant dose in the $\text{H}_2\text{O}_2/\text{Fe}^{2+}$ system was evaluated (sample L1, 24-h oxidation period) as shown in Figure 3. The obtained results indicated that at a $\text{H}_2\text{O}_2/\text{COD}$ m/m of 0.1/1 ($[\text{H}_2\text{O}_2]_0 = 60$ mM), removal of the organic load was 35%, which is similar (36%) to the $\text{S}_2\text{O}_8^{2-}/\text{Fe}^{2+}$ system at a $\text{S}_2\text{O}_8^{2-}/\text{COD}$ m/m of 1/1 ($[\text{S}_2\text{O}_8^{2-}]_0 = 600$ mM). The COD and DOC removal increased by 31% and 39%, respectively, according to the increase in the H_2O_2 concentration from 60 mM to 600 mM. At the latter dose, the removal was 66% and 60%, respectively. Notably, the utilisation of H_2O_2 was complete at all oxidant concentrations studied.

According to Deng and Ezyske's [22] study, the thermal persulphate oxidation of landfill leachate showed the effective removal of the ammoniacal nitrogen; the COD removal remained moderate in comparison with the Fenton process. The DN removal in the current study similarly showed promising results for the $\text{S}_2\text{O}_8^{2-}/\text{Fe}^{2+}$ system (Figures 2 and 3). The DN removal after the Fenton treatment at a $[\text{H}_2\text{O}_2]_0$ of 60 and 600 mM was 2.5% and 19%, respectively. In comparison, the Fe^{2+} -activated persulphate treatment showed 2–3 times higher removal efficacy at the same oxidant doses. Considerably higher efficacy of the DN removal by the ferrous ion-activated persulphate treatment favours the application of a biological post-treatment to achieve additional removal in COD, if necessary. The DN removal by the $\text{SO}_4^{\bullet-}$ -based system is initiated by

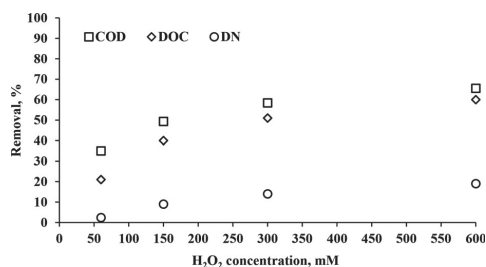


Figure 3. COD, DOC and DN removal versus H_2O_2 concentration by the Fenton treatment of sample L1 ($[\text{Fe}^{2+}]_0 = 6-60$ mM at a fixed $\text{H}_2\text{O}_2/\text{Fe}^{2+}$ molar ratio of 10/1; 24-h oxidation period).

the ammonia and ammonium nitrogen (reductive ammoniacal nitrogen) that donate electrons to $\text{SO}_4^{\cdot-}$, and thereby, the nitrogen is oxidised to a higher valence state, like N_2 . [22] On the other hand, HO^\bullet practically cannot oxidise ammoniacal nitrogen [13]; this explains the advantageous application of $\text{SO}_4^{\cdot-}$ -AOT over HO^\bullet -AOT for the DN removal.

In the case of the phenolic micropollutants content reduction, the application of the Fenton process at a $[\text{H}_2\text{O}_2]_0$ of 60 mM resulted in 60%; a further increase in oxidant dose up to a $[\text{H}_2\text{O}_2]_0$ of 300 mM resulted in over 90% of TPh elimination.

During the sample L1 treatment by the $\text{S}_2\text{O}_8^{2-}/\text{Fe}^{2+}$ and $\text{H}_2\text{O}_2/\text{Fe}^{2+}$ systems, the changes in temperature were measured as well. The results of the Fenton treatment at a $[\text{H}_2\text{O}_2]_0$ of 600 mM indicated a 12°C increase in temperature (initial sample temperature was 21°C). On the contrary, the application of Fe^{2+} -activated persulphate process at the same oxidant concentration of 600 mM proved to have a negligible exothermic effect. Furthermore, the production of excessive foam caused by CO_2 and O_2 evolution as a result of H_2O_2 decomposition was observed in the Fenton treatment trials.

Blank experiments with non-activated persulphate at a $[\text{S}_2\text{O}_8^{2-}]_0$ of 150 and 300 mM (pH 3, 24-h oxidation period) were also performed. The treatment of L1 resulted in 6–11% of COD, 3–10% of DOC, 11–20% of DN and 79–86% of TPh removal. In the application of the non-activated persulphate treatment ($[\text{S}_2\text{O}_8^{2-}]_0 = 150$ mM) on L2, a considerable removal of COD (20%) and less-effective DOC (8%) and DN (13%) elimination were observed. Therefore, the activation of persulphate proved essential in improving the removal of total organic load, specific phenolic micropollutants and nitrogen compounds during the landfill leachate treatment.

The comparison of the two Fe^{2+} -activated radical-based AOTs verified that the Fenton process is more efficient for organic load removal from landfill leachate. Conversely, the nitrogen content and the phenolic micropollutants abatement were significantly higher by the $\text{S}_2\text{O}_8^{2-}/\text{Fe}^{2+}$ than by the $\text{H}_2\text{O}_2/\text{Fe}^{2+}$ system. In addition, the $\text{S}_2\text{O}_8^{2-}/\text{Fe}^{2+}$ process has no restrictions by temperature rise or excessive foam formation. Thus, the application of Fe^{2+} -activated persulphate treatment is suitable as a wastewater pretreatment step for subsequent biological treatment.

3.3. Effect of the oxidation time

The removal of organic contaminants by the Fe^{2+} -activated persulphate oxidation is known to be a more time-consuming process as compared to the Fenton

oxidation.[27] Thus, experiments with an oxidation time of 1, 2, 4, 6 and 24 h were performed to find out the effect of the oxidation time on the removal of organic and inorganic contaminants from the landfill leachate. Notably, the duration of the coagulation step of ferric hydroxy complexes in all the trials was ~22 h. The reagent concentrations for the $\text{S}_2\text{O}_8^{2-}/\text{Fe}^{2+}$ system were $[\text{S}_2\text{O}_8^{2-}]_0 = 330$ mM ($\text{S}_2\text{O}_8^{2-}/\text{COD}$ m/m of 0.25/1), $[\text{Fe}^{2+}]_0 = 66$ mM ($\text{S}_2\text{O}_8^{2-}/\text{Fe}^{2+}$ m/m of 5/1), and for the $\text{H}_2\text{O}_2/\text{Fe}^{2+}$ system $[\text{H}_2\text{O}_2]_0 = 660$ mM ($\text{H}_2\text{O}_2/\text{COD}$ m/m of 0.5/1), $[\text{Fe}^{2+}]_0 = 66$ mM ($\text{H}_2\text{O}_2/\text{Fe}^{2+}$ m/m of 10/1). The results of the studied AOTs application for the treatment of sample L2 in COD and DOC removal are presented in Figure 4.

The COD removal remained unchanged after treatment with a 6-h oxidation step in both applied systems and resulted in 30% and 59% for the $\text{S}_2\text{O}_8^{2-}/\text{Fe}^{2+}$ and $\text{H}_2\text{O}_2/\text{Fe}^{2+}$ processes, respectively. In addition, the DOC elimination was similar with 24% and 45% for the $\text{S}_2\text{O}_8^{2-}/\text{Fe}^{2+}$ and the $\text{H}_2\text{O}_2/\text{Fe}^{2+}$ system. No further increase in the COD and DOC removal occurred after the treatment with a 24-h oxidation period. The elimination of DN from the leachate by the $\text{S}_2\text{O}_8^{2-}/\text{Fe}^{2+}$ system resulted in 29% after treatment with a 24-h oxidation step; the removal was lower in the case of the $\text{H}_2\text{O}_2/\text{Fe}^{2+}$ system, remaining at 18% after the same oxidation duration. Remarkably, the removal of phenolic micropollutants was over 90% after treatment with a 1-h oxidation step in both applied systems.

The oxidant in the $\text{H}_2\text{O}_2/\text{Fe}^{2+}$ treatment was completely utilised as the measurement of residual hydrogen peroxide resulted in negligible residual concentration after a 1-h oxidation period. In the case of the $\text{S}_2\text{O}_8^{2-}/\text{Fe}^{2+}$ system application, the utilisation of oxidant was partial in all the trials and comprised only 32% after a 24-h oxidation step.

Nevertheless, the application of both Fe^{2+} -activated systems proved to be effective in the landfill leachate

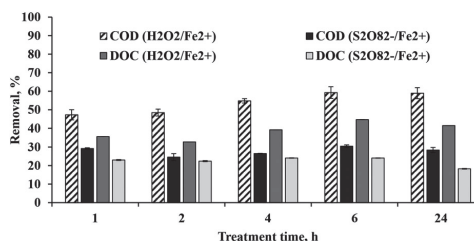
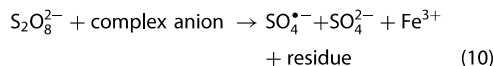
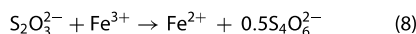


Figure 4. COD and DOC removal versus oxidation time by the $\text{S}_2\text{O}_8^{2-}/\text{Fe}^{2+}$ and $\text{H}_2\text{O}_2/\text{Fe}^{2+}$ treatments of sample L2 (for the $\text{S}_2\text{O}_8^{2-}/\text{Fe}^{2+}$ system: $[\text{S}_2\text{O}_8^{2-}]_0 = 330$ mM, $[\text{Fe}^{2+}]_0 = 66$ mM; for the $\text{H}_2\text{O}_2/\text{Fe}^{2+}$ system: $[\text{H}_2\text{O}_2]_0 = 660$ mM, $[\text{Fe}^{2+}]_0 = 66$ mM).

treatment after 4–6 h of oxidation period. Notably, the persulphate steady decomposition and $\text{SO}_4^{\bullet-}$ selective oxidation were more advantageous for phenolic micropollutants degradation and nitrogen removal from the landfill leachate.

3.4 Effect of the reductant concentration

The main drawback of the activated persulphate process is the lack of direct activator reduction by persulphate, as demonstrated in Equation (4) for the Fenton process. Therefore, to increase the process efficacy, it is necessary to advance the reduction in Fe^{3+} formed in the $\text{S}_2\text{O}_8^{2-}/\text{Fe}^{2+}$ system. According to Liang et al., [39] the addition of thiosulphate ($\text{S}_2\text{O}_3^{2-}$) to the persulphate system could convert Fe^{3+} to the lower valence state Fe^{2+} for the activation of persulphate destruction. $\text{S}_2\text{O}_3^{2-}$ is a powerful reductant due to the sulphur oxidation state (+II). Thus, $\text{S}_2\text{O}_3^{2-}$ has an equal capacity to donate and accept electrons; in addition, it has been successfully used in biological wastewater treatment. [42] A potential reaction mechanism for the ferrous ion-activated persulphate system in the presence of thiosulphate to produce $\text{SO}_4^{\bullet-}$ was proposed by Liang et al. [39]:



Therefore, the efficacy of the $\text{S}_2\text{O}_3^{2-}$ addition to the Fe^{2+} -activated persulphate treatment at a $[\text{S}_2\text{O}_8^{2-}]_0$ of 330 mM and $[\text{Fe}^{2+}]_0$ of 66 mM, corresponding to $\text{S}_2\text{O}_8^{2-}/\text{COD}$ m/m of 0.5/1 and $\text{S}_2\text{O}_8^{2-}/\text{Fe}^{2+}$ m/m of 10/1, was studied as presented in Figure 5.

Accordingly, the COD removal was the same (29%) for the landfill leachate treatment without thiosulphate

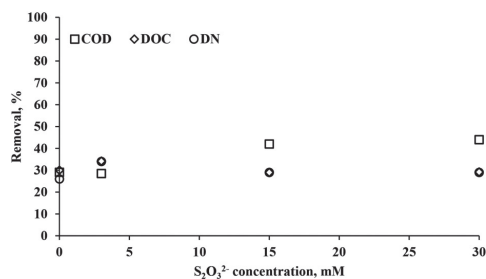


Figure 5. COD, DOC and DN removal versus $\text{S}_2\text{O}_3^{2-}$ concentration by the Fe^{2+} -activated persulphate treatment of sample L1 ($[\text{S}_2\text{O}_8^{2-}]_0 = 300$ mM, $[\text{Fe}^{2+}]_0 = 30$ mM; 24-h oxidation period).

addition and at a $\text{S}_2\text{O}_8^{2-}/\text{Fe}^{2+}/\text{S}_2\text{O}_3^{2-}$ m/m/m of 10/1/0.1 ($[\text{S}_2\text{O}_3^{2-}]_0 = 3$ mM), respectively. A fivefold increase in the reductant dose to a $[\text{S}_2\text{O}_3^{2-}]_0$ of 15 mM resulted in supplementary 13% removal of COD; a 10-fold increase to a $[\text{S}_2\text{O}_3^{2-}]_0$ of 30 mM demonstrated a 15% additional removal of COD as compared to the experiment without thiosulphate addition. The use of thiosulphate also improved the DN removal, and thus, the reductant addition (3–30 mM) increased the system efficacy up to 5% (only the $\text{S}_2\text{O}_8^{2-}/\text{Fe}^{2+}$ system removed 26% of DN).

Based on the obtained results, the application of thiosulphate as a reductant in the activated persulphate process can be recommended for landfill leachate treatment and potentially for other wastewaters as an important agent to increase COD and DN removal.

4. Conclusions

The results of this study give valuable knowledge for the application of ferrous ion-activated persulphate treatment for landfill leachate. The efficacy of the COD removal in the $\text{S}_2\text{O}_8^{2-}/\text{Fe}^{2+}$ treatment resulted in modest efficacy compared to that of the Fenton treatment. A twofold difference in the COD removal at the same oxidant/COD m/m (varied from 0.1/1 to 1/1, corresponding to $[\text{oxidant}]_0$ variation from 60 to 600 mM) was indicated in the $\text{S}_2\text{O}_8^{2-}/\text{Fe}^{2+}$ and $\text{H}_2\text{O}_2/\text{Fe}^{2+}$ treatments (16–36% and 35–66%, respectively). Conversely, the removal of DN resulted in up to 39% and 19% at a $\text{S}_2\text{O}_8^{2-}/\text{COD}$ m/m of 1/1 (at a $\text{S}_2\text{O}_8^{2-}/\text{Fe}^{2+}$ m/m of 10/1) and $\text{H}_2\text{O}_2/\text{COD}$ m/m of 1/1 (at a $\text{H}_2\text{O}_2/\text{Fe}^{2+}$ m/m of 10/1), respectively. The removal of phenolic micropollutants was near to 90% and more in all Fe^{2+} -activated persulphate and hydrogen peroxide experiments. Furthermore, the ferrous ion-activated persulphate treatment does not need supplementary adjustment concerning the temperature and excessive foam formation as in the case of the $\text{H}_2\text{O}_2/\text{Fe}^{2+}$ system. The modest COD removal efficacy in the $\text{S}_2\text{O}_8^{2-}/\text{Fe}^{2+}$ treatment can be improved by the addition of thiosulphate as a reducing agent. Moreover, the application of $\text{S}_2\text{O}_8^{2-}/\text{Fe}^{2+}/\text{S}_2\text{O}_3^{2-}$ m/m/m of 10/1/0.1 decreased the DN content by additional 5% compared to the $\text{S}_2\text{O}_8^{2-}/\text{Fe}^{2+}/\text{S}_2\text{O}_3^{2-}$ m/m/m of 10/1/0. Thus, the ferrous ion-activated persulphate treatment with optimised process conditions could be a promising technology for landfill leachate treatment.

Acknowledgements

The authors would like to thank Ms. Sigrid Turja for her assistance with the experiments.

Disclosure statement

No potential conflict of interest was reported by the authors.

Funding

The financial support provided by institutional research funding IUT (1-7) of the Estonian Ministry of Education and Research is gratefully acknowledged.

References

- [1] Zhang QQ, Tian BH, Zhang X, Ghulam A, Fang C-R, He R. Investigation on characteristics of leachate and concentrated leachate in three landfill leachate treatment plants. *Waste Manage.* 2013;33:2277–2286.
- [2] Xie B, Lv Z, Lv BY, Gu YX. Treatment of mature landfill leachate by biofilters and Fenton oxidation. *Waste Manage.* 2010;30:2108–2112.
- [3] Oller I, Malato S, Sánchez-Pérez JA. Combination of advanced oxidation processes and biological treatments for wastewater decontamination – a review. *Sci Total Environ.* 2011;409:4141–4166.
- [4] Fang F, Abbas AA, Chen YP, Liu ZP, Gao X, Guo JS. Anaerobic/aerobic/coagulation treatment of leachate from a municipal solid wastes incineration plant. *Environ Technol.* 2012;33:927–935.
- [5] Huang J, Chen J, Xie Z, Xu X. Treatment of nanofiltration concentrates of mature landfill leachate by a coupled process of coagulation and internal micro-electrolysis adding hydrogen peroxide. *Environ Technol.* 2015;36:1001–1007.
- [6] Renou S, Givaudan JG, Poulain S, Dirassouyan F, Moulin P. Landfill leachate treatment: review and opportunity. *J Hazard Mater.* 2008;150:468–493.
- [7] Cheibub AF, Campos JC, da Fonseca FV. Removal of COD from a stabilized landfill leachate by physicochemical and advanced oxidative process. *J Environ Sci Health A.* 2014;49:1718–1726.
- [8] Bashir MJK, Aziz HA, Abu Amr SS, Sethupathi S, Aun Ng C, Lim JW. The competency of various applied strategies in treating tropical municipal landfill leachate. *Desalination Water Treat.* 2015;54:2382–2395.
- [9] Rosario-Ortiz FL, Wert EC, Snyder SA. Evaluation of UV/H₂O₂ treatment for the oxidation of pharmaceuticals in wastewater. *Water Res.* 2010;44:1440–1448.
- [10] Wang JL, Xu LJ. Advanced oxidation processes for wastewater treatment: formation of hydroxyl radical and application. *Crit Rev Environ Sci Technol.* 2012;42:251–325.
- [11] Sáez C, Cañizares P, Llanos J, Rodrigo MA. The treatment of actual industrial wastewaters using electrochemical techniques. *Electrocatalysis.* 2013;4:252–258.
- [12] Deng Y, Englehardt JD. Treatment of landfill leachate by the Fenton process. *Water Res.* 2006;40:3683–3694.
- [13] Gotvajn AŽ, Zagorc-Končan J, Cotman M. Fenton's oxidative treatment of municipal landfill leachate as an alternative to biological process. *Desalination.* 2011;275:269–275.
- [14] Singh SK, Tang WZ, Tachiev G. Fenton treatment of landfill leachate under different COD loading factors. *Waste Manage.* 2013;33:2116–2122.
- [15] Luo Y, Guo W, Ngo HH, et al. A review on the occurrence of micropollutants in the aquatic environment and their fate and removal during wastewater treatment. *Sci Total Environ.* 2014;473–474:619–641.
- [16] Guo R, Xie X, Chen J. The degradation of antibiotic amoxicillin in the Fenton-activated sludge combined system. *Environ Technol.* 2015;36:844–851.
- [17] Neyens E, Baeyens J. A review of classic Fenton's peroxidation as an advanced oxidation technique. *J Hazard Mater.* 2003;98:33–50.
- [18] Babuponnusami A, Muthukumar K. A review on Fenton and improvements to the Fenton process for wastewater treatment. *J Environ Chem Eng.* 2014;2:557–572.
- [19] Kochany J, Lipczynska-Kochany E. Utilization of landfill leachate parameters for pretreatment by Fenton reaction and struvite precipitation – a comparative study. *J Hazard Mater.* 2009;166:248–254.
- [20] Cortez S, Teixeira P, Oliveira R, Mota M. Evaluation of Fenton and ozone-based advanced oxidation processes as mature landfill leachate pre-treatments. *J Environ Manage.* 2011;92:749–755.
- [21] Moravia WG, Amaral MCS, Lange LC. Evaluation of landfill leachate treatment by advanced oxidative process by Fenton's reagent combined with membrane separation system. *Waste Manage.* 2013;33:89–101.
- [22] Deng Y, Ezyseke CM. Sulfate radical-advanced oxidation process (SR-AOP) for simultaneous removal of refractory organic contaminants and ammonia in landfill leachate. *Water Res.* 2011;45:6189–6194.
- [23] Chou Y-C, Lo S-L, Kuo J, Yeh C-J. A study on microwave oxidation of landfill leachate – Contributions of microwave-specific effects. *J Hazard Mater.* 2013;246–247:79–86.
- [24] Tsitonaki A, Petri B, Crimi M, Mosabaek H, Siegrist RL, Bjerg PL. In situ chemical oxidation of contaminated soil and groundwater using persulfate: a review. *Crit Rev Environ Sci Technol.* 2010;40:55–91.
- [25] Zhang B-T, Zhang Y, Teng Y, Fan M. Sulfate radical and its application in decontamination technologies. *Crit Rev Environ Sci Technol.* 2015;45:1756–1800.
- [26] Antoniou MG, Cruz AA, Dionysiou DD. Degradation of microcystin-LR using sulfate radicals generated through photolysis, thermolysis and e-transfer mechanisms. *Appl Catal B: Environ.* 2010;96:290–298.
- [27] Romero A, Santos A, Vicente F, Gonzalez C. Diuron abatement using activated persulphate: effect of pH, Fe(II) and oxidant dose. *Chem Eng J.* 2010;162:257–265.
- [28] Chen W-S, Su Y-C. Removal of dinitrotoluenes in wastewater by sono-activated persulfate. *Ultrason Sonochem.* 2012;19:921–927.
- [29] Abu Amr SS, Aziz HA, Adlan MH, Bashir MJK. Optimization of semi-aerobic stabilized leachate treatment using ozone/Fenton's reagent in the advanced oxidation process. *J Environ Sci Health A.* 2013;48:720–729.
- [30] Chu W, Wang YR, Leung HF. Synergy of sulfate and hydroxyl radicals in UV/S₂O₈²⁻/H₂O₂ oxidation of iodinated X-ray contrast medium iopromide. *Chem Eng J.* 2011;178:154–160.
- [31] Liang C, Su H-W. Identification of sulfate and hydroxyl radicals in thermally activated persulfate. *Ind Eng Chem Res.* 2009;48:5558–5562.
- [32] Ji Y, Ferronato C, Salvador A, Yang X, Chovelon J-M. Degradation of ciprofloxacin and sulfamethoxazole by

- ferrous-activated persulfate: implications for remediation of groundwater contaminated by antibiotics. *Sci Total Environ.* 2014;472:800–808.
- [33] APHA (American Public Health Association). Standard methods for the examination of water and wastewater. 22nd ed. Washington DC: American Water Works Association, Water Environment Federation; 2012.
- [34] Dulova N, Trapido M. Application of Fenton's reaction for food-processing wastewater treatment. *J Adv Oxid Technol.* 2011;12:9–16.
- [35] Dulov A, Dulova N, Trapido M. Combined physicochemical treatment of textile and mixed industrial wastewater. *Ozone: Sci Eng.* 2011;33:285–293.
- [36] Sof'ina NA, Beklemishev MK, Kapanadze AL, Dolmanova IF. Sorption catalytic method for the chromium determination. *Mosc Univ Chem Bull.* 2003;44:189–198 [in Russian].
- [37] Eisenberg GM. Colorimetric determination of hydrogen peroxide. *Ind Eng Chem Anal Ed.* 1943;15:327–328.
- [38] Wu X, Gu X, Lu S, et al. Degradation of trichloroethylene in aqueous solution by persulfate activated with citric acid chelated ferrous ion. *Chem Eng J.* 2014;255:585–592.
- [39] Liang C, Bruell CJ, Marley MC, Sperry KL. Persulfate oxidation for in situ remediation of TCE. I. Activated by ferrous ion with and without a persulfate-thiosulfate redox couple. *Chemosphere.* 2004;55:1213–1223.
- [40] Kusic H, Peternel I, Koprivanac N, Loncaric Bozic A. Iron-activated persulfate oxidation of an azo dye in model wastewater: influence of iron activator type on process optimization. *J Environ Eng.* 2011;137:454–463.
- [41] Liang C, Liang C-P, Chen C-C. pH dependence of persulfate activation by EDTA/Fe(III) for degradation of trichloroethylene. *J Contam Hydrol.* 2009;106:173–182.
- [42] Qian J, Lu H, Cui Y, Wei L, Liu R, Chen G-H. Investigation on thiosulfate-involved organics and nitrogen removal by a sulfur cycle-based biological wastewater treatment process. *Water Res.* 2015;69:295–306.

PAPER III

Kattel, E., Trapido, M., Dulova, N. Oxidative degradation of emerging micropollutant acesulfame in aqueous matrices by UVA-induced $\text{H}_2\text{O}_2/\text{Fe}^{2+}$ and $\text{S}_2\text{O}_8^{2-}/\text{Fe}^{2+}$ processes. – *Chemosphere*, 2017, 171, 528–536.

Reproduced with the permission of Elsevier.



Oxidative degradation of emerging micropollutant acesulfame in aqueous matrices by UVA-induced $\text{H}_2\text{O}_2/\text{Fe}^{2+}$ and $\text{S}_2\text{O}_8^{2-}/\text{Fe}^{2+}$ processes



Eneliis Kattel*, Marina Trapido, Niina Dulova

Tallinn University of Technology, Department of Chemical Engineering, Ehitajate tee 5, 19086 Tallinn, Estonia

HIGHLIGHTS

- UVA light effectively induced the $\text{H}_2\text{O}_2/\text{Fe}^{2+}$ and $\text{S}_2\text{O}_8^{2-}/\text{Fe}^{2+}$ processes.
- ACE was 100% degraded at pH 3 by the UVA/ $\text{H}_2\text{O}_2/\text{Fe}^{2+}$ and UVA/ $\text{S}_2\text{O}_8^{2-}/\text{Fe}^{2+}$ systems.
- Mineralization of ACE was generally lower than degradation in all studied processes.
- Hydroxyl radical was proposed to be predominant in the UVA/ $\text{S}_2\text{O}_8^{2-}/\text{Fe}^{2+}$ system.
- Natural water matrices strongly affected the target compound degradation efficacy.

ARTICLE INFO

Article history:

Received 7 July 2016

Received in revised form

9 November 2016

Accepted 20 December 2016

Available online 22 December 2016

Handling Editor: Jun Huang

Keywords:

Artificial sweetener

UVA-irradiation

Activated persulfate

Photo-Fenton process

Water treatment

ABSTRACT

In the present study, UVA/ $\text{H}_2\text{O}_2/\text{Fe}^{2+}$ and UVA/ $\text{S}_2\text{O}_8^{2-}/\text{Fe}^{2+}$ processes were applied to degrade the artificial sweetener, acesulfame (ACE) in ultrapure water (UW), groundwater (GW), and secondary effluent (WW). The degradation time and mineralization of 75 μM of ACE determined the efficacy of the procedures. The results indicated that the UVA-induced $\text{H}_2\text{O}_2/\text{Fe}^{2+}$ and $\text{S}_2\text{O}_8^{2-}/\text{Fe}^{2+}$ systems are a promising alternative for the removal of ACE from different aqueous matrices as both studied processes completely degraded the target compound at an ACE/oxidant/ Fe^{2+} molar ratio of 1/10/1 and pH 3. In the case of UVA-induced systems application without pH adjustment, the ACE decomposition was achieved only in ultrapure water. The maximum mineralization of ACE in ultrapure water by the UVA/ $\text{H}_2\text{O}_2/\text{Fe}^{2+}$ system (molar ratio of 1/10/1) at pH 3 resulted in residual TOC of 18.3%. The oxidative effectiveness of the UVA/ $\text{S}_2\text{O}_8^{2-}/\text{Fe}^{2+}$ system was proved to be mainly formed by the hydroxyl radicals. The obtained results indicate that UVA light can be successfully used for the oxidation of the studied artificial sweetener in various aqueous matrices with carefully adjusted process conditions.

© 2016 Elsevier Ltd. All rights reserved.

1. Introduction

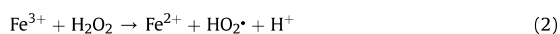
The ubiquitous occurrence of artificial sweeteners (AS) in the environment has raised the concern of them being an emerging micropollutant (Kokotou et al., 2012; Lange et al., 2012). Mostly, these substances are not metabolized by human and get excreted to sewage (Klug and von Rymon Lipinski, 2012). Amongst AS, acesulfame (ACE) is one of the most detected compound ($\mu\text{g/L}$ to mg/L) in wastewater, surface water and groundwater (Buerge et al., 2009; Lange et al., 2012). Reduced (<50%) elimination of ACE in

wastewater treatment plants (WWTPs) by traditional purification processes is the prime reason for its detection at a higher level in the aqueous environment (Scheurer et al., 2009). Additionally, ACE is resistant to biological degradation and therefore acts as a wastewater indicator to measure the anthropogenic impact (Buerge et al., 2009; Scheurer et al., 2009). Gardner (2014) reported that a daily intake of ACE at 15 mg/kg body weight was harmless for human. Nonetheless, study by Stolte et al. (2013) indicated low, but detectable hazards of ACE at concentrations > 1000 mg/L to water fleas *Daphnia magna*, duckweed *Lemna minor*, and green algae *Scenedesmus vacuolatus*. Under environmental conditions, the photo-degradation of ACE in natural aqueous matrices takes place but some photo-transformation products are found to be more toxic than the parent compound (Gan et al., 2014; Sang et al., 2014).

* Corresponding author.

E-mail address: eneliis.kattel@ttu.ee (E. Kattel).

Hence, suitable techniques for removal of ACE from environmental compartments are required. The removal of ACE in aqueous matrices has been studied by the application of biological treatment (Tran et al., 2015), simulated sunlight (Gan et al., 2014), UVC radiation (Coiffard et al., 1999; Sang et al., 2014; Scheurer et al., 2014), ozonation (Scheurer et al., 2012), photocatalytic oxidation (Li et al., 2016), electro-oxidation (Punturat and Huang, 2016), and granulated activated carbon (GAC) filtration (Lange et al., 2012). The conventional water treatment technologies such as biological treatment and GAC filtration have shown inadequate ACE removal efficiencies ($\leq 23\%$, respectively), whereas promising results of complete elimination obtained by the application of several above-mentioned advanced oxidation technologies (AOTs) indicated the perspective of radical-based processes for the degradation of ACE. Among other AOTs, the Fenton and photo-Fenton processes are well-known to be extremely useful in the degradation of numerous classes of organic micropollutants (Pignatello et al., 2006; Litter and Quici, 2010; Trapido et al., 2014; Ribeiro et al., 2015). The generation of hydroxyl radicals ($\text{HO}\cdot$) in the classical Fenton process (Eq. (1)) leads to fast and non-selective oxidation degradation of organic contaminants (Pignatello et al., 2006). The formed ferric iron (Fe^{3+}) can catalyze H_2O_2 to form hydroperoxyl radicals ($\text{HO}_2\cdot$) via the Fenton-like reaction that is responsible for the regeneration of activator and maintain the high efficacy of the Fenton reaction (Eq. (2)) (Babuponnusami and Muthukumar, 2014).



The Fenton system's exposure to UV radiation induces more intensive generation of $\text{HO}\cdot$ as a result of the UV photolysis of the formed Fe^{3+} hydroxocomplexes (Eq. (3)) (Litter and Quici, 2010). The application of the photo-Fenton process has been successfully adopted to enhance the target compound degradation (Xu et al., 2009; Trapido et al., 2014).



In the recent decade, purification of aqueous matrices from a wide range of organic micropollutants is increasingly performed by processes based on the generation of sulfate radical ($\text{SO}_4^{\cdot-}$) (Tsitonaki et al., 2010; Epold et al., 2015; Zhang et al., 2015). $\text{SO}_4^{\cdot-}$ are strong oxidative species similar to $\text{HO}\cdot$ and thus, $\text{SO}_4^{\cdot-}$ -based AOTs are applied also for *in situ* soil and groundwater remediation. A stable oxidant, persulfate ($\text{S}_2\text{O}_8^{2-}$) when activated by transition metals, heat, UV or US irradiation, alkaline pH, activated carbon, hydrogen peroxide or ozone produces $\text{SO}_4^{\cdot-}$ (Tsitonaki et al., 2010; Matzek and Carter, 2016). Fe^{2+} is non-toxic and environmental friendly and thus, the widest used transition metal for $\text{S}_2\text{O}_8^{2-}$ activation. However, generation type of $\text{SO}_4^{\cdot-}$ by Fe^{2+} has some limitations. Accordingly, a quick conversion of Fe^{2+} into Fe^{3+} (Eq. (4)) occurs and the excessive Fe^{2+} scavenges $\text{SO}_4^{\cdot-}$ (Eq. (5)), thereby reducing the efficacy of the pollutant degradation (Liang et al., 2004; Vicente et al., 2011; Matzek and Carter, 2016). Besides, UV light induces the cleavage of peroxide bond in $\text{S}_2\text{O}_8^{2-}$ generating a pair of sulfate radicals (Eq. (6)) (Tsitonaki et al., 2010).



AS are the relatively new group of emerging pollutants and the

information about their occurrence and fate in the environment is still scarce. The available literature is mainly focused on the removal of sucralose. Till date, elimination of other AS from different environmental compartments has not been fully evaluated. Therefore, the present study aimed to evaluate and compare the degradation of ACE in aqueous matrices by UV-induced hydroxyl and sulfate radical-based processes through the assessment of target compound degradation and mineralization efficacy. The presence of the UVA radiation in the sunlight impelled the use of the UVA lamp in the experiments. The efficacy of ACE decomposition by the selected AOTs was studied in ultrapure water (UW), groundwater (GW) and secondary treatment effluent (WW). The treatment was carried out at various oxidant and ferrous iron concentrations as well as at differently adjusted pH values. Also, the radicals in the UVA/ $\text{S}_2\text{O}_8^{2-}$ / Fe^{2+} system were identified. According to the available literature and to the authors' best knowledge, this is the first study related to the UVA/ H_2O_2 / Fe^{2+} and UVA/ $\text{S}_2\text{O}_8^{2-}$ / Fe^{2+} process application for the treatment of ACE in different aqueous matrices.

2. Experimental

2.1. Chemicals

Acetulfame potassium ($\text{C}_4\text{H}_4\text{KNO}_4\text{S}$, $\geq 99\%$, molecular weight 201.24 g/mol) (Fig. 1), hydrogen peroxide (H_2O_2 , PERDROGENTM, $\geq 30\%$), sodium persulfate ($\text{Na}_2\text{S}_2\text{O}_8$, $\geq 99\%$), ferrous sulfate heptahydrate ($\text{FeSO}_4 \cdot 7\text{H}_2\text{O}$, $\geq 99\%$), potassium phosphate dibasic (K_2HPO_4 , $\geq 98\%$), potassium phosphate monobasic (KH_2PO_4 , $\geq 98\%$), sulfuric acid (H_2SO_4 , 95–98%) and sodium sulfite (Na_2SO_3 , $\geq 98\%$) were purchased from Sigma-Aldrich. Acetonitrile (CH_3CN , LiChrosolv[®]), ethanol ($\text{C}_2\text{H}_6\text{O}$, EtOH, 99%), acetic acid (glacial) ($\text{CH}_3\text{CO}_2\text{H}$, 100%), and tertiary butanol ($(\text{CH}_3)_3\text{COH}$, *t*-BuOH, $\geq 99\%$) were purchased from Merck KGaA. All the other chemicals were of analytical grade and used without further purification. Stock solutions were prepared in ultrapure water (Millipore Simplicity[®] UV System, Merck, Germany).

2.2. Properties of groundwater and wastewater

WW collected from the outlet of the secondary treatment of a local municipal WWTP (Tallinn, Estonia), and GW without preceding purification (borehole depth 19 m, Harjumaa, Estonia) were used as real aqueous matrices for ACE degradation. The samples were collected in November 2015 and the main parameters are given in Table 1.

2.3. Experimental procedure

Activated persulfate and hydrogen peroxide treatment were conducted in a batch mode at ambient room temperature (22 ± 1 °C). ACE UW solutions (75 μM , 0.8 L) were treated in a 1.0-L cylindrical glass reactor with a permanent agitation speed (400 rpm) for 2 h with UVA, UVA/ H_2O_2 , UVA/ H_2O_2 / Fe^{2+} , UVA/ Fe^{2+} , UVA/ $\text{S}_2\text{O}_8^{2-}$, UVA/ $\text{S}_2\text{O}_8^{2-}$ / Fe^{2+} , H_2O_2 / Fe^{2+} and $\text{S}_2\text{O}_8^{2-}$ / Fe^{2+} systems. The treatment was carried out in buffered solutions at pH 5.8 and

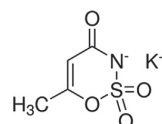


Fig. 1. Chemical structure of ACE.

Table 1
Chemical composition and main parameters of groundwater and secondary effluent from a local municipal WWTP (hereinafter “wastewater”).

Parameter	Unit	Groundwater (GW)	Wastewater (WW)
pH		7.75	7.20
Alkalinity	mgCaCO ₃ /L	650 ± 0	370 ± 15
Conductivity	µS/cm	617 ± 1	1022 ± 1
Total organic carbon (TOC)	mg/L	4.3	13.2
Fe ²⁺	mg/L	0.03	0
Total Fe	mg/L	0.1	0
F ⁻	mg/L	0.2	BDL ^a
Cl ⁻	mg/L	87	450
NO ₃ ⁻	mg/L	BDL	64
PO ₄ ³⁻	mg/L	BDL	12
SO ₄ ²⁻	mg/L	41	75

^a BDL – below detection limit.

7.4 as well as in non-buffered solutions with pH adjusted to 3 or without any adjustment. The pH of the samples was adjusted to 3 by using H₂SO₄, and to 5.8 or 7.4 by using phosphate buffer (K₂HPO₄ and KH₂PO₄) aqueous solutions. The ferrous iron source (FeSO₄·7H₂O) was added and after its complete dissolution, the reaction was initiated by adding Na₂S₂O₈ or H₂O₂ and simultaneous exposure to the UVA lamp that was turned on at least 5 min before the trial to provide a constant output. A low-pressure mercury lamp (11 W OSRAM Dulux S BLUE) located in a quartz tube inside the reactor was used as an UVA source (Fig. S1). The average irradiance entering the solution in the reactor measured by spectrometer (Ocean Optics USB2000+) equipped with SpectraSuite software was 2.2 mW/cm². A water cooling jacket was used to keep the constant temperature in the reactor. Sample aliquots were taken at pre-determined time intervals. The oxidation quenching was done by the addition of EtOH (sample/EtOH volume ratio of 10/1) or Na₂SO₃ at a [oxidant]₀/SO₃²⁻ molar ratio (m/m) of 1/10 for HPLC or TOC analysis, respectively. All experiments were duplicated; the final data shows the results of at least three parallel replicates with error less than 5% and are presented as mean ± standard deviation.

2.4. Identification of hydroxyl and sulfate radicals

Radical scavengers were used to identify the radicals formed during the UVA/S₂O₈²⁻/Fe²⁺ process at pH 3 and 5.8. To differentiate the role of HO• and SO₄•⁻ in ACE oxidation by the UVA/S₂O₈²⁻/Fe²⁺ system two radical probes, EtOH and *t*-BuOH, were employed. An excessive amount of scavenger was spiked into the reaction solutions before the catalyst and oxidant addition at an ACE/[scavenger]₀ m/m of 1/500 ([scavenger]₀ = 37.5 mM). In the case of UVA/Fe²⁺ process at pH 3, the addition of *t*-BuOH at an ACE/*t*-BuOH molar ratio of 1/500 was studied.

2.5. Analytical methods

ACE concentration was quantified using HPLC (YL-Instrument 9300, China). The HPLC was equipped with a Waters Bridge C18 (150 × 3.0 mm inner diameter, 3.5 µm particle size) column and UV/Vis detector. The analysis was performed using an isocratic method with a mobile phase mixture of 10% acetonitrile and 90% acetic acid (0.1%) aqueous solution. Samples (20 µL) were analyzed at the flow rate of 200 µL/min and wavelength of 230 nm. The concentration of ACE was determined by using the standard multipoint calibration.

The total organic carbon (TOC) was measured by a TOC analyzer multi N/C[®] 3100 (Analytik Jena, Germany). The ion chromatography with chemical suppression of the eluent conductivity was used to measure the concentrations of anions (761 Compact IC, Metrohm Ltd., Switzerland). The pH was measured using a digital pH/lon

meter (Mettler Toledo S220, Switzerland) and the electrical conductivity was measured using a digital EC meter (HQ 430d flexi, HACH Company, USA). The initial hydrogen peroxide concentration in the stock solutions was measured spectrophotometrically at λ = 254 nm; the residual hydrogen peroxide concentration in the treated samples was measured spectrophotometrically at λ = 410 nm with titanium sulfate by a hydrogen peroxide-Ti⁴⁺ complex formation (Eisenberg, 1943) by a UV/Vis spectrophotometer (GENESYS 10S, Thermo Scientific, USA). The residual persulfate concentration in the treated samples was measured spectrophotometrically at λ = 352 nm by a sodium iodide reaction with persulfate towards the formation of I₂ (Liang et al., 2008). The alkalinity of groundwater and secondary effluent was measured by titration with hydrochloric acid (0.1 M) in the presence of methyl orange (APHA, 2012).

3. Results and discussion

3.1. Effect of initial concentrations of oxidants

The influence of two UVA-irradiated oxidative systems to the degradation efficacy of ACE (75 µM) in ultrapure water was investigated. The UVA/oxidant/Fe²⁺ trials with different oxidant concentrations were performed by using 150, 375, 750 and 1500 µM of H₂O₂ or S₂O₈²⁻, respectively. Corresponding molar ratios of ACE/[oxidant] varied from 1/2 to 1/20, whereas the molar ratio of ACE/Fe²⁺ was fixed at 1/1 ([Fe²⁺]₀ = 75 µM); pH of the system was adjusted to 3 to maintain the valence of iron(II). The stoichiometric value of the ACE/[oxidant] molar ratio was calculated as 1/11 and 1/10.5 for hydrogen peroxide and persulfate, respectively, assuming the complete oxidation of the target compound. The results presented in Fig. 2 indicate that the degradation of ACE with time is increasing simultaneously with the initial oxidant concentration of 150 µM to 750 µM in both studied systems.

Intrinsic to persulfate oxidation the accumulation of Fe(III) in the reaction system (Eqs. (4)–(5)) (Zhang et al., 2015; Matzek and Carter, 2016) was likely responsible for a slower ACE decomposition as compared to the photo-Fenton process. Thus, the target compound degradation was achieved in a longer period (30–45 min) in the UVA/S₂O₈²⁻/Fe²⁺ process than in the UVA/H₂O₂/Fe²⁺ process (10–30 min) irrespective of the oxidant concentration applied in the range of 150–750 µM. Further increase in oxidants concentration to 1500 µM had no favorable effect on ACE degradation as the treatment was prolonged to 15 min for the UVA/H₂O₂/Fe²⁺ process and remained 30 min for the UVA/S₂O₈²⁻/Fe²⁺ process, respectively. This phenomenon is most likely caused by the excessive amount of oxidant that in the case of fixed concentration of Fe²⁺ of 75 µM was presumably responsible for the scavenging of radicals (Eqs. (7)–(8)) and subsequently resulting in negligible

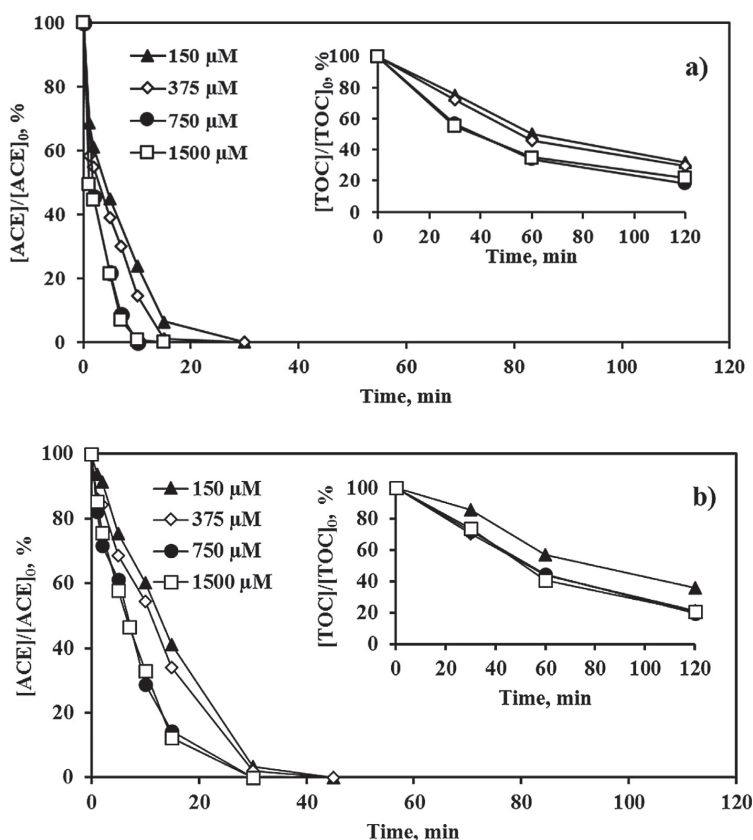
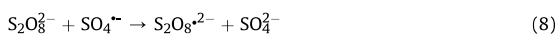


Fig. 2. Degradation and mineralization of ACE by the UVA/H₂O₂/Fe²⁺ (a) and UVA/S₂O₈²⁻/Fe²⁺ (b) processes at different initial oxidant concentrations at pH 3 ([ACE]₀ = 75 μM, [Fe²⁺]₀ = 75 μM).

treatment efficacy enhancement or even reduction in the S₂O₈²⁻- and H₂O₂-based oxidative system, respectively (Pignatello et al., 2006; Matzek and Carter, 2016).



In this study, a decline in TOC content measured the mineralization of ACE by the studied processes. As can be seen from Fig. 2, the mineralization of the target compound after 120 min of treatment in the investigated systems was similar with 1500 μM oxidant concentration (approximately 80%).

Both the activation ability as well as the stability of the studied oxidants were measured and assessed. Accordingly, hydrogen peroxide used in the UVA/H₂O₂/Fe²⁺ system was completely utilized after 2-h treatment at a [H₂O₂]₀ of 150–1500 μM. In the case of the UVA/S₂O₈²⁻/Fe²⁺ system, the residual concentration of persulfate steadily increased with the increase in applied [S₂O₈²⁻]₀ after 2 h of oxidation and resulted in the residue of 1.6% and 85% from the initial concentration of 150 and 1500 μM, respectively.

Among the studied ACE/[oxidant]/Fe²⁺ molar ratios, the 1/10/1 was the most efficient one taking into account the decrease of ACE concentration and TOC, and the stability as well as the consumption

of the oxidants. However, the effect of activator concentration was further studied to estimate the possibility to reduce the ferrous iron (Fe²⁺) consumption but maintain plausible treatment efficacy.

3.2. Effect of initial concentration of ferrous ion

To examine the effect of the addition of Fe²⁺ to UVA-irradiated oxidation system the blank trials without Fe²⁺ were conducted. The results of UVA/H₂O₂ and UVA/S₂O₈²⁻ processes indicated that the addition of Fe²⁺ is essential to accelerate ACE degradation and mineralization as after 2 h of treatment, the residual ACE concentration was 80.9% for the UVA/H₂O₂ and 60.7% for the UVA/S₂O₈²⁻ system. Notably, the mineralization was negligible in both the studied systems. Similar results were observed for the UVA-induced degradation of a hormone melatonin, where Fe²⁺ was added to the system to enhance the degradation of the target compound (Xu et al., 2009).

The effect of initial activator concentration was studied at a [Fe²⁺]₀ of 15, 37.5, 75 and 150 μM that corresponds to an [oxidant]/Fe²⁺ molar ratio of 10/0.2, 10/0.5, 10/1 and 10/2. The experiments were performed at the fixed ACE/[oxidant] m/m of 1/10 ([ACE]₀ = 75 μM, [oxidant]₀ = 750 μM) and at pH 3. The results of the UVA/H₂O₂/Fe²⁺ and UVA/S₂O₈²⁻/Fe²⁺ processes applied for the ACE degradation and mineralization are shown in Fig. 3.

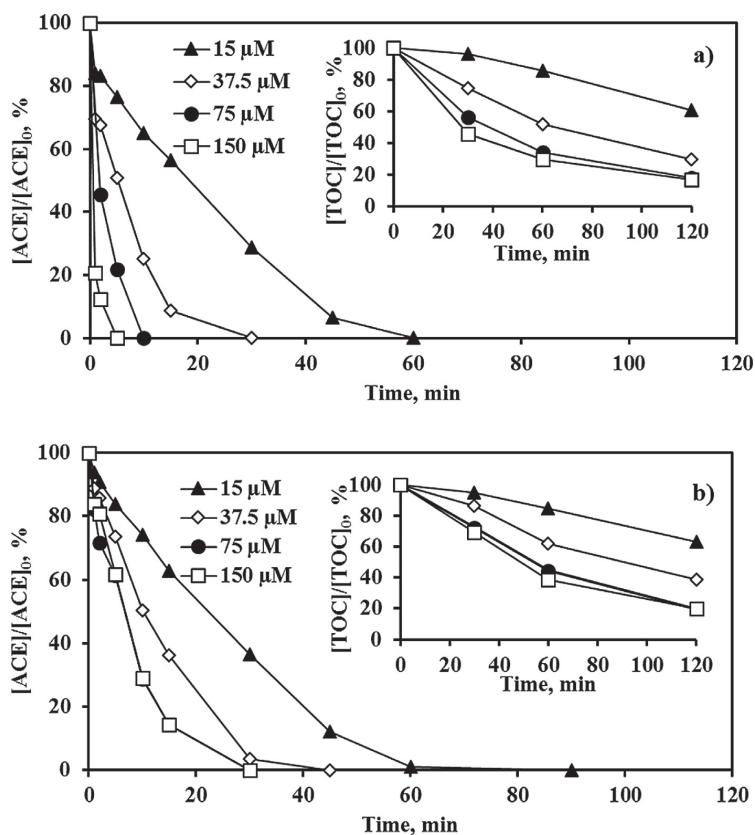


Fig. 3. Degradation and mineralization of ACE by the UVA/H₂O₂/Fe²⁺ (a) and UVA/S₂O₈²⁻/Fe²⁺ (b) processes at different [Fe²⁺]₀ at pH 3 ([ACE]₀ = 75 μM, [oxidant]₀ = 750 μM).

The data obtained from the UVA/H₂O₂/Fe²⁺ process indicated that the increase in iron concentration from 15 to 150 μM enhanced the efficacy of ACE degradation. Accordingly, the time for complete degradation of ACE was 60 min of treatment for 15 μM of [Fe²⁺]₀ while for 150 μM of [Fe²⁺]₀ the time was 5 min. In the case of UVA/S₂O₈²⁻/Fe²⁺ process, the efficacy of ACE degradation was improved with the increase in [Fe²⁺]₀ from 15 to 75 μM; further increase in [Fe²⁺]₀ to 150 μM resulted in analogous efficacy.

The latter observation could be explained by the fact that excess Fe²⁺ acts as a scavenger of SO₄^{•-} (Eq. (5)) and therefore reduces the degradation efficacy of the target compound by generating less reactive species (Matzek and Carter, 2016).

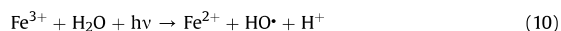
In the UVA/H₂O₂/Fe²⁺ system, the dissociation of oxidant after 2 h of treatment was about 100% in the studied range of [Fe²⁺]₀. However, in the UVA/S₂O₈²⁻/Fe²⁺ system, the maximum dissociation of S₂O₈²⁻ (57%) was reached at 75 μM of [Fe²⁺]₀, indicating the highest activation efficacy at a S₂O₈²⁻/Fe²⁺ m/m of 10/1. The latter was also consistent with the result of ACE degradation.

The mineralization of ACE by the processes applied proved to have a similar pattern. Accordingly, the increase in applied [Fe²⁺]₀ resulted in improved ACE mineralization over 40% by the UVA/H₂O₂/Fe²⁺ (Fig. 3a) and UVA/S₂O₈²⁻/Fe²⁺ (Fig. 3b) processes. In the UVA/H₂O₂/Fe²⁺ system, the 10-fold increase of ferrous iron concentration from 15 to 150 μM after 2-h treatment resulted in 17.1% of residual TOC, whereas the latter for [Fe²⁺]₀ of 75 μM was 18.3%

(Fig. 3a). In the UVA/S₂O₈²⁻/Fe²⁺ system, the [TOC]/[TOC]₀ after 2-h treatment was 63% for 15 μM of [Fe²⁺]₀, 19.7% for 75 μM of Fe²⁺ and 20% for 150 μM of Fe²⁺ (Fig. 3b).

Overall, the experiments proved that the most effective strategy for the degradation and mineralization of ACE were obtained at [Fe²⁺]₀ of 75 μM. Therefore, a ACE/oxidant/Fe²⁺ molar ratio of 1/10/1 was used in all the further studies.

Furthermore, the efficacy of UVA/Fe²⁺ system ([Fe²⁺]₀ = 75 μM) without oxidant was also studied. The results proved that the ACE decomposition (100%) and mineralization (41.5%) occurs in the presence of Fe²⁺ in a 2-h treatment. Dainton and Jones (1965) and Airey and Dainton (1966) proposed that exposure to light induces ferrous iron to reduce a hydrated electron (e_{aq}⁻) (Eq. (9)). Additionally, the exposure of iron-containing aqueous solution to UV or UV-Vis radiation could facilitate the generation of hydroxyl radicals by photo-reduction of Fe³⁺ and hydroxylated Fe³⁺ to Fe²⁺ via Eqs. (3) and (10), respectively. On the other hand, the presence of oxygen promotes the generation of superoxide (O₂⁻) and subsequently hydrogen peroxide as shown by Eqs. (11)–(12); then hydroxyl radicals could be produced by the Fenton reaction (Eq. (1)) (Pouran et al., 2015).





Based on this knowledge, the degradation of ACE in the UVA/ Fe^{2+} system was potentially stimulated by the $\text{HO}\cdot$. The discussion covering the role of radicals will appear in Section 3.4.

3.3. Effect of pH

Both of the radical-based oxidation systems were examined at different pH values: 3 and 5.8 (corresponding to the initial pH of ACE solution) in non-buffered solutions as well as 5.8 and 7.4 in buffered systems. The pH value was adjusted to 3 to provide the presence of activator in its ferrous form, which proved to have the higher potential in activation of H_2O_2 and $\text{S}_2\text{O}_8^{2-}$ than Fe^{3+} (Pignatello et al., 2006; Babuponnusami and Muthukumar, 2014 and Matzek and Carter, 2016). The effect of pH value of the applied UVA/ $\text{H}_2\text{O}_2/\text{Fe}^{2+}$ and UVA/ $\text{S}_2\text{O}_8^{2-}/\text{Fe}^{2+}$ treatments at molar ratio of 1/10/1, corresponding to $[\text{oxidant}]_0 = 750 \mu\text{M}$ and $[\text{Fe}^{2+}]_0 = 75 \mu\text{M}$, is presented in Fig. 4.

The obtained results expectedly indicated that the buffered medium inhibits the degradation of ACE at $\text{pH}_{\text{buffer}}$ 5.8 and 7.4, whereas in non-buffered solution at pH 5.8 the complete

degradation of ACE was achieved in 60 and 90 min of oxidation by the UVA/ $\text{H}_2\text{O}_2/\text{Fe}^{2+}$ and UVA/ $\text{S}_2\text{O}_8^{2-}/\text{Fe}^{2+}$ systems, respectively. Notably, the pH was 3.90 and 3.30 after the 2-h treatment by the activated H_2O_2 and $\text{S}_2\text{O}_8^{2-}$ process, respectively, with the fast drop in pH value to 3.91–3.98 during the first minute in the non-buffered oxidative systems. In the UVA/ $\text{H}_2\text{O}_2/\text{Fe}^{2+}$ system (Fig. 4a), the residual ACE concentration was 72.9% at $\text{pH}_{\text{buffer}}$ 5.8 and 86.7% at $\text{pH}_{\text{buffer}}$ 7.4, respectively. In the UVA/ $\text{S}_2\text{O}_8^{2-}/\text{Fe}^{2+}$ system (Fig. 4b), the residual ACE concentration was 47.9% at $\text{pH}_{\text{buffer}}$ 5.8 and 64.9% at $\text{pH}_{\text{buffer}}$ 7.4, respectively. In general, the ACE degradation in the buffered solution at $\text{pH}_{\text{buffer}}$ 5.8 and 7.4 by the UVA/ $\text{S}_2\text{O}_8^{2-}/\text{Fe}^{2+}$ process occurred up to 25% more effective over the UVA/ $\text{H}_2\text{O}_2/\text{Fe}^{2+}$ process. The efficacy of persulfate-based system supported the results obtained by Xu et al. (2016) for the degradation of sucralose that the co-existence of $\text{SO}_4^{\cdot-}$ and $\text{HO}\cdot$ at higher pH in persulfate oxidative system is responsible for the degradation of ACE.

In non-buffered systems, a significant decrease in TOC with the increase of pH value was observed; thus the residual TOC content was 18.3% at pH 3 and 59.5% at pH 5.8 in the UVA/ $\text{H}_2\text{O}_2/\text{Fe}^{2+}$ system and 19.7% at pH 3 and 47.4% at pH 5.8 in the UVA/ $\text{S}_2\text{O}_8^{2-}/\text{Fe}^{2+}$ system. The buffer addition to the studied systems resulted in negligible ACE mineralization. Gan et al. (2014) also found in the experiments of ACE photolysis under simulated sunlight that the

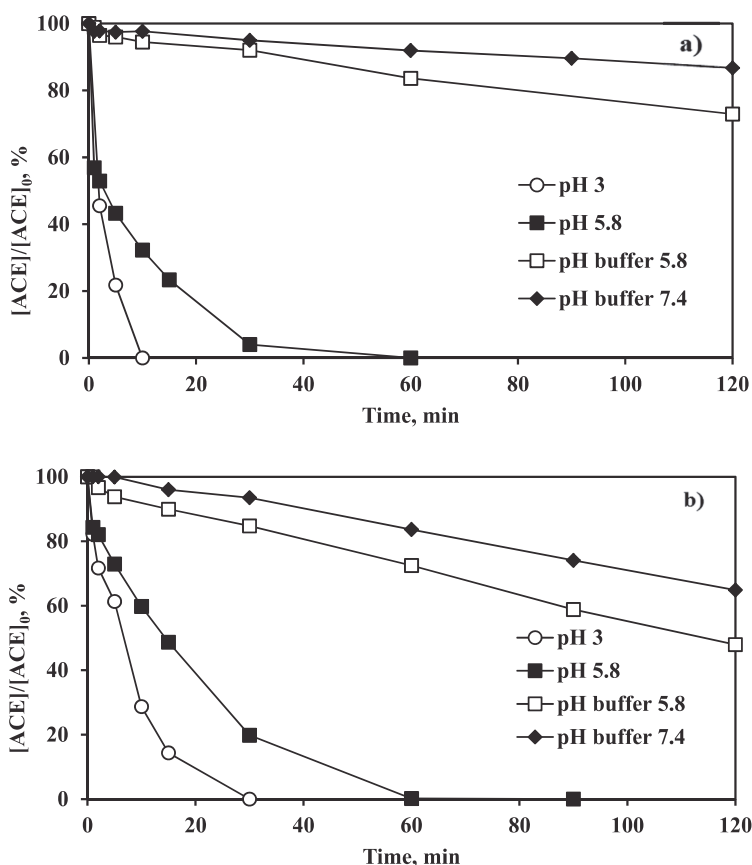


Fig. 4. Degradation of ACE by the UVA/ $\text{H}_2\text{O}_2/\text{Fe}^{2+}$ (a) and UVA/ $\text{S}_2\text{O}_8^{2-}/\text{Fe}^{2+}$ (b) processes at different pH-s in buffered and non-buffered systems ($[\text{ACE}]_0 = 75 \mu\text{M}$, $[\text{oxidant}]_0 = 750 \mu\text{M}$, $[\text{Fe}^{2+}]_0 = 75 \mu\text{M}$).

compound ($[ACE]_0 = 0.6 \mu\text{M}$) degradation occurred faster at pH 4 than at pH 7 or 9, but with the generation of more persistent intermediates rather than mineralization. According to Legrini et al. (1993), the pH value around 3 is also more advantageous for the solubility of ferric hydroxocomplexes and $\text{Fe}(\text{OH})^{2+}$ photo-activity (Eq. (3)). Thus, the degradation efficacy of ACE by the UVA-induced iron-activated AOTs was strongly influenced by the initial pH and the inhibiting properties of an aqueous matrix. The acidic conditions (pH 3 or 5.8) without the buffering capability for both, H_2O_2 and $\text{S}_2\text{O}_8^{2-}$ -based oxidative systems proved to be advantageous for the target contaminant concentration decrease.

3.4. Identification of active radicals in the UVA-induced iron-activated persulfate system

The species responsible for the degradation of ACE in the UVA/ $\text{S}_2\text{O}_8^{2-}/\text{Fe}^{2+}$ system were determined by the addition of radical scavengers. Molecular probes, EtOH and *t*-BuOH, were used to identify the proportion of sulfate or hydroxyl radicals in the oxidative system. It is well studied in the literature that EtOH is used to scavenge both, $\text{SO}_4^{\cdot-}$ and HO^{\cdot} , with a reaction rates of $(1.6\text{--}7.7) \times 10^7 \text{ L}/(\text{mol s})$ and $(1.2\text{--}2.8) \times 10^9 \text{ L}/(\text{mol s})$, respectively (Anipsitakis and Dionysiou, 2004). To differentiate the contributions of $\text{SO}_4^{\cdot-}$ and HO^{\cdot} , *t*-BuOH was used as it is more selective towards HO^{\cdot} scavenging. The reaction rates of *t*-BuOH with HO^{\cdot} are $(3.8\text{--}7.6) \times 10^8 \text{ L}/(\text{mol s})$ compared to $(4\text{--}9.1) \times 10^5 \text{ L}/(\text{mol s})$ with $\text{SO}_4^{\cdot-}$ (Anipsitakis and Dionysiou, 2004; Oh et al., 2016). Based on this data, the prevalence of sulfate or hydroxyl radicals was estimated by adding excess EtOH and *t*-BuOH into the UVA/ $\text{S}_2\text{O}_8^{2-}/\text{Fe}^{2+}$ system. The estimation was done by estimating the degradation efficacy of ACE after adding the molecular probes. As presented in Table 2, the results demonstrated the predominance of the hydroxyl radicals at both studied pH-s.

The addition of *t*-BuOH decreased the treatment efficacy at pH 3 by about 60% and the addition of EtOH by more than 80%. At pH 5.8, the corresponding results were more than 30% (*t*-BuOH) and 45% (EtOH). These results suggest that in the UVA-induced ferrous ion-activated persulfate system both HO^{\cdot} and $\text{SO}_4^{\cdot-}$ were involved in the degradation of ACE, but the HO^{\cdot} proved to have the dominant role. The obtained results of higher reactivity of hydroxyl radicals towards the oxidation of ACE than sulfate radicals are in agreements with the findings of Toth et al. (2012).

The presence of HO^{\cdot} in the UVA/ Fe^{2+} system at similar conditions was studied by the addition of *t*-BuOH. After 30 min of treatment, the residual concentration of ACE was 77.8%, whereas the presence of scavenger reduced the degradation of ACE by about 20%. Hence, the HO^{\cdot} generated in the system proved to be at least partially responsible for the degradation of the target compound.

3.5. Effect of water matrix

The degradation of ACE was also examined in environmental samples such as GW and WW. The treatment efficacy by the UVA/ $\text{H}_2\text{O}_2/\text{Fe}^{2+}$ and UVA/ $\text{S}_2\text{O}_8^{2-}/\text{Fe}^{2+}$ processes at a molar ratio of 1/10/1

Table 2
Degradation of ACE by the UVA/ $\text{S}_2\text{O}_8^{2-}/\text{Fe}^{2+}$ process in the presence and absence of radical scavengers after 15 min of treatment ($[ACE]_0 = 75 \mu\text{M}$, $[\text{S}_2\text{O}_8^{2-}]_0 = 750 \mu\text{M}$, $[\text{Fe}^{2+}]_0 = 75 \mu\text{M}$).

	Without scavengers ($[ACE]/[ACE]_0$, %)		With scavengers ($[ACE]/[ACE]_0$, %)	
			<i>t</i> -BuOH	EtOH
pH 3	14.3		76.5	96.5
pH 5.8	48.7		82.5	93.9

was compared at adjusted pH 3 and initial pH values of the studied matrices. The results of the trials are given in Table 3.

Oxidation experiments with natural matrices indicated considerably lower ACE degradation efficacy as compared with UW trials. Accordingly, the trials at initial pH (7.75) resulted in 6.5 and 5.5% degradation effectiveness of ACE in GW by the UVA/ $\text{H}_2\text{O}_2/\text{Fe}^{2+}$ and UVA/ $\text{S}_2\text{O}_8^{2-}/\text{Fe}^{2+}$ process, respectively. At pH 3, the 100% decomposition of ACE was attained in 30 min by the UVA/ $\text{H}_2\text{O}_2/\text{Fe}^{2+}$ process; the particular effect was reached in 2-fold longer oxidation period, in 60 min, by the UVA/ $\text{S}_2\text{O}_8^{2-}/\text{Fe}^{2+}$ process. The degradation of ACE in WW at initial pH of 7.20 was similar to GW, resulting in 7.9% by the UVA/ $\text{H}_2\text{O}_2/\text{Fe}^{2+}$ and 4.8% by the UVA/ $\text{S}_2\text{O}_8^{2-}/\text{Fe}^{2+}$ process after 120 min of treatment. In strongly acidic conditions, the complete degradation of ACE in WW was reached in 1-h and in 2-h treatment by the UVA/ $\text{H}_2\text{O}_2/\text{Fe}^{2+}$ and UVA/ $\text{S}_2\text{O}_8^{2-}/\text{Fe}^{2+}$ processes, respectively. It should be noted that ACE was not detected in GW and WW samples before artificial contamination in the laboratory. Scheurer et al. (2014) ascertained that 34–37% of ACE ($[ACE]_0 = 0.06 \mu\text{M}$) were degraded in tap water and waterworks water (pre-treated with activated carbon) by applying a 10-min UVC-radiation ($1000 \text{ J}/\text{m}^2$) treatment. The results of this study also indicated that the target compound degradation is influenced by the pH; thus, the efficacy of ACE degradation was 85% at pH 5, around 80% at pH 7–8 and near 60% at pH 11. Li et al. (2016) found out that $30 \mu\text{M}$ ACE was completely removed from seawater by using UVC/ TiO_2 system (ACE/ TiO_2 m/m of 1/20) within 60 min of treatment. Scheurer et al. (2012) proved that >99% of $1.5 \mu\text{M}$ ACE could be degraded in WWTP influent and effluent by $1 \text{ mg}/\text{L}$ ozone and 25 min of contact time. Moreover, the complete ACE degradation and mineralization ($[ACE]_0 = 600 \mu\text{M}$) in biologically pre-treated and untreated domestic wastewater by electrochemical oxidation was observed in 30–120 min, depending on the material of the anode (Punturat and Huang, 2016).

The results presented in Table 3 suggest that environmental aqueous matrices have noticeable inhibitory properties leading to declining in the efficacy of ACE degradation even at pH 3. Matrices in the current study had considerable alkalinity and content of various inorganic ions (Table 1). Subsequently, all these substances were potentially involved in the radical scavenging processes in the oxidative systems.

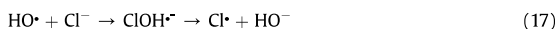
The buffering properties of bicarbonate (HCO_3^-) and carbonate (CO_3^{2-}) ions may contribute to the inhibition of AOTs application for aqueous matrices treatment (Grebel et al., 2010; Bennedsen et al., 2012). In the studied systems, the HO^{\cdot} and $\text{SO}_4^{\cdot-}$ scavenging by alkalinity via Eqs. (13)–(16) becomes more relevant with the increase in pH (Grebel et al., 2010; Vicente et al., 2011; Bennedsen et al., 2012; Rubio et al., 2013). This may be the reason of rather low efficacy of the ACE treatment in GW and WW at initial pH values. In addition, bicarbonates are known to absorb light leading to the uneven dispersion of radiation in the aqueous environment (Grebel et al., 2010).



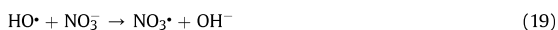
Similarly, chloride ions (Cl^-) are reported to be effective scavengers of HO^{\cdot} and $\text{SO}_4^{\cdot-}$ via Eqs. (17)–(18) (Liao et al., 2001; Grebel et al., 2010; Fang et al., 2012; Caregnato et al., 2013), although some studies indicated an increase in treatment efficacy (Monteagudo et al., 2015; Xu et al., 2016).

Table 3Degradation of ACE by the UVA/H₂O₂/Fe²⁺ and UVA/S₂O₈²⁻/Fe²⁺ processes in aqueous matrices at different pH ([ACE]₀ = 75 μM, [oxidant]₀ = 750 μM, [Fe²⁺]₀ = 75 μM).

Matrix		[ACE]/[ACE] ₀ , %							
		UVA/H ₂ O ₂ /Fe ²⁺				UVA/S ₂ O ₈ ²⁻ /Fe ²⁺			
		15 min	30 min	60 min	120 min	15 min	30 min	60 min	120 min
Initial pH	UW ^a	23.4	4.0	0	–	48.7	19.8	0.2	0
	GW ^b	93.8	93.8	93.8	93.5	99.2	98.1	97.4	94.5
	WW ^c	96	94.3	93.8	92.3	95.5	95.5	95.5	95.2
pH 3	UW	0	–	–	–	14.3	0	–	–
	GW	3.9	0	–	–	48.0	12.6	0	–
	WW	14.0	0.7	0	–	62.9	40.7	6.3	0

^a UW – ultrapure water.^b GW – groundwater.^c WW – wastewater collected from the outlet of the secondary treatment of a municipal WWTP.

Moreover, nitrate ions (NO₃⁻) intensively react with HO• and SO₄^{•-} through Eqs. (19)–(20) that commonly result in the inhibition of the target organic pollutant oxidation (Xu et al., 2016).



Finally, fluoride ions (F⁻) in the studied systems may slightly decrease the HO• properties as less reactive inorganic species are generated through the reaction between HO• and F⁻, but they are usually recognized as poor radical scavengers together with sulfate (SO₄²⁻) and phosphate ions (PO₄³⁻) (Pignatello et al., 2006).

Therefore, the impact of matrix on the degradation of ACE was mainly influenced by the presence of various inorganic ions as well as by the initial pH of the samples. To improve the ACE decomposition efficacy in different matrices prudent adjustment of the pH need to be provided.

4. Conclusions

The present study focused on the application of UVA-induced H₂O₂/Fe²⁺ and S₂O₈²⁻/Fe²⁺ processes towards the degradation of artificial sweetener ACE. The results indicated that at acidic conditions in UW, the complete and fast degradation of ACE was achieved by both the studied oxidative systems with the oxidant concentration of 750 μM and the Fe²⁺ concentration of 75 μM. The experiments on the effects of oxidant and Fe²⁺ concentration indicated that these concentrations give the highest efficacy of both processes regarding ACE degradation and mineralization. The effect of pH was significant, particularly in the application for GW and WW, where the pH of 3 favored the complete degradation of ACE. The application of the UVA/H₂O₂/Fe²⁺ and UVA/S₂O₈²⁻/Fe²⁺ treatment to GW and WW at initial pH of 7.75 and 7.20, respectively, resulted in 4.8–7.7% of ACE degradation. The latter could be instigated by neutral pH region and consequently, formation of non-soluble ferric hydroxocomplexes during oxidation as well as by inhibitory properties of inorganic ions presented in the water matrices. The identification of species responsible for the ACE degradation in the UVA/S₂O₈²⁻/Fe²⁺ system indicated that both radicals, SO₄^{•-} and HO•, were present, but the HO• were the predominant radicals. The results of this study demonstrate the feasibility of the UVA-induced H₂O₂/Fe²⁺ and S₂O₈²⁻/Fe²⁺ processes for the degradation of ACE in different aqueous matrices with preceding acidification. The use of UVA suggests that these

processes have the potential to be used under natural sunlight that contributes to the sustainable water processing technology.

Acknowledgments

The financial support provided by institutional research funding IUT (1–7) of the Estonian Ministry of Education and Research is gratefully acknowledged. The authors would like to thank Marge Nõmmik, M.Sc., and Sandra Salom, M.Sc., for their assistance with the experiments.

Appendix A. Supplementary data

Supplementary data related to this article can be found at <http://dx.doi.org/10.1016/j.chemosphere.2016.12.104>.

References

- Airey, P.L., Dainton, F.S., 1966. The photochemistry of aqueous solutions of Fe(II). 1. Photoelectron detachment from ferrous and ferrocyanide ions. *Proc. R. Soc. Lond. A29*, 340–352.
- Anipsitakis, G.P., Dionysiou, D.D., 2004. Radical generation by the interaction of transition metals with common oxidants. *Environ. Sci. Technol.* 38, 3705–3712.
- APHA (American Public Health Association), 2012. *Standard Methods for the Examination of Water and Wastewater*, twenty-second ed. American Water Works Association, Water Environment Federation, Washington DC.
- Babuponnusami, A., Muthukumar, K., 2014. A review on Fenton and improvements to the Fenton process for wastewater treatment. *J. Environ. Chem. Eng.* 2, 557–572.
- Bennedsen, L.R., Muff, J., Søgaard, E.G., 2012. Influence of chloride and carbonates on the reactivity of activated persulfate. *Chemosphere* 86, 1092–1097.
- Buerge, I.J., Buser, H.-R., Kahle, M., Müller, M.D., Poiger, T., 2009. Ubiquitous occurrence of the artificial sweetener acesulfame in the aquatic environment: an ideal chemical marker of domestic wastewater in groundwater. *Environ. Sci. Technol.* 43, 4381–4385.
- Caregnato, P., Rosso, J.A., Soler, J.M., Arques, A., Mártire, D.O., Gonzalez, M.C., 2013. Chloride anion effect on the advanced oxidation processes of methidathion and dimethoate: role of Cl₂^{•-} radical. *Water Res.* 47, 351–362.
- Coiffard, C.A.C., Coiffard, L.J.M., De Roock-Holtzauer, Y.M.R., 1999. Photodegradation kinetics of acesulfame-K solutions under UV light: effect of pH. *Z. Leb. Unters Forsch A* 208, 6–9.
- Dainton, F.S., Jones, F.T., 1965. Photo- and radiation-chemistry of low temperature aqueous glasses: Part 1. – mineral acid glasses containing N₂O and Fe²⁺ ions. *Trans. Faraday Soc.* 61, 1681–1700.
- Eisenberg, G.M., 1943. Colorimetric determination of hydrogen peroxide. *Ind. Eng. Chem. Anal. Ed.* 15, 327–328.
- Epold, I., Trapido, M., Dulova, N., 2015. Degradation of levofloxacin in aqueous solutions by Fenton, ferrous ion-activated persulfate and combined Fenton/persulfate systems. *Chem. Eng. J.* 279, 452–462.
- Fang, G.D., Dionysiou, D., Wang, Y., Al-Abed, S.R., Zhou, D.M., 2012. Sulfate radical-based degradation of polychlorinated biphenyls: effects of chloride ion and reaction kinetics. *J. Hazard. Mater.* 227–228, 394–401.
- Gan, Z., Sun, H., Wang, R., Hu, H., Zhang, P., Ren, X., 2014. Transformation of acesulfame in water under natural sunlight: joint effect of photolysis and biodegradation. *Water Res.* 64, 113–122.
- Gardner, C., 2014. Non-nutritive sweeteners: evidence for benefit vs. risk. *Curr. Opin. Lipidol.* 25, 80–84.
- Grebel, J.E., Pignatello, J.J., Mitch, W.A., 2010. Effect of halide ions and carbonates on

- organic contaminant degradation by hydroxyl radical-based advanced oxidation processes in saline waters. *Environ. Sci. Technol.* 44, 6822–6828.
- Klug, C., von Rymon Lipinski, G.-W., 2012. Acesulfame potassium. In: O'Brien Nabors, L. (Ed.), *Alternative Sweeteners*, fourth ed. CRC Press, Taylor and Francis Group, Florida, p. 18.
- Kokotou, M.G., Asimakopoulos, A.G., Thomaidis, N.S., 2012. Artificial sweeteners as emerging pollutants in the environment: analytical methodologies and environmental impact. *Anal. Methods* 4, 3057–3070.
- Lange, F.T., Scheurer, M., Brauch, H.-J., 2012. Artificial sweeteners – a recently recognized class of emerging environmental contaminants: a review. *Anal. Bioanal. Chem.* 403, 2503–2518.
- Legrini, O., Oliveros, E., Braun, A.M., 1993. Photochemical processes for water treatment. *Chem. Rev.* 93, 671–698.
- Li, A.J., Schmitz, O.J., Stephan, S., Lenzen, C., Yue, P.Y.-K., Li, K., Li, H., Leung, K.S.-Y., 2016. Photocatalytic transformation of acesulfame: transformation products identification and embryotoxicity study. *Water Res.* 89, 68–75.
- Liang, C., Bruell, C.J., Marley, M.C., Sperry, K.L., 2004. Persulfate oxidation for in situ remediation of TCE. I. Activated by ferrous ion with and without a persulfate-thiosulfate redox couple. *Chemosphere* 55, 1213–1223.
- Liang, C., Huang, C.-F., Mohanty, N., Kurakalva, R.M., 2008. A rapid spectrophotometric determination of persulfate anion in ISCO. *Chemosphere* 73 (9), 1540–1543.
- Liao, C.-H., Kang, S.-F., Wu, F.-A., 2001. Hydroxyl radical scavenging role of chloride and bicarbonate ions in the H₂O₂/UV process. *Chemosphere* 44, 1193–1200.
- Litter, M.I., Quici, N., 2010. Photochemical advanced oxidation processes for water and wastewater treatment. *Recent Pat. Eng.* 4, 217–241.
- Matzek, L.W., Carter, K.E., 2016. Activated persulfate for organic chemical degradation: a review. *Chemosphere* 151, 178–188.
- Monteagudo, J.M., Durán, A., González, R., Expósito, A.J., 2015. In situ chemical oxidation of carbamazepine solutions using persulfate simultaneously activated by heat energy, UV light, Fe²⁺ ions, and H₂O₂. *Appl. Catal. B Environ.* 176–177, 120–129.
- Oh, W.-D., Dong, Z., Lim, T.-T., 2016. Generation of sulfate radical through heterogeneous catalysis for organic contaminants removal: current development, challenges and prospects. *Appl. Catal. B Environ.* 194, 169–201.
- Pignatello, J.J., Oliveros, E., Mackay, E.A., 2006. Advanced oxidation processes for organic contaminant destruction based on the Fenton reaction and related chemistry. *Crit. Rev. Environ. Sci. Technol.* 36, 1–84.
- Pouran, S.R., Aziz, A.R.A., Daud, W.M.A.W., 2015. Review on the main advances in photo-Fenton oxidation system for recalcitrant wastewaters. *J. Ind. Eng. Chem.* 21, 53–69.
- Punturat, V., Huang, K.-L., 2016. Degradation of acesulfame in aqueous solutions by electro-oxidation. *J. Taiwan Inst. Chem. Eng.* 63, 286–294.
- Ribeiro, A.R., Nunes, O.C., Pereira, M.F.R., Silva, A.M.T., 2015. An overview on the advanced oxidation processes applied for the treatment of water pollutants defined in the recently launched Directive 2013/39/EU. *Environ. Int.* 75, 33–51.
- Rubio, D., Nebot, E., Casanueva, J.F., Pulgarin, C., 2013. Comparative effect of simulated solar light, UV, UV/H₂O₂ and photo-Fenton treatment (UV-Vis/H₂O₂/Fe²⁺,³⁺) in the *Escherichia coli* inactivation in artificial seawater. *Water Res.* 47, 6367–6379.
- Sang, Z., Jiang, Y., Tsoi, Y.-K., Leung, K.S.-Y., 2014. Evaluating the environmental impact of artificial sweeteners: a study of their distributions, photodegradation and toxicities. *Water Res.* 52, 260–274.
- Scheurer, M., Brauch, H.-J., Lange, F.T., 2009. Analysis and occurrence of seven artificial sweeteners in German waste water and surface water and in soil aquifer treatment (SAT). *Anal. Bioanal. Chem.* 394, 1585–1594.
- Scheurer, M., Godejohann, M., Wick, A., Happel, O., Ternes, T.A., Brauch, H.-J., Ruck, W.K., Lange, F.T., 2012. Structural elucidation of main ozonation products of the artificial sweeteners cyclamate and acesulfame. *Environ. Sci. Pollut. Res. Int.* 19, 1107–1118.
- Scheurer, M., Schmutz, B., Happel, O., Brauch, H.-J., Wülser, R., Storck, F.R., 2014. Transformation of the artificial sweetener acesulfame by UV light. *Sci. Total Environ.* 481, 425–432.
- Stolte, S., Steudte, S., Schebb, N.H., Willenberg, I., Stepnowski, P., 2013. Ecotoxicity of artificial sweeteners and steviolosides. *Environ. Int.* 60, 123–127.
- Toth, J.E., Rickman, K.A., Verner, A.R., Kiddle, J.J., Mezyk, S.P., 2012. Reaction kinetics and efficiencies for the hydroxyl and sulfate radical based oxidation of artificial sweeteners in water. *J. Phys. Chem. A* 116, 9819–9824.
- Tran, N.H., Gan, J., Nguyen, V.T., Chen, H., You, L., Duarah, A., Zhang, L., Gin, K.Y.-H., 2015. Sorption and biodegradation of artificial sweeteners in activated sludge processes. *Biores. Technol.* 197, 329–338.
- Trapido, M., Epold, I., Bolobajev, J., Dulova, N., 2014. Emerging micropollutants in water/wastewater: growing demand on removal technologies. *Environ. Sci. Pollut. Res.* 21, 12217–12222.
- Tsionaki, A., Petri, B., Crimi, M., Mosabaek, H., Siegrist, R.L., Bjerg, P.L., 2010. In situ chemical oxidation of contaminated soil and groundwater using persulfate: a review. *Crit. Rev. Environ. Sci. Technol.* 40, 55–91.
- Vicente, F., Santos, A., Romero, A., Rodriguez, S., 2011. Kinetic study of diuron oxidation and mineralization by persulfate: effects of temperature, oxidant concentration and iron dosage method. *Chem. Eng. J.* 170, 127–135.
- Xu, X.-R., Li, X.-Y., Li, X.-Z., Li, H.-B., 2009. Degradation of melatonin by UV, UV/H₂O₂, Fe²⁺/H₂O₂ and UV/H₂O₂/Fe²⁺ processes. *Sep. Purif. Technol.* 68, 261–266.
- Xu, Y., Lin, Z., Zhang, H., 2016. Mineralization of sucralose by UV-based oxidation processes: UV/PDS versus UV/H₂O₂. *Chem. Eng. J.* 285, 392–401.
- Zhang, B.-T., Zhang, Y., Teng, Y., Fan, M., 2015. Sulfate radical and its application in decontamination technologies. *Crit. Rev. Environ. Sci. Technol.* 45, 1756–1800.

PAPER IV

Dulova, N., **Kattel, E.**, Trapido, M. Degradation of naproxen by ferrous ion-activated hydrogen peroxide, persulfate and combined hydrogen peroxide/persulfate processes: the effect of citric acid addition. – *Chemical Engineering Journal*, 2017, 318, 254–263.

Reproduced with the permission of Elsevier.



Degradation of naproxen by ferrous ion-activated hydrogen peroxide, persulfate and combined hydrogen peroxide/persulfate processes: The effect of citric acid addition



Niina Dulova*, Eneliis Kattel, Marina Trapido

Department of Chemical Engineering, Tallinn University of Technology, Ehitajate tee 5, Tallinn 19086, Estonia

HIGHLIGHTS

- Addition of CA showed promoting effect on NPX degradation by all systems at $\text{pH}_0 > 3$.
- $\text{S}_2\text{O}_8^{2-}/\text{Fe}^{2+}/\text{CA}$ proved the most effective in NPX degradation at a wide range of pH.
- Non-purgeable organic carbon was degraded gradually during the NPX mineralization.
- HO^\cdot was proposed as the predominant radical in activated $\text{H}_2\text{O}_2/\text{S}_2\text{O}_8^{2-}$ systems.
- NPX transformation products were identified in all CA- Fe^{2+} -activated systems.

ARTICLE INFO

Article history:
Available online 4 July 2016

Keywords:
Naproxen
Chelating agent
Fenton process
Ferrous ion-activated persulfate
In situ chemical oxidation

ABSTRACT

Naproxen (NPX), a widely used non-steroidal anti-inflammatory drug, has been detected extensively in different environmental systems at concentrations ranging from ng/L to $\mu\text{g/L}$, which may have a detrimental effect on human health and natural ecosystems. In this study, the degradation of NPX by citric acid (CA) chelated ferrous ion-activated hydrogen peroxide, persulfate and an innovative combined hydrogen peroxide/persulfate system was evaluated. The addition of CA at an appropriate complexation ratio considerably improved the target compound decomposition by the applied systems. Among the studied processes, the $\text{S}_2\text{O}_8^{2-}/\text{Fe}^{2+}/\text{CA}$ system showed the highest performance in NPX degradation at a wide range of pH followed by the combined $\text{H}_2\text{O}_2/\text{S}_2\text{O}_8^{2-}/\text{Fe}^{2+}/\text{CA}$ process. Limited elimination of non-purgeable organic carbon (NPOC) was observed during the mineralization of NPX by the examined systems. The results of radicals scavenging experiments indicated that both HO^\cdot and SO_3^\cdot contributed to the overall oxidation performance in the activated $\text{S}_2\text{O}_8^{2-}$ and $\text{H}_2\text{O}_2/\text{S}_2\text{O}_8^{2-}$ systems, but the former was the principal radical in the combined process. Transformation products (TPs) were identified using LC–MS analysis in the CA- Fe^{2+} -activated systems. Potential NPX degradation mechanism was subsequently proposed revealing hydroxylation with the subsequent decarboxylation or demethoxylation as the main step of the TPs formation. The findings of this study strongly suggest that the CA- Fe^{2+} -activated $\text{S}_2\text{O}_8^{2-}$ and combined $\text{H}_2\text{O}_2/\text{S}_2\text{O}_8^{2-}$ oxidation are promising treatment technologies for the abatement of NPX pollution in natural aqueous matrices.

© 2016 Elsevier B.V. All rights reserved.

1. Introduction

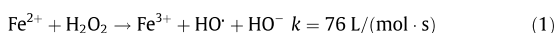
The introduction of non-steroidal anti-inflammatory drugs (NSAIDs) into natural matrices such as drinking water, surface water, groundwater, seawater, sediments and soil is an emerging problem due to their potential harmful effect on human health and natural ecosystems [1–4]. Most of NSAIDs are not fully

metabolized after application, only partially oxidized by conventional treatment processes used in wastewater treatment plants, and as a result found in the environment in an unchanged or slightly modified active form [5]. Naproxen (NPX) is a non-steroidal anti-inflammatory drug with analgesic and antipyretic properties, widely used for the treatment of rheumatoid arthritis as well as in the veterinary medicine. Similarly to other NSAIDs, NPX and its intermediates have been detected in different environments at concentrations ranging from ng/L to $\mu\text{g/L}$ [6–8]. Therefore, the development of effective remediation technology for

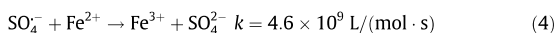
* Corresponding author.
E-mail address: niina.dulova@ttu.ee (N. Dulova).

elimination of NSAIDs, including NPX, from natural matrices, such as groundwater, is of great scientific and public interest.

Among the various chemical, physical and biological technologies used in the remediation of organically contaminated groundwater, *in situ* chemical oxidation (ISCO) is the most promising one due to its feasibility to degrade a wide range of bio-recalcitrant contaminants, relatively fast treatment and cost-effectiveness as well as potentially enhanced post-oxidation microbial activity [9,10]. The ISCO is typically implemented by the application of systems based on hydrogen peroxide (H₂O₂), permanganate (MnO₄⁻), ozone (O₃), persulfate (S₂O₈²⁻), or a combination of them [9,11,12]. The Fenton treatment is widely studied and used technology for *in situ* groundwater and soil remediation based on the generation of hydroxyl radicals (HO•) from iron-activated hydrogen peroxide decomposition [13]. The commonly accepted Fenton mechanism consists of a chain reaction, where Eq. (1) is known as the Fenton reaction implying the oxidation of ferrous iron ions (Fe²⁺) to decompose H₂O₂ into HO• and Eq. (2) is so-called Fenton-like reaction representing the activator regeneration by H₂O₂ decomposition into hydroperoxyl radical (HO₂) [14,15]:



Persulfate is an alternative ISCO oxidant, which has the potential to overcome some limitations associated with activated hydrogen peroxide environmental applications [16–19]. The activation of persulfate by heat, UVC light or ultrasound (US), transition metal, base, peroxide or ozone leads to the generation of sulfate radicals (SO₄^{-•}) [12,20,21]. Among different transition metals used in persulfate activation [22], iron in its ferrous form is the most frequently studied activator for ISCO applications [12,16,18]. However, ferrous ion-activated persulfate oxidation has its limitations related mainly to the fast conversion of Fe²⁺ into Fe³⁺ via Eq. (3) leading to the rapid termination of persulfate activation and the fast scavenging of SO₄^{-•} by excessive Fe²⁺ through Eq. (4) eventually causing the reduction in treatment efficacy [16,23,24]:



Moreover, in the both above-mentioned ISCO technologies iron is used initially in a soluble Fe²⁺ form to activate oxidant; however aqueous iron is relatively insoluble at the ambient pH ≥ 5 of most natural aquifer systems and tend to precipitate in the form of amorphous ferric oxyhydroxides [25]. Thus, to adjust the availability of Fe²⁺ and to stabilize its amount in aqueous matrices at natural pH values, chelating agents such as ethylenediaminetetraacetic acid (EDTA) [17,26], ethylenediaminedisuccinate (EDDS) [27–29], sodium polyphosphates (STPP, TSPP) [17,27], oxalic acid (OA) [26,29], tartaric acid [26,29] and citric acid/citrates (CA) [17,27,29] could be employed in ISCO applications. The latter, CA, proved to be the most feasible chelating agent both for Fe²⁺-activated hydrogen peroxide and persulfate oxidation of chlorophenols [27] and the most efficient one for aniline decomposition by Fe²⁺-activated persulfate system [29].

Therefore, in the present study the potential of H₂O₂/Fe²⁺/CA, S₂O₈²⁻/Fe²⁺/CA and combined H₂O₂/S₂O₈²⁻/Fe²⁺/CA systems in NPX decomposition was assessed. According to the available literature, the application of radical-based advanced oxidation technologies (AOTs), including UVC/H₂O₂ system [30,31], O₃/H₂O₂ and O₃/UVC processes [32], O₃/TiO₂ oxidation [32], sonolysis and combined US/Fenton/TiO₂ system [33], photo-Fenton and photo-Fenton-like systems [31,34], photocatalysis [32], and thermally activated persulfate oxidation [35], proved to be a promising solution for NPX

degradation in aqueous matrices. However, the application of Fe²⁺-activated persulfate and combined hydrogen peroxide/persulfate systems for NPX decomposition in aqueous solution was not previously evaluated.

The main objective of this study was to investigate and compare the degradation of NPX by citric acid chelated ferrous ion-activated hydrogen peroxide, persulfate and innovative combined hydrogen peroxide/persulfate systems. The effect of pH and different initial oxidant, activator and chelating agent concentrations were evaluated. The consumption of hydrogen peroxide and persulfate as well as mineralization and degradation mechanism of NPX were also studied. It is expected that the results of this study can provide valuable information on the degradation of NPX by these radical-based AOTs applied as an ISCO approach for groundwater remediation.

2. Materials and methods

2.1. Chemicals and materials

All chemicals were of the highest purity commercially available and used without further purification. Naproxen (Fig. 1; C₁₄H₁₄O₃, ≥98%, molecular weight 230.26 g/mol, pK_a = 4.45 [36], hydrogen peroxide (H₂O₂, PERDROGENTM, ≥30%), sodium persulfate (Na₂S₂O₈, ≥99%), ferrous sulfate heptahydrate (FeSO₄·7H₂O, ≥99%), citric acid monohydrate (C₆H₈O₇·H₂O, ≥99%), sodium sulfite (Na₂SO₃, ≥98%), sodium hydroxide (NaOH, ≥98%), and sulfuric acid (H₂SO₄, 95–98%) were purchased from Sigma-Aldrich. Acetonitrile (CH₃CN, LiChrosolv[®]), ethanol (C₂H₆O, EtOH, 99%), formic acid (CH₂O₂, 99%), and tertiary butanol ((CH₃)₃COH, *t*-BuOH, ≥99%) were purchased from Merck KGaA. Ultrapure water, generated by a Millipore Simplicity[®] UV System, was used for the preparation of all solutions used in the non-activated and activated hydrogen peroxide, persulfate and combined hydrogen peroxide/persulfate oxidation experiments.

2.2. Experimental procedure

The laboratory-scale experiments of the activated hydrogen peroxide (H₂O₂), persulfate (S₂O₈²⁻) and combined H₂O₂/S₂O₈²⁻ systems were performed in batch mode at ambient room temperature (22 ± 1 °C). No buffer solution was used to avoid any interference related to potential reactions between hydroxyl and sulfate radicals and buffer species. NPX solutions (75 μM, 0.4 L) were treated in a 0.6-L cylindrical glass reactor with a permanent agitation speed (400 rpm) for a period of 3 h. The pH of the samples was adjusted to 3, 5, 7 or 9 by NaOH or H₂SO₄ aqueous solutions. The activator (FeSO₄·7H₂O, Fe²⁺) or activator/chelating agent (C₆H₈O₇·H₂O, CA) was added, and after complete dissolution of the activator or chelated activator, the oxidation was initiated by adding hydrogen peroxide and/or sodium persulfate. In the case of combined H₂O₂/S₂O₈²⁻ system, both oxidants were added simultaneously. Samples were withdrawn at pre-determined time intervals, corresponding to 0, 1, 5, 10, 15, 30, 60, 120 and 180 min. The oxidation quenching was done by the addition of Na₂SO₃ at a [oxidant]₀/SO₃²⁻ molar ratio (m/m) of 1/10 or by the addition of 1 M NaOH solution to adjust the pH to ~9. The experiments on NPX oxidation with non-activated

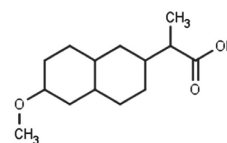


Fig. 1. Molecular structure of NPX.

hydrogen peroxide or persulfate were conducted in identical reactors and treatment conditions for the respective activated oxidation trials. All experiments were duplicated; the results of the analysis are presented as the mean with a standard deviation of at least three parallel replicates less than 5%.

2.3. Identification of hydroxyl and sulfate radicals

Radical scavengers were applied to identify the radicals formed during the $S_2O_8^{2-}/Fe^{2+}$ and combined $H_2O_2/S_2O_8^{2-}/Fe^{2+}$ processes. To differentiate the role of $HO\cdot$ and $SO_4\cdot^-$ in NPX degradation by the $S_2O_8^{2-}/Fe^{2+}$ and $H_2O_2/S_2O_8^{2-}/Fe^{2+}$ systems two radical probes, EtOH and *t*-BuOH, were employed. An excessive amount of scavenger was spiked into the reaction solutions before the activator or chelated activator and the oxidant addition at a $NPX/[scavenger]_0$ m/m of 1/500.

2.4. Analytical methods

The pH was measured using a digital pH/Ion meter (Mettler Toledo S220). The initial hydrogen peroxide concentration in the stock solutions was measured spectrophotometrically at $\lambda = 254$ nm (the molar extinction coefficient of H_2O_2 at 254 nm is 19.6 L/(mol·cm)); the residual hydrogen peroxide concentration in the treated samples was measured spectrophotometrically at $\lambda = 410$ nm with titanium sulfate by a hydrogen peroxide- Ti^{4+} complex formation [37] by a Helios- β UV/VIS spectrophotometer (Thermo Electron Corporation). The residual persulfate concentration in the treated samples was measured spectrophotometrically at $\lambda = 446$ nm with *o*-dianisidine by a *o*-dianisidine-peroxydisulfate complex formation [38]. The Fe^{2+} concentration in the solution was measured spectrophotometrically at $\lambda = 492$ nm using the *o*-phenanthroline method [39]. The non-purgeable organic carbon (NPOC) was measured by a TOC analyzer multi N/C[®] 3100 (Analytik Jena).

The evolution of NPX concentration was monitored by means of a high performance liquid chromatography combined with diode array detector (HPLC-PDA, Prominence SPD-M20A, Shimadzu) equipped with a Phenomenex Gemini (150 × 2.0 mm, 1.7 μ m) NX-C18 (110 Å, 5 μ m) column. The isocratic method with a solvent mixture of 40% acetonitrile and 60% formic acid (0.1%) aqueous solution was applied. The flow rate was kept at 0.2 mL/min. Samples were scanned at 190–800 nm and analyzed at $\lambda = 232$ nm. The concentration of NPX was determined by using the standard multipoint calibration.

2.5. Identification of NPX transformation products

The samples from selected trials were analyzed by the high-performance liquid chromatography combined with mass spectrometer (HPLC-MS, Shimadzu LC-MS 2020). Phenomenex Gemini-NX 5u C18 110A 150 × 2.0 mm column, inner diameter 1.7 μ m, was used with isocratic eluents mixture, 0.3% formic acid aqueous solution (60%) and acetonitrile (40%), and total flow rate of 0.2 mL/min. Mass spectra were acquired in full-scan mode (scanning in the range 50–500 *m/z*). The instrument was operated in positive ESI mode and the results obtained with MS detector were handled using Shimadzu LabSolutions software.

3. Results and discussion

3.1. Ferrous ion-activated oxidation

As presented in Fig. 2(a,b), the degradation of NPX was negligible by direct hydrogen peroxide and persulfate oxidation while it

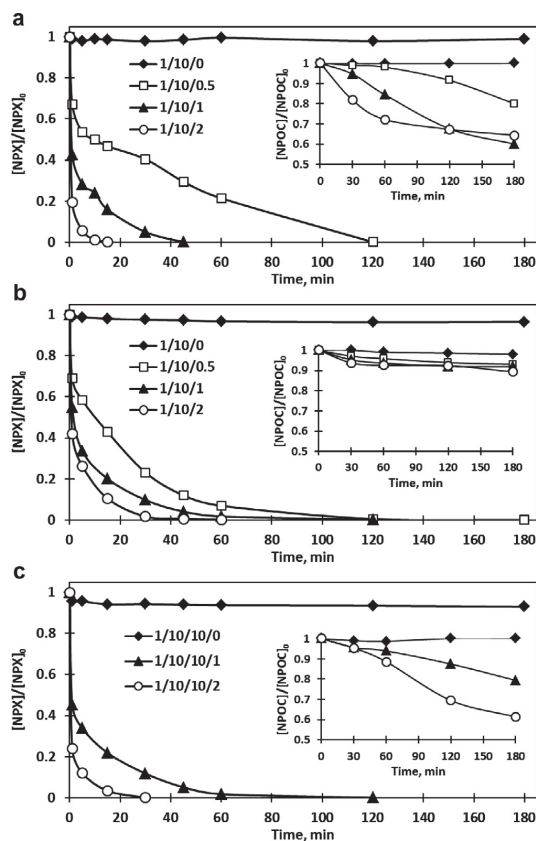


Fig. 2. NPX degradation and NPOC reduction by (a) the H_2O_2/Fe^{2+} process ($NPX/H_2O_2/Fe^{2+}$ is a molar ratio, $[H_2O_2]_0 = 750 \mu M$), (b) the $S_2O_8^{2-}/Fe^{2+}$ process ($NPX/S_2O_8^{2-}/Fe^{2+}$ is a molar ratio, $[S_2O_8^{2-}]_0 = 750 \mu M$), (c) the $H_2O_2/S_2O_8^{2-}/Fe^{2+}$ process ($NPX/H_2O_2/S_2O_8^{2-}/Fe^{2+}$ is a molar ratio, $[H_2O_2]_0 = [S_2O_8^{2-}]_0 = 750 \mu M$): effect of initial Fe^{2+} concentration ($pH_0 = 3$).

was considerably accelerated by ferrous ion activation of both oxidants. Accordingly, the increase in applied activator dose at a fixed oxidant initial concentration of 750 μM , corresponding to a NPX/H_2O_2 and $NPX/S_2O_8^{2-}$ m/m of 1/10 for the H_2O_2/Fe^{2+} and $S_2O_8^{2-}/Fe^{2+}$ system, respectively, resulted in a stable improvement in the NPX degradation efficacy. Overall, the efficacy of target compound degradation in the $S_2O_8^{2-}/Fe^{2+}$ process was lower compared with the H_2O_2/Fe^{2+} process at the same $NPX/oxidant/Fe^{2+}$ ratios. For instance, the application of $NPX/oxidant/Fe^{2+}$ m/m/m of 1/10/1 resulted in >99% NPX removal after 45 and 120 min of the Fe^{2+} -activated H_2O_2 and $S_2O_8^{2-}$, respectively. The tendency of NPX mineralization proved similar to the target compound degradation trend for the studied systems and in general was enhanced with increases in the activator dose (Fig. 2(a,b)). Conversely, the mineralization was considerably lower than the target compound removal, and thus the highest obtained NPOC reduction under the studied treatment conditions was 40% at a $NPX/H_2O_2/Fe^{2+}$ m/m/m of 1/10/1 and 11% at a $NPX/S_2O_8^{2-}/Fe^{2+}$ m/m/m of 1/10/2; mainly indicating the accumulation of NPX transformation products (TPs) in the oxidized solution. Notably, both the tendency of NPOC removal and NPX degradation were consistent with the dissociation of oxidant, which was more complete in the case of the elevated activator dose (Table 1).

It should be noted that in the $\text{H}_2\text{O}_2/\text{Fe}^{2+}$ and $\text{S}_2\text{O}_8^{2-}/\text{Fe}^{2+}$ system, the entire reaction was divided into two stages: the first period of fast NPX degradation and the second period of gradual NPX oxidation. Consequently, more than 45% and 54% of NPX was removed during the first minute and the rest of the 120 min oxidation, respectively, in the $\text{S}_2\text{O}_8^{2-}/\text{Fe}^{2+}$ system at a NPX/ $\text{S}_2\text{O}_8^{2-}/\text{Fe}^{2+}$ m/m/m of 1/10/1. In the case of $\text{H}_2\text{O}_2/\text{Fe}^{2+}$ process (NPX/ $\text{H}_2\text{O}_2/\text{Fe}^{2+}$ m/m/m 1/10/1), almost 57% and 43% of NPX was degraded during the first period and the rest of the 45 min oxidation indicating higher efficacy of this process in NPX decomposition during the second period as compared to the $\text{S}_2\text{O}_8^{2-}/\text{Fe}^{2+}$ system. This finding was also supported by Fe^{2+} concentration profile measurements in reaction mixture. The obtained results indicated a fast drop in the Fe^{2+} concentration to 27.5% and 25.8% from the initial concentration of 75 μM during the first minute of oxidation in the $\text{H}_2\text{O}_2/\text{Fe}^{2+}$ (NPX/ $\text{H}_2\text{O}_2/\text{Fe}^{2+}$ m/m/m 1/10/1) and $\text{S}_2\text{O}_8^{2-}/\text{Fe}^{2+}$ (NPX/ $\text{S}_2\text{O}_8^{2-}/\text{Fe}^{2+}$ m/m/m 1/10/1) system, respectively. However, the Fe^{2+} concentration in solution started to increase after 5 min of the $\text{H}_2\text{O}_2/\text{Fe}^{2+}$ oxidation reaching a plateau at $\sim 36 \mu\text{M}$ after 30 min. In the $\text{S}_2\text{O}_8^{2-}/\text{Fe}^{2+}$ system no increase in the Fe^{2+} concentration during the rest of 120 min oxidation was observed. The latter observation is consistent with the previously reported studies [17,40,41] and could be explained by rapid generation of SO_4^- through the dissociation of $\text{S}_2\text{O}_8^{2-}$ immediately after the activation and fast accumulation of Fe^{3+} , which is most likely subsequently slowly reduced in the reaction with organic radicals (R $^\cdot$) as presented in Eq. (5):



Therefore, in order to facilitate the Fe^{3+} reduction in ferrous ion-activated persulfate processes as well as to evaluate the superiority and synergetic effect of the $\text{H}_2\text{O}_2/\text{Fe}^{2+}$, $\text{S}_2\text{O}_8^{2-}/\text{Fe}^{2+}$ and $\text{S}_2\text{O}_8^{2-}/\text{H}_2\text{O}_2$ systems the combined $\text{H}_2\text{O}_2/\text{S}_2\text{O}_8^{2-}/\text{Fe}^{2+}$ system was studied (Fig. 2(c)). The chemistry of the latter process is still uncertain: the suggested activation mechanisms include the HO^\cdot generation from H_2O_2 or the heat release from the exothermic H_2O_2 reactions [12]. The efficacy of NPX degradation by the peroxide-activated $\text{S}_2\text{O}_8^{2-}$ was assessed at a NPX/ $\text{H}_2\text{O}_2/\text{S}_2\text{O}_8^{2-}$ m/m/m of 1/10/10; the

results indicated less than 4% NPX degradation and negligible NPOC reduction after 180 min of oxidation. It should be noted that similar to the $\text{H}_2\text{O}_2/\text{Fe}^{2+}$ and $\text{S}_2\text{O}_8^{2-}/\text{Fe}^{2+}$ oxidation the two stage mechanism of reaction was observed in the combined $\text{H}_2\text{O}_2/\text{S}_2\text{O}_8^{2-}/\text{Fe}^{2+}$ system. The results presented in Fig. 2 clearly indicated a more fast decrease in NPX concentration during the first minute in the $\text{H}_2\text{O}_2/\text{S}_2\text{O}_8^{2-}/\text{Fe}^{2+}$ process compared with the $\text{H}_2\text{O}_2/\text{Fe}^{2+}$ and $\text{S}_2\text{O}_8^{2-}/\text{Fe}^{2+}$ systems, demonstrating the synergetic action of both processes. On the other hand, taking into consideration the two-fold higher activator dose added into the Fe^{2+} -activated $\text{H}_2\text{O}_2/\text{S}_2\text{O}_8^{2-}$ system, the overall efficacy of the $\text{H}_2\text{O}_2/\text{S}_2\text{O}_8^{2-}/\text{Fe}^{2+}$ process in NPX decomposition was in general higher than in the $\text{S}_2\text{O}_8^{2-}/\text{Fe}^{2+}$ system but to a certain degree lower than in the $\text{H}_2\text{O}_2/\text{Fe}^{2+}$ process, mainly suggesting the existence of concurrent reactions of the oxidants with the activator in the $\text{H}_2\text{O}_2/\text{S}_2\text{O}_8^{2-}/\text{Fe}^{2+}$ system. Accordingly, 40%, 8% and 21(39)% of the initial NPOC concentration was removed after 180 min of oxidation by the $\text{H}_2\text{O}_2/\text{Fe}^{2+}$ system at a NPX/ $\text{H}_2\text{O}_2/\text{Fe}^{2+}$ m/m/m of 1/10/1, the $\text{S}_2\text{O}_8^{2-}/\text{Fe}^{2+}$ system at a NPX/ $\text{S}_2\text{O}_8^{2-}/\text{Fe}^{2+}$ m/m/m of 1/10/1, and the combined $\text{H}_2\text{O}_2/\text{S}_2\text{O}_8^{2-}/\text{Fe}^{2+}$ system at a NPX/ $\text{H}_2\text{O}_2/\text{S}_2\text{O}_8^{2-}/\text{Fe}^{2+}$ m/m/m/m of 1/10/10/1(2), respectively (Fig. 2).

In the combined $\text{H}_2\text{O}_2/\text{S}_2\text{O}_8^{2-}/\text{Fe}^{2+}$ system, the measurement of residual concentrations of $\text{S}_2\text{O}_8^{2-}$ was interfered with the presence of H_2O_2 in samples. In contrast, the presence of residual $\text{S}_2\text{O}_8^{2-}$ still permitted the measurement of undissociated H_2O_2 (Table 1). Accordingly, the increase in activator dose improved the consumption of H_2O_2 in the combined system, and only 6% of residual oxidant was detected after 180 min of oxidation at a NPX/ $\text{H}_2\text{O}_2/\text{S}_2\text{O}_8^{2-}/\text{Fe}^{2+}$ m/m/m/m of 1/10/10/2.

The pH value of the aqueous matrix is known to be a limiting factor in iron-activated ISCO applications. Therefore, the effect of pH_0 on the decomposition of NPX in the studied systems was evaluated and the results are presented in Fig. 3. The efficacy of NPX decomposition was found to decrease steadily with the increase in the pH_0 value in the $\text{H}_2\text{O}_2/\text{Fe}^{2+}$ and $\text{H}_2\text{O}_2/\text{S}_2\text{O}_8^{2-}/\text{Fe}^{2+}$ system. Although Fe^{2+} salts are quite soluble in aqueous matrices even at neutral pH values, ferrous ions tend to co-precipitate with amorphous ferric oxyhydroxides if the pH is brought up above 3 [42]. As a result, the efficacy of organic compounds oxidative degradation by the Fenton and related systems usually the highest at a pH value ~ 3 mainly due to the speciation of Fe^{3+} [15,42]. In the case of $\text{S}_2\text{O}_8^{2-}/\text{Fe}^{2+}$ process, the results revealed the comparable performance of NPX degradation and mineralization at pH_0 values of 3, 5 and 7, suggesting a high potential of this system for ISCO applications at natural pH values. These findings are consistent with the previous studies regarding organic pollutants degradation by the Fe^{2+} -activated $\text{S}_2\text{O}_8^{2-}$ systems [41,43]. It should be noted that the solution pH in all trials decreased to around 3–4 after 180 min of oxidation, mainly due to acidity of activator and oxidant as well as formation of acidic intermediate product during the reactions (Table 1).

3.2. Citric acid chelated ferrous ion-activated oxidation

To evaluate the effect of chelating agent concentration on NPX degradation in the $\text{H}_2\text{O}_2/\text{Fe}^{2+}/\text{CA}$, $\text{S}_2\text{O}_8^{2-}/\text{Fe}^{2+}/\text{CA}$ and $\text{H}_2\text{O}_2/\text{S}_2\text{O}_8^{2-}/\text{Fe}^{2+}/\text{CA}$ system the experiments were conducted at different metal/ligand molar ratios. Citric acid has three carboxyl dentates, and thus will completely chelate Fe^{2+} to form a hexacoordinated complex at a Fe^{2+}/CA molar ratio of 1/2. Thus, four Fe^{2+}/CA molar ratios of 1/0.1, 1/0.5, 1/1 and 1/2 were studied at the same NPX/ H_2O_2 , NPX/ $\text{S}_2\text{O}_8^{2-}$ or NPX/ $\text{H}_2\text{O}_2/\text{S}_2\text{O}_8^{2-}$ molar ratio of 1/10, 1/10 or 1/10/10, respectively. Fig. 4 shows the NPX degradation and NPOC removal profiles for different CA- Fe^{2+} -activated oxidation systems at pH_0 3. It should be noted that in the case of CA- Fe^{2+} -activated processes, the overall NPOC concentration consisted of NPOC_{NPX}

Table 1
Final pH values and residual oxidant concentrations in different Fe^{2+} -activated systems under various treatment conditions ([NPX] $_0$ = 75 μM , t = 180 min).

Process	Molar ratio	pH $_0$	pH	[oxidant],% remained	
$\text{H}_2\text{O}_2/\text{Fe}^{2+}$	NPX/ $\text{H}_2\text{O}_2/\text{Fe}^{2+}$			[H_2O_2]	
		1/10/0	3	3.00	99.8
		1/10/0.5	3	2.99	22.2
		1/10/1	3	2.96	3.9
		1/10/2	3	2.95	0
		1/10/1	5	3.55	8.0
		1/10/1	7	4.01	31.1
$\text{S}_2\text{O}_8^{2-}/\text{Fe}^{2+}$	NPX/ $\text{S}_2\text{O}_8^{2-}/\text{Fe}^{2+}$			[$\text{S}_2\text{O}_8^{2-}$]	
		1/10/0	3	2.96	98.4
		1/10/0.5	3	2.94	84.8
		1/10/1	3	2.90	73.7
		1/10/2	3	2.88	66.9
		1/10/1	5	3.27	83.8
		1/10/1	7	3.54	88.1
$\text{H}_2\text{O}_2/\text{S}_2\text{O}_8^{2-}/\text{Fe}^{2+}$	NPX/ $\text{H}_2\text{O}_2/\text{S}_2\text{O}_8^{2-}/\text{Fe}^{2+}$			[H_2O_2]	
		1/10/10/0	3	2.98	97.9
		1/10/10/1	3	2.86	38.8
		1/10/10/2	3	2.72	5.7
		1/10/10/1	5	3.17	46.5
		1/10/10/1	7	3.35	59.0
		1/10/10/1	9	3.54	69.1

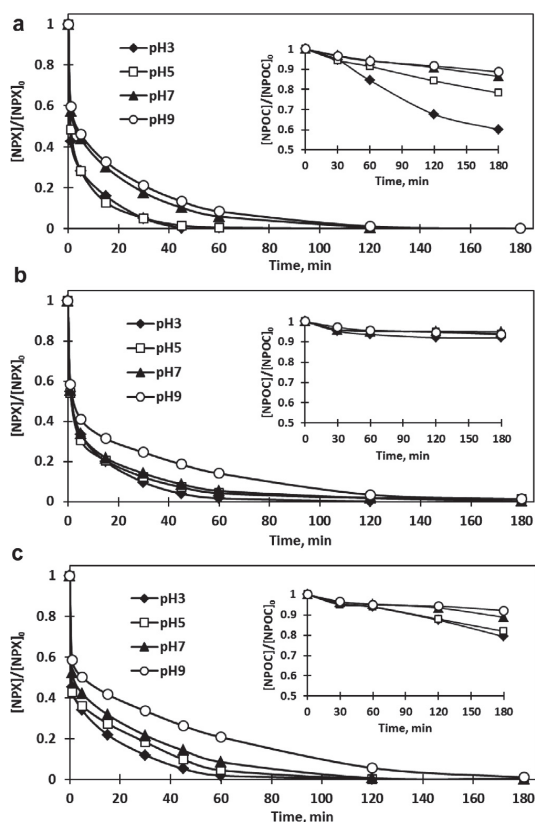


Fig. 3. NPX degradation and NPOC reduction by (a) the $\text{H}_2\text{O}_2/\text{Fe}^{2+}$ process (NPX/ $\text{H}_2\text{O}_2/\text{Fe}^{2+}$ molar ratio of 1/10/1), (b) the $\text{S}_2\text{O}_8^{2-}/\text{Fe}^{2+}$ process (NPX/ $\text{S}_2\text{O}_8^{2-}/\text{Fe}^{2+}$ molar ratio of 1/10/1), (c) the $\text{H}_2\text{O}_2/\text{S}_2\text{O}_8^{2-}/\text{Fe}^{2+}$ process (NPX/ $\text{H}_2\text{O}_2/\text{S}_2\text{O}_8^{2-}/\text{Fe}^{2+}$ molar ratio of 1/10/10/1): effect of initial pH ($[\text{NPX}]_0 = 75 \mu\text{M}$).

and NPOC_{CA} . Among the studied oxidation processes, the highest improvement in target compound degradation and oxidant dissociation, as presented in Table 2, was observed in the $\text{S}_2\text{O}_8^{2-}/\text{Fe}^{2+}/\text{CA}$ system. Accordingly, the noticeable enhancement of NPX degradation and $\text{S}_2\text{O}_8^{2-}$ activation was observed at Fe^{2+}/CA molar ratios of 1/0.5 and 1/1 resulting in more than 99.9% NPX destruction after 60 and 45 min of oxidation, respectively, and more than 50% $\text{S}_2\text{O}_8^{2-}$ dissociation after 180 min of oxidation. A further increase in the chelating ligand concentration led to decrease in the oxidation efficacy. Other studies conducted at uncontrolled pH also reported effective organic contaminants degradation and $\text{S}_2\text{O}_8^{2-}$ activation in the $\text{S}_2\text{O}_8^{2-}/\text{Fe}^{2+}/\text{CA}$ systems with prudently optimized chelating agent concentration [17,27]. In the case of the classical $\text{H}_2\text{O}_2/\text{Fe}^{2+}$ system the addition of CA inhibited the efficacy of NPX degradation at the studied treatment conditions. Moreover, a clear strengthening of the inhibitive effect with the increase in the CA dose was observed. Accordingly, 95%, 89.8% and 79.3% of NPX were removed at a NPX/ $\text{H}_2\text{O}_2/\text{Fe}^{2+}/\text{CA}$ m/m/m/m of 1/10/1/0, 1/10/1/0.1 and 1/10/1/1, respectively, after 30 min of oxidation. In the same way, the H_2O_2 dissociation was evidently suppressed in the $\text{H}_2\text{O}_2/\text{Fe}^{2+}/\text{CA}$ system as presented in Table 2. Several reasons could be suggested to explain the inhibition of NPX degradation as well as H_2O_2 dissociation efficacy in the $\text{H}_2\text{O}_2/\text{Fe}^{2+}$ caused by the addition of chelating agent. Firstly, the strong complexation with CA

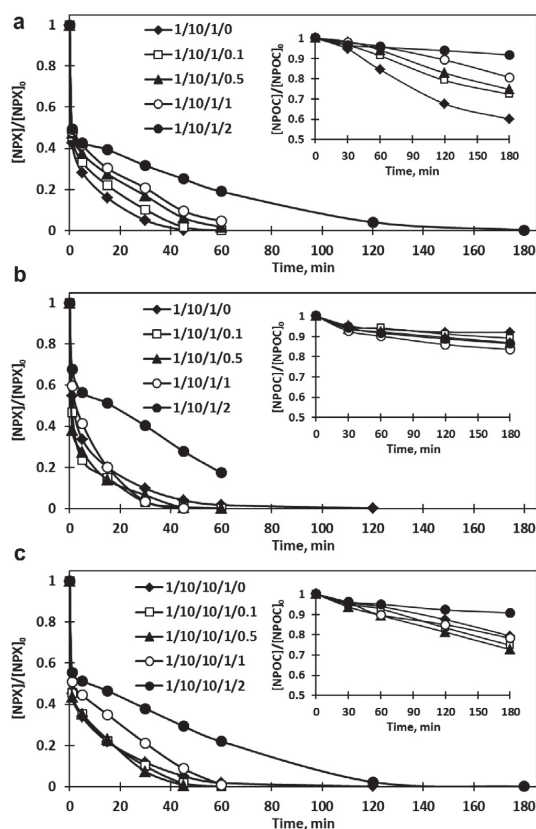


Fig. 4. NPX degradation and NPOC reduction by (a) the $\text{H}_2\text{O}_2/\text{Fe}^{2+}/\text{CA}$ process (NPX/ $\text{H}_2\text{O}_2/\text{Fe}^{2+}/\text{CA}$ is a molar ratio), (b) the $\text{S}_2\text{O}_8^{2-}/\text{Fe}^{2+}/\text{CA}$ process (NPX/ $\text{S}_2\text{O}_8^{2-}/\text{Fe}^{2+}/\text{CA}$ is a molar ratio), (c) the $\text{H}_2\text{O}_2/\text{S}_2\text{O}_8^{2-}/\text{Fe}^{2+}/\text{CA}$ process (NPX/ $\text{H}_2\text{O}_2/\text{S}_2\text{O}_8^{2-}/\text{Fe}^{2+}/\text{CA}$ is a molar ratio): effect of initial CA concentration ($[\text{Fe}^{2+}]_0 = 75 \mu\text{M}$, $\text{pH}_0 = 3$).

caused unavailability of soluble Fe^{2+} to react with H_2O_2 . Secondly, the chelating agent played a role of HO^\bullet scavenger ($k_{\text{CA},\text{HO}^\bullet} = 5.0 \times 10^7 \text{ L}/(\text{mol}\cdot\text{s})$ [44]), which in turn suppressed the destruction of NPX. Finally, the direct activator regeneration through Eq. (2) was more efficient than the CA assisted mechanism via Eq. (5) or the combined action of both reactions.

Compared to the Fe^{2+} -activated oxidation, the NPX degradation was enhanced in the $\text{H}_2\text{O}_2/\text{S}_2\text{O}_8^{2-}/\text{Fe}^{2+}/\text{CA}$ system when the appropriate concentration of CA was added, while the observed improvement was less significant as compared to the $\text{S}_2\text{O}_8^{2-}/\text{Fe}^{2+}$ system, mainly due to the influence of the $\text{H}_2\text{O}_2/\text{Fe}^{2+}$ fragment of the system chemistry. Notably, the NPX degradation in the $\text{S}_2\text{O}_8^{2-}/\text{Fe}^{2+}/\text{CA}$ and $\text{H}_2\text{O}_2/\text{S}_2\text{O}_8^{2-}/\text{Fe}^{2+}/\text{CA}$ systems was similar to that in the non-chelated processes and went through two stages, indicating the $\text{S}_2\text{O}_8^{2-}/\text{Fe}^{2+}$ fragment influence on the combined system mechanism. Thus, the highest improvement in NPX degradation and total mineralization was observed at a Fe^{2+}/CA molar ratio of 1/0.5 resulting in complete NPX destruction in less than 60 min of oxidation and 27.4% NPOC removal after 180 min of reaction. As in the case of the other two systems, an evident decrease in the NPX degradation and the overall mineralization was observed in the combined system at a Fe^{2+}/CA m/m of 1/2. This finding is consistent with the previous studies which demonstrated that the full complexation of Fe^{2+} by CA resulted in the reduced

Table 2

Final pH values and residual oxidant concentrations in different CA-Fe²⁺-activated systems under various treatment conditions ([NPX]₀ = 75 μM, t = 180 min).

Process	Molar ratio	pH ₀	pH	[oxidant],% remained
H ₂ O ₂ /Fe ²⁺ /CA	NPX/H ₂ O ₂ /Fe ²⁺ /CA			[H ₂ O ₂]
	1/10/1/0.1	3	2.96	4.3
	1/10/1/0.5	3	2.95	9.1
	1/10/1/1	3	2.93	15.8
	1/10/1/2	3	2.90	55.2
	1/10/1/0.1	5	3.85	2.7
	1/10/1/0.5	5	3.77	0.0
	1/10/1/1	5	3.74	1.2
	1/10/1/0.1	7	3.89	5.3
	1/10/1/1	7	3.77	1.9
	1/10/1/1	9	3.81	2.4
	S ₂ O ₈ ²⁻ /Fe ²⁺ /CA	NPX/S ₂ O ₈ ²⁻ /Fe ²⁺ /CA		
1/10/1/0.1		3	2.88	70.1
1/10/1/0.5		3	2.84	47.5
1/10/1/1		3	2.75	43.5
1/10/1/2		3	2.72	56.4
1/10/1/0.1		5	3.25	69.8
1/10/1/0.5		5	3.14	32.4
1/10/1/1		5	3.04	30.7
1/10/1/0.1		7	3.35	77.7
1/10/1/1		7	3.06	40.2
1/10/1/1		9	3.09	41.9
H ₂ O ₂ /S ₂ O ₈ ²⁻ /Fe ²⁺ /CA		NPX/H ₂ O ₂ /S ₂ O ₈ ²⁻ /Fe ²⁺ /CA		
	1/10/10/1/0.1	3	2.80	23.8
	1/10/10/1/0.5	3	2.77	26.3
	1/10/10/1/1	3	2.73	39.2
	1/10/10/1/2	3	2.71	70.7
	1/10/10/2/1	3	2.70	9.8
	1/10/10/2/2	3	2.59	23.1
	1/10/10/1/0.1	5	3.17	28.9
	1/10/10/1/0.5	5	2.99	20.2
	1/10/10/1/1	5	2.96	28.7
	1/10/10/1/0.1	7	3.16	41.5
	1/10/10/1/1	7	3.02	30.5
1/10/10/1/1	9	3.04	33.0	

availability of Fe²⁺ in solution along with the declined efficacy of oxidant dissociation and organic contaminant degradation [27,29,40].

In the case of CA-Fe²⁺-activated systems at pH₀ > 3, the important role of CA was to stabilize iron ions in solution by the combined mechanism including the decrease of solution pH₀, the formation of CA-Fe²⁺/Fe³⁺ complexes, and as a result the prevention of Fe³⁺ from precipitating into ferric oxyhydroxides. From Fig. 5 and Table 2, it can be seen that an increase in the pH₀ to 5 noticeably improved the efficacy of the H₂O₂/Fe²⁺/CA system in NPX degradation and oxidant activation as compared to the H₂O₂/Fe²⁺ process. The improved NPX degradation was observed even at a low Fe²⁺/CA molar ratio of 1/0.1 with more than 99.9% NPX removal in 60 min of oxidation as compared to the similar percent removal of NPX after 120 min of the non-chelated oxidation. The highest enhancement in NPX destruction and total mineralization as well as H₂O₂ dissociation was attained at a Fe²⁺/CA of 1/0.5. In the case of the S₂O₈²⁻/Fe²⁺/CA and combined H₂O₂/S₂O₈²⁻/Fe²⁺/CA system, the improvement in target compound degradation efficacy was also more evident at pH 5 as compared to the results obtained at pH 3 with the highest oxidation effectiveness observed at the same Fe²⁺/CA m/m of 1/1 and 1/0.5, respectively. A further increase in the pH₀ value revealed that irrespective of the applied oxidation process, the efficacy of NPX degradation and total mineralization was similar at pH 5, 7 and 9 (Fig. 6). Therefore, according to the results presented in Figs. 4–6 and Table 2, the S₂O₈²⁻/Fe²⁺/CA process proved the most effective and particularly promising technique for NPX degradation at a

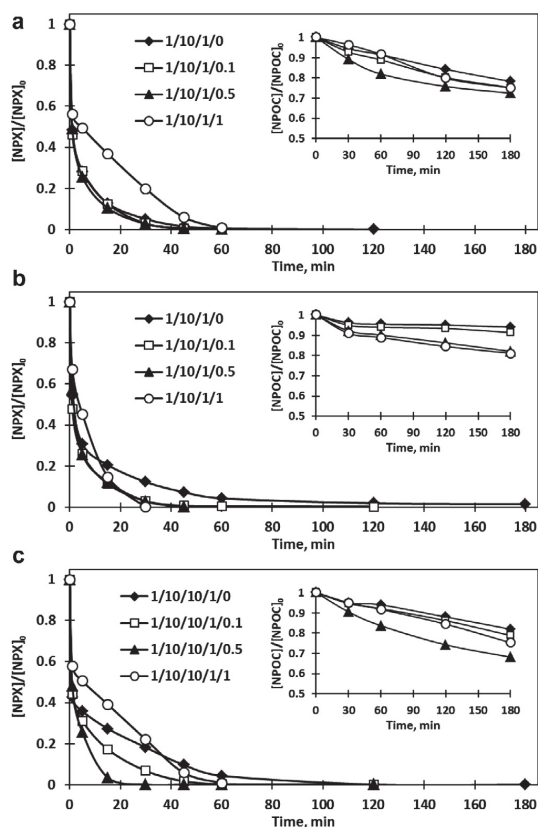


Fig. 5. NPX degradation and NPOC reduction by (a) the H₂O₂/Fe²⁺/CA process (NPX/H₂O₂/Fe²⁺/CA is a molar ratio), (b) the S₂O₈²⁻/Fe²⁺/CA process (NPX/S₂O₈²⁻/Fe²⁺/CA is a molar ratio), (c) the H₂O₂/S₂O₈²⁻/Fe²⁺/CA process (NPX/H₂O₂/S₂O₈²⁻/Fe²⁺/CA is a molar ratio): effect of initial CA concentration ([Fe²⁺]₀ = 75 μM, pH₀ = 5).

wide range of pH values followed by the CA-Fe²⁺ activated combined system. Notably, the solution pH was not controlled during the reaction and the final pH values in these reactions are presented in Table 2. In the case of the H₂O₂ and S₂O₈²⁻ dissociation extent in the studied CA-Fe²⁺-activated processes, the lowest residual concentrations were observed at pH 5 rather than pH 3 and the activation efficacy steadily decreased when the pH value was above 5 (Table 2). Similar to the findings of Liang et al. [45] regarding to EDTA-Fe²⁺/Fe³⁺ complexes formation, this phenomenon could be explained by different predominant forms of the CA-Fe²⁺ complex, such as Fe²⁺H₂CA, Fe²⁺HCA, Fe²⁺CA, Fe²⁺(OH)CA and Fe²⁺(OH)₂CA, depending on the pH, which are mainly responsible for the Fe²⁺ availability in solution. Hence, the efficacy of oxidant activation could be dependent on the composition of mixed iron/ligand complexes at different pH values. As a result, when pH was raised to 5, the moderate concentration of hydroxyl ions led to an appropriate mixed chelation. A further increase in pH to neutral and alkaline conditions generated sufficient hydroxyl ions and resulted in an excessive mixed chelation leading to decrease in the availability of Fe²⁺.

To sum up, the comparison of results obtained in the non-chelated and CA-chelated Fe²⁺-activated systems at the same treatment conditions indicated that the addition of chelating ligand proved effective to improve the NPX degradation at a wide range

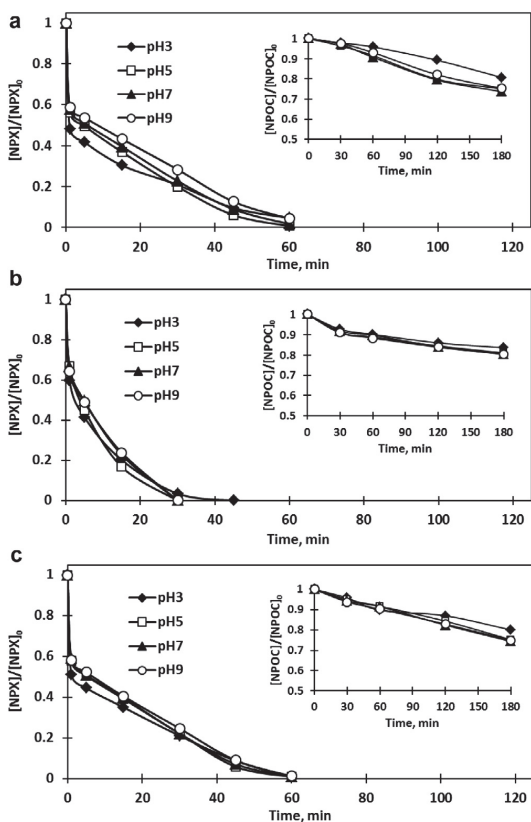


Fig. 6. NPX degradation and NPOC reduction by (a) the $\text{H}_2\text{O}_2/\text{Fe}^{2+}/\text{CA}$ process (NPX/ $\text{H}_2\text{O}_2/\text{Fe}^{2+}/\text{CA}$ molar ratio of 1/10/1/1), (b) the $\text{S}_2\text{O}_8^{2-}/\text{Fe}^{2+}/\text{CA}$ process (NPX/ $\text{S}_2\text{O}_8^{2-}/\text{Fe}^{2+}/\text{CA}$ molar ratio of 1/10/1/1), (c) the $\text{H}_2\text{O}_2/\text{S}_2\text{O}_8^{2-}/\text{Fe}^{2+}/\text{CA}$ process (NPX/ $\text{H}_2\text{O}_2/\text{S}_2\text{O}_8^{2-}/\text{Fe}^{2+}/\text{CA}$ molar ratio of 1/10/10/1/1): effect of initial pH ($[\text{NPX}]_0 = 75 \mu\text{M}$).

of pH probably due to the combined actions including the decrease of pH, the buffering of Fe^{2+} availability, and the prevention of Fe^{3+} precipitation in the studied processes. Therefore, the presence of CA played an important role in maintaining Fe^{2+} stable in aqueous solution, which favored the NPX destruction by the $\text{H}_2\text{O}_2/\text{Fe}^{2+}/\text{CA}$, $\text{H}_2\text{O}_2/\text{S}_2\text{O}_8^{2-}/\text{Fe}^{2+}/\text{CA}$, and especially $\text{S}_2\text{O}_8^{2-}/\text{Fe}^{2+}/\text{CA}$ process.

3.3. Identification of active radicals in citric acid chelated ferrous ion-activated persulfate and hydrogen peroxide/persulfate systems

To identify the predominant oxidative species and obtain a further insight into the reaction mechanism of NPX degradation by the $\text{S}_2\text{O}_8^{2-}/\text{Fe}^{2+}$, $\text{S}_2\text{O}_8^{2-}/\text{Fe}^{2+}/\text{CA}$, $\text{H}_2\text{O}_2/\text{S}_2\text{O}_8^{2-}/\text{Fe}^{2+}$ and $\text{H}_2\text{O}_2/\text{S}_2\text{O}_8^{2-}/\text{Fe}^{2+}/\text{CA}$ systems, scavenging studies using radical probes were carried out. The experiments were conducted with the addition of EtOH, reacting at high and comparable rates with HO^\cdot ($1.2 \times 10^9 - 2.8 \times 10^9 \text{ L}(\text{mol}\cdot\text{s})$) and $\text{SO}_4^{\cdot-}$ ($1.6 \times 10^7 - 7.7 \times 10^7 \text{ L}(\text{mol}\cdot\text{s})$), and *t*-BuOH, which is more effective scavenger for HO^\cdot ($3.8 \times 10^8 - 7.6 \times 10^8 \text{ L}(\text{mol}\cdot\text{s})$) than for $\text{SO}_4^{\cdot-}$ ($4 \times 10^5 - 9.1 \times 10^5 \text{ L}(\text{mol}\cdot\text{s})$) [22,46]. Based on these characteristics, the presence of HO^\cdot was identified by adding excess *t*-BuOH into the studied systems. The effect of $\text{SO}_4^{\cdot-}$ was estimated by comparing the difference between the degradation efficacy of NPX after adding excess *t*-BuOH and EtOH.

The results in Table 3 indicated that irrespective of the pH_0 value, the addition of excess *t*-BuOH decreased the efficacy of NPX degradation by about 14% and 15% for the $\text{S}_2\text{O}_8^{2-}/\text{Fe}^{2+}$ and $\text{S}_2\text{O}_8^{2-}/\text{Fe}^{2+}/\text{CA}$ systems, respectively, suggesting that HO^\cdot was involved in the both cases. The obtained results are consistent with the findings of Ji et al. [47] and Wu et al. [40].

For the combined process, the scavenging effect of excess *t*-BuOH was expectedly higher and accordingly the increase in the residual NPX concentration by about 65% and 50% was observed in the non-chelated and CA-chelated Fe^{2+} -activated system at $\text{pH}_0 = 3$, respectively. In the case of trials at $\text{pH}_0 = 7$, the presence of excess *t*-BuOH decreased the efficacy of NPX degradation by about 54% and 49% for the $\text{H}_2\text{O}_2/\text{S}_2\text{O}_8^{2-}/\text{Fe}^{2+}$ and $\text{H}_2\text{O}_2/\text{S}_2\text{O}_8^{2-}/\text{Fe}^{2+}/\text{CA}$ systems, respectively, indicating that the generation of HO^\cdot was more affected by the pH_0 in the non-chelated system. The addition of excess EtOH drastically inhibited the degradation of NPX in all studied systems. The small amount of NPX degradation that could not be eliminated by the addition of excess EtOH was most likely attributed to the generation of reductants, such as O_2^\cdot , in the studied systems [40]. These findings suggested that both HO^\cdot and $\text{SO}_4^{\cdot-}$ contributed to the degradation of NPX in the studied systems, whereas HO^\cdot proved the predominant oxidative species in the activated $\text{H}_2\text{O}_2/\text{S}_2\text{O}_8^{2-}$ process.

3.4. Identification of major transformation products

The same transformation products were identified during the oxidation of NPX by the $\text{H}_2\text{O}_2/\text{Fe}^{2+}/\text{CA}$, $\text{S}_2\text{O}_8^{2-}/\text{Fe}^{2+}/\text{CA}$ and $\text{H}_2\text{O}_2/\text{S}_2\text{O}_8^{2-}/\text{Fe}^{2+}/\text{CA}$ systems using LC–MS analysis as presented in Table 4. According to the results of the scavenging trials, both HO^\cdot and $\text{SO}_4^{\cdot-}$ were responsible for the destruction of NPX in the studied systems. In contrast, it is well known that $\text{SO}_4^{\cdot-}$ shares the similar reaction mechanisms with HO^\cdot , namely hydrogen abstraction, hydroxyl addition to unsaturated carbon including double bond and aromatic rings, and electron transfer which is more prevailing for $\text{SO}_4^{\cdot-}$ [48]. Irrespective of the applied oxidation system, the main step of the formation of the TPs was proposed to be hydroxylation (TP1a and TP1b), which is a common reaction pathway in both HO^\cdot and $\text{SO}_4^{\cdot-}$ reaction with aromatic molecules [15,49], with the subsequent decarboxylation (TP2–TP4) or demethoxylation (TP5).

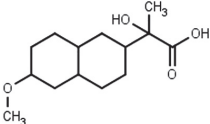
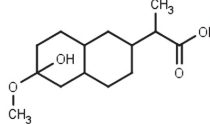
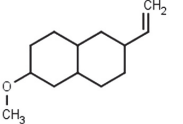
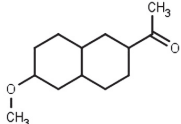
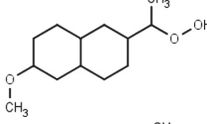
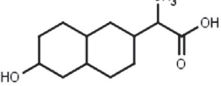
Unfortunately, the MS data did not allow to differentiate which site was preferentially attacked by the radicals and where the exact position of hydroxylation occurred, thus TP1a and TP1b structures were proposed based on the suggested routes (A and B) for the formation of other identified products (TP2–TP5) (Fig. 7). In the route A, the initial attack of $\text{HO}^\cdot/\text{SO}_4^{\cdot-}$ in methyl position results in formation of TP1a, which sequentially yields the peroxy radical to produce further TP2 (2-Methoxy-6-vinylnaphthalene) [35,50,51], TP3 (2-Acetyl-6-methoxynaphthalene) [35,50,52] and TP4 (1-(6-Methoxynaphthalen-2-yl)ethyl hydroperoxide) [52]. In the route B, the

Table 3
Degradation of NPX at different conditions.

Process ^a	pH_0	[NPX],% removed		
		Without scavenger	<i>t</i> -BuOH	EtOH
$\text{S}_2\text{O}_8^{2-}/\text{Fe}^{2+}$	3	90.3	76.1	14.6
	7	85.8	73.2	13.5
$\text{S}_2\text{O}_8^{2-}/\text{Fe}^{2+}/\text{CA}$	3	96.5	81.2	19.3
	7	99.9	85.1	21.7
$\text{H}_2\text{O}_2/\text{S}_2\text{O}_8^{2-}/\text{Fe}^{2+}$	3	88.2	23.2	6.4
	7	78.5	24.8	9.0
$\text{H}_2\text{O}_2/\text{S}_2\text{O}_8^{2-}/\text{Fe}^{2+}/\text{CA}$	3	78.9	29.2	16.8
	7	77.9	28.6	19.4

^a Experimental condition: $[\text{NPX}]_0 = [\text{Fe}^{2+}]_0 = [\text{CA}]_0 = 75 \mu\text{M}$, $[\text{H}_2\text{O}_2]_0 = [\text{S}_2\text{O}_8^{2-}]_0 = 750 \mu\text{M}$, $[\text{t-BuOH}]_0 = [\text{EtOH}]_0 = 37.5 \text{ mM}$, $t = 30 \text{ min}$.

Table 4
Proposed structures of the transformation products (TPs) of NPX presumed using LC–MS analysis.

Compound	Molecular weight	$[M + H]^+$, m/z	Reaction pathway	Chemical structure
TP1a	246	247	+{HO} -{H}	
TP1b	246	247	+{HO} -{H}	
TP2	184	185	+{HO} -{H2O} -{COOH}	
TP3	200	201	+{HO} -2{H} -{COOH}	
TP4	218	219	+{HO} -{H} -{COOH} +{HO}	
TP5	216	217	+{HO} -{CH3O}	

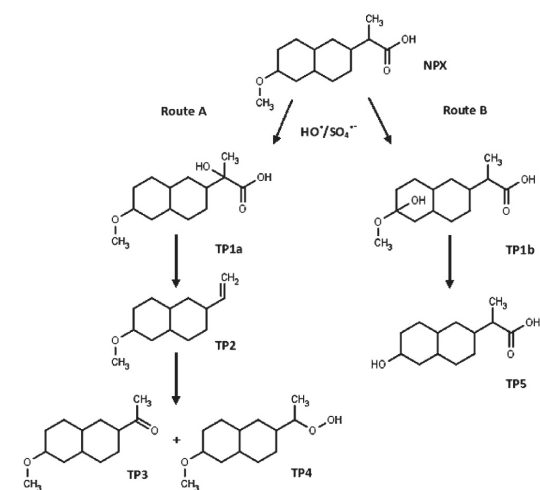


Fig. 7. Proposed reaction pathways for degradation of NPX in the studied systems.

attack of $\text{HO}^\bullet/\text{SO}_4^{\bullet-}$ in ring position occupied by methoxyl group leads to formation of TP1b, causing the subsequent demethoxylation to form TP5 (2-(6-Hydroxy-2-naphthyl)propanoic acid) [53]. It should be noted that the concentration of TPs increased with increasing reaction time to the maximum, and then gradually declined to below detection limit after complete destruction of NPX in the studied systems. The TP2 and TP3 were the two major TPs determined during the degradation of NPX by all studied systems. These intermediates were also previously reported in the literature as the most common NPX degradation by-products by other radical-based oxidation processes [35,50–52].

4. Conclusions

This study explored the degradation of NPX under different experimental conditions by H_2O_2 , $\text{S}_2\text{O}_8^{2-}$ and combined $\text{H}_2\text{O}_2/\text{S}_2\text{O}_8^{2-}$ activated with citric acid chelated ferrous ion. The addition of CA at an appropriate complexation ratio substantially improved the NPX destruction by the oxidation processes. The efficacy in the target compound oxidation was the highest in the $\text{S}_2\text{O}_8^{2-}/\text{Fe}^{2+}/\text{CA}$ process followed by the $\text{H}_2\text{O}_2/\text{S}_2\text{O}_8^{2-}/\text{Fe}^{2+}/\text{CA}$ process. Irrespective of the applied system, the mineralization of NPX was limitedly achieved. The results of the quenching studies suggested that both

HO^\cdot and SO_4^\cdot contributed to the degradation of NPX in the activated $\text{S}_2\text{O}_8^{2-}$ and $\text{H}_2\text{O}_2/\text{S}_2\text{O}_8^{2-}$ systems, while HO^\cdot proved the predominant radical in the combined process. Potential degradation mechanism of NPX was proposed based on the identified transformation products and included hydroxylation with the subsequent decarboxylation or demethoxylation. This study demonstrates that CA- Fe^{2+} -activated $\text{S}_2\text{O}_8^{2-}$ and combined $\text{H}_2\text{O}_2/\text{S}_2\text{O}_8^{2-}$ oxidation are effective treatment technologies for the degradation of NPX in aqueous solution at a wide range of pH and provides valuable information on the potential ISCO application of these technologies for the removal of NPX from the contaminated groundwater.

Acknowledgments

The authors are thankful to Irina Epold, Ph.D, and Tatjana Tjuljukova, M.Sc., for their assistance with the experiments. The financial support provided by institutional research funding IUT (1-7) of the Estonian Ministry of Education and Research is gratefully acknowledged.

References

- M. Isidori, M. Lavorgna, A. Nardelli, A. Parrella, L. Previtara, M. Rubino, Ecotoxicity of naproxen and its phototransformation products, *Sci. Total Environ.* 348 (2005) 93–101.
- K. Fent, A.A. Weston, D. Caminada, Ecotoxicology of human pharmaceuticals, *Aquat. Toxicol.* 76 (2006) 122–159.
- J.-J. Jiang, C.-L. Lee, M.-D. Fang, Emerging organic contaminants in coastal waters: anthropogenic impact, environmental release and ecological risk, *Mar. Pollut. Bull.* 85 (2014) 391–399.
- A. Barra Caracciolo, E. Topp, P. Grenni, Pharmaceuticals in the environment: biodegradation and effects on natural microbial communities. A review, *J. Pharm. Biomed. Anal.* 106 (2015) 25–36.
- D. Wojcieszynska, D. Domaradzka, K. Hupert-Kocurek, U. Guzik, Bacterial degradation of naproxen – undisclosed pollutant in the environment, *J. Environ. Manage.* 145 (2014) 157–161.
- T.A. Ternes, Occurrence of drugs in German sewage treatment plants and rivers, *Water Res.* 32 (1998) 3245–3260.
- C. Fernández, M. González-Doncel, J. Pro, G. Carbonell, J.V. Tarazona, Occurrence of pharmaceutically active compounds in surface waters of the henares-jarama-tajo river system (madrid, Spain) and a potential risk characterization, *Sci. Total Environ.* 408 (2010) 543–551.
- E. Marco-Urrea, M. Pérez-Trujillo, P. Blázquez, T. Vicent, G. Caminal, Biodegradation of the analgesic naproxen by *Trametes versicolor* and identification of intermediates using HPLC-DAD-MS and NMR, *Bioresour. Technol.* 101 (2010) 2159–2166.
- R.J. Watts, A.L. Teel, Treatment of contaminated soils and groundwater using ISCO, *Pract. Period Hazard. Toxic Radioact. Waste Manage.* 10 (2006) 2–9.
- I. Innocenti, I. Verginelli, F. Massetti, D. Piscitelli, R. Gavasci, R. Baciocchi, Pilot-scale ISCO treatment of a MtBE contaminated site using a Fenton-like process, *Sci. Total Environ.* 485–486 (2014) 726–738.
- F.J. Krems, R.L. Siegrist, M.L. Crimi, R.F. Furrer, B.G. Petri, ISCO for groundwater remediation: analysis of field applications and performance, *Ground Water Monit. Rem.* 30 (2010) 42–53.
- A. Tsitonaki, B. Petri, M. Crimi, H. Mosbaek, R.L. Siegrist, P.L. Bjerg, In situ chemical oxidation of contaminated soil and groundwater using persulfate: a review, *Crit. Rev. Environ. Sci. Technol.* 40 (2010) 55–91.
- Venny, S. Gan, H.K. Ng, Current status and prospects of Fenton oxidation for the decontamination of persistent organic pollutants (POPs) in soils, *Chem. Eng. J.* 213 (2012) 295–317.
- R. Chen, J.J. Pignatello, Role of quinone intermediates as electron shuttles in Fenton and photoassisted Fenton oxidations of aromatic compounds, *Environ. Sci. Technol.* 31 (1997) 2399–2406.
- A. Babuponnusami, K. Muthukumar, A review on Fenton and improvements to the Fenton process for wastewater treatment, *J. Environ. Chem. Eng.* 2 (2014) 557–572.
- C. Liang, C.J. Bruell, M.C. Marley, K.L. Sperry, Persulfate oxidation for in situ remediation of TCE. I. Activated by ferrous ion with and without a persulfate-thiosulfate redox couple, *Chemosphere* 55 (2004) 1213–1223.
- C. Liang, C.J. Bruell, M.C. Marley, K.L. Sperry, Persulfate oxidation for in situ remediation of TCE. II. Activated by chelated ferrous ion, *Chemosphere* 55 (2004) 1225–1233.
- J. Lemaire, M. Buès, T. Kabeche, K. Hanna, M.-O. Simonnot, Oxidant selection to treat an aged PAH contaminated soil by in situ chemical oxidation, *J. Environ. Chem. Eng.* 1 (2013) 1261–1268.
- X. Liao, D. Zhao, X. Yan, S.G. Huling, Identification of persulfate oxidation products of polycyclic aromatic hydrocarbon during remediation of contaminated soil, *J. Hazard. Mater.* 276 (2014) 26–34.
- W.-S. Chen, Y.-C. Su, Removal of dinitrotoluenes in wastewater by sono-activated persulfate, *Ultrason. Sonochem.* 19 (2012) 921–927.
- S.S. Abu Amr, H.A. Aziz, M.N. Adlan, M.J.K. Bashir, Pretreatment of stabilized leachate using ozone/persulfate oxidation process, *Chem. Eng. J.* 221 (2013) 492–499.
- G.P. Anipsitakis, D.D. Dionysiou, Radical generation by the interaction of transition metals with common oxidants, *Environ. Sci. Technol.* 38 (2004) 3705–3712.
- G.V. Buxton, T.N. Malone, G.A. Salmon, Reaction of SO_4^\cdot with Fe^{2+} , Mn^{2+} and Cu^{2+} in aqueous solution, *J. Chem. Soc. Faraday Trans.* 93 (1997) 2893–2897.
- O.A. Travina, Y.N. Kozlov, A.P. Pural', I.Y. Rodko, Synergism of the action of the sulfite oxidation initiators, iron and peroxydisulfate ions, *Russ. J. Phys. Chem.* 73 (1999) 1215–1219.
- J.J. Pignatello, K. Baehr, Ferric complexes as catalysts for Fenton degradation of 2,4-D and metolachlor in soil, *J. Environ. Qual.* 23 (1994) 365–370.
- A. De Luca, R.F. Dantas, S. Esplugas, Assessment of iron chelates efficiency for photo-Fenton at neutral pH, *Water Res.* 61 (2014) 232–242.
- A. Rastogi, S.R. Al-Abed, D.D. Dionysiou, Effect of inorganic, synthetic and naturally occurring chelating agents on Fe(II) mediated advanced oxidation of chlorophenols, *Water Res.* 43 (2009) 684–694.
- D. Han, J. Wan, Y. Ma, Y. Wang, M. Huang, Y. Chen, D. Li, Z. Guan, Y. Li, Enhanced decolorization of Orange G in a Fe(II)-EDDS activated persulfate process by accelerating the regeneration of ferrous iron with hydroxylamine, *Chem. Eng. J.* 256 (2014) 316–323.
- D. Han, J. Wan, Y. Ma, Y. Wang, Y. Li, D. Li, Z. Guan, New insights into the role of organic chelating agents in Fe(II) activated persulfate processes, *Chem. Eng. J.* 269 (2015) 425–433.
- Z. Shu, J.R. Bolton, M. Belosevic, M.G. El Din, Photodegradation of emerging micropollutants using the medium-pressure UV/ H_2O_2 Advanced Oxidation Process, *Water Res.* 47 (2013) 2881–2889.
- F. Mendez-Arriaga, R. Almanza, Water remediation by UV-vis/ H_2O_2 process, photo-Fenton-like oxidation, and zeolite ZSM5, *Desalin. Water Treat.* 52 (2014) 5822–5832.
- F.J. Benitez, J.L. Acero, F.J. Real, G. Roldan, F. Casas, Comparison of different chemical oxidation treatments for the removal of selected pharmaceuticals in water matrices, *Chem. Eng. J.* 168 (2011) 1149–1156.
- J.-K. Im, J. Yoon, N. Her, J. Han, K.-D. Zoh, Y. Yoon, Sonocatalytic- TiO_2 nanotube, Fenton, and CCl_4 reactions for enhanced oxidation, and their applications to acetaminophen and naproxen degradation, *Sep. Purif. Technol.* 141 (2015) 1–9.
- N. Klammerth, S. Malato, A. Agüera, A. Fernández-Alba, Photo-Fenton and modified photo-Fenton at neutral pH for the treatment of emerging contaminants in wastewater treatment plant effluents: a comparison, *Water Res.* 47 (2013) 833–840.
- A. Gauch, A.M. Tuğan, N. Kibbi, Naproxen abatement by thermally activated persulfate in aqueous, *Chem. Eng. J.* 279 (2015) 861–873.
- S. Zorita, L. Mårtensson, L. Mathiasson, Occurrence and removal of pharmaceuticals in a municipal sewage treatment system in the south of Sweden, *Sci. Total Environ.* 407 (2009) 2760–2770.
- G.M. Eisenberg, Colorimetric determination of hydrogen peroxide, *Ind. Eng. Chem. Anal. Ed.* 15 (1943) 327–328.
- N.A. Sofina, M.K. Beklemishev, A.L. Kapanadze, I.F. Dolmanova, Sorption-catalytic Method for the Chromium Determination, 44, Moscow Univ. Chem. Bull., 2003, pp. 189–198 (in Russian).
- E. Merck, Iron, The Testing of Water, Merck, Darmstadt, 1994, pp. 107–110.
- X. Wu, X. Gu, S. Lu, M. Xu, X. Zhang, Z. Miao, Z. Qiu, Q. Sui, Degradation of trichloroethylene in aqueous solution by persulfate activated with citric acid chelated ferrous ion, *Chem. Eng. J.* 255 (2014) 585–592.
- I. Epold, M. Trapido, N. Dulova, Degradation of levofloxacin in aqueous solutions by Fenton, ferrous ion-activated persulfate and combined Fenton/persulfate systems, *Chem. Eng. J.* 279 (2015) 452–462.
- J.J. Pignatello, E. Oliveros, A. MacKay, Advanced oxidation processes for organic contaminant destruction based on the Fenton reaction and related chemistry, *Crit. Rev. Environ. Sci. Technol.* 36 (2006) 1–84.
- A. Romero, A. Santos, F. Vicente, C. González, Diuron abatement using activated persulfate: effect of pH, Fe(II) and oxidant dosage, *Chem. Eng. J.* 162 (2010) 257–265.
- N. Quici, M.E. Morgada, R.T. Gettar, M. Bolte, M.I. Litter, Photocatalytic degradation of citric acid under different conditions: TiO_2 heterogeneous photocatalysis against homogeneous photolytic processes promoted by Fe(III) and H_2O_2 , *Appl. Catal. B Environ.* 71 (2007) 117–124.
- C. Liang, C.-P. Liang, C.-C. Chen, pH dependence of persulfate activation by EDTA/Fe(III) for degradation of trichloroethylene, *J. Contam. Hydrol.* 106 (2009) 173–182.
- G.V. Buxton, C.L. Greenstock, W.P. Helman, A.B. Ross, Critical review of rate constants for reactions of hydrated electrons, hydrogen atoms and hydroxyl radicals ($^\cdot\text{OH}/^\cdot\text{O}^\cdot$) in aqueous solution, *J. Phys. Chem. Ref. Data* 17 (1988) 513–886.
- Y. Ji, C. Ferronato, A. Salvador, X. Yang, J.-M. Chovelon, Degradation of ciprofloxacin and sulfamethoxazole by ferrous-activated persulfate: implications for remediation of groundwater contaminated by antibiotics, *Sci. Total Environ.* 472 (2014) 800–808.
- J.A. Khan, X. He, N.S. Shah, H.M. Khan, E. Hapeshi, D. Fatta-Kassinos, D.D. Dionysiou, Kinetic and mechanism investigation on the photochemical degradation of atrazine with activated H_2O_2 , $\text{S}_2\text{O}_8^{2-}$ and HSO_5^\cdot , *Chem. Eng. J.* 252 (2014) 393–403.

- [49] M.G. Antoniou, A.A. De La Cruz, D.D. Dionysiou, Intermediates and reaction pathways from the degradation of microcystin-LR with sulfate radicals, *Environ. Sci. Technol.* 44 (2010) 7238–7244.
- [50] E. Arany, R.K. Szabó, L. Apáti, T. Alapi, I. Illisz, P. Mazellier, A. Dombi, K. Gajda-Schranz, Degradation of naproxen by UV, VUV photolysis and their combination, *J. Hazard. Mater.* 262 (2013) 151–157.
- [51] R. Marotta, D. Spasiano, I. Di Somma, R. Andreozzi, Photodegradation of naproxen and its photoproducts in aqueous solution at 254 nm: a kinetic investigation, *Water Res.* 47 (2013) 373–383.
- [52] N. Jallouli, K. Elghniji, O. Hentati, A.R. Ribeiro, A.M.T. Silva, M. Ksibi, UV and solar photo-degradation of naproxen: TiO₂ catalyst effect, reaction kinetics, products identification and toxicity assessment, *J. Hazard. Mater.* 304 (2016) 329–336.
- [53] C.-J.M. Chin, T.-Y. Chen, M. Lee, C.-F. Chang, Y.-T. Liu, Y.-T. Kuo, Effective anodic oxidation of naproxen by platinum nanoparticles coated FTO glass, *J. Hazard. Mater.* 277 (2014) 110–119.

CURRICULUM VITAE

Personal data

Name: Eneliis Kattel
Date of birth: 26.07.1989
Place of birth: Tallinn, Estonia
Citizenship: Estonian

Contact data

E-mail: eneliis.kattel@ttu.ee

Education

2014– ...	Tallinn University of Technology, PhD studies (Chemical and Materials Technology)
2014–2016	Estonian Centre for Engineering Pedagogy, Additional Speciality of Technical teachers (Engineering Pedagogy)
2011–2013	Tallinn University of Technology, MSc in Engineering
2011–2013	Tallinn University of Technology, BSc in Engineering
1996–2008	Saku Gymnasium, high school education

Language competence/skills

Estonian	native speaker
English	fluent
Russian	beginner
German	beginner

Special courses

July 2017	2nd Summer School on Environmental Applications of Advanced Oxidation Processes and Training School on Advanced Treatment Technologies and Contaminants of Emerging Concern (NEREUS COST Action ES1403)"; Porto, Portugal
June 2017	"Resource Wisdom" workshop held by Ministry of the Environment of Estonia and Induco Ltd. Finland; Ministry of the Environment of Estonia, Tallinn, Estonia
August 2016	Courses on "Homogeneous catalysis" and "Fate of Organic Chemicals in the Environment"; 26th Jyväskylä Summer School, University of Jyväskylä, Finland
June 2016	NEREUS "Cristina Becerra-Castro" Training School on "Methods for detecting and quantifying antibiotic resistant bacteria and antibiotic resistance genes in the environment"; IDAEA-CSIC, Barcelona, Spain
May–June 2012	Two-week intensive programme „Sustainable Management and Technology“; Artois University (The Institute of Technology in Bethune), Bethune, France

Professional employment

2017–2018	Tallinn University of Technology, Early Stage Researcher
2015–2017	Tallinn University of Technology, Research Staff
2013–2014	Tallinn University of Technology, Engineer

Defended theses

Master's Degree: Purification of pyrolysis water from oil shale processing with the Fenton-process and ozonation, Tallinn University of Technology, Faculty of Chemical and Materials Technology, Department of Chemical Engineering, 2013.

Supervisors: Marina Trapido, Anna Goi

Main areas of scientific work

1. Biosciences and Environment; 1.8. Research relating to the State of the Environment and to Environmental Protection; CERCS SPECIALTY: T270 Environmental technology, pollution control

1. Biosciences and Environment; 1.9. Research into Substances Hazardous to the Environment; CERCS SPECIALTY: P305 Environmental chemistry

4. Natural Sciences and Engineering; 4.11. Chemistry and Chemical Technology; CERCS SPECIALTY: P305 Environmental chemistry

Involvement in research projects

VIR16015 Water emissions and their reduction in village communities - villages in Baltic Sea Region as pilots (VillageWaters).

IUT1-7 Chemical engineering approach to removal of priority pollutants and emerging micropollutants from water/wastewater and soil: implementation and optimization of advanced oxidation technologies.

AR12017 Removing biologically non-readily degradable substances from wastewater with physical-chemical and biological methods to decrease the pollution load of aquatic environment (CHEMBIO).

ETF7812 Peroxidation for remediation of chlorinated hydrocarbons contaminated soil.

Awards

2017	Association of Chemistry and the Environment (ACE) scholarship to participate in the 18th European Meeting on Environmental Chemistry (EMEC 18) (26–29 November 2017, Porto, Portugal)
2017	Kristjan Jaak short study scholarship (2nd Summer School on Environmental Applications of Advanced Oxidation Processes and Training School on Advanced Treatment Technologies and Contaminants of Emerging Concern (NEREUS COST Action ES1403) (10–14 July 2017, Porto, Portugal)
2017	Tallinn City Government, Jaan Poska scholarship

- 2016 ERF Dora Plus program (activity 1) scholarship for the participation with oral presentation in 1st International Conference on Sustainable Water Processing (11–14 September 2016, Sitges, Spain)
- 2016 COST (European Cooperation in Science and Technology) grant to participate in NEREUS “Cristina Becerra-Castro” Training School on “Methods for detecting and quantifying antibiotic resistant bacteria and antibiotic resistance genes in the environment” (13–14 June 2016, IDAEA-CSIC, Barcelona, Spain)

Supervised dissertations

Maarja Sammelselg, Master's Degree, 2017, (sup) Niina Dulova; Eneliis Kattel, Degradation of amoxicillin in different aqueous matrices by photo-activated hydrogen peroxide, Tallinn University of Technology, School of Engineering, Department of Materials and Environmental Technology.

Balpreet Kaur, Master's Degree, 2017, (sup) Niina Dulova; Eneliis Kattel, Degradation of amoxicillin in aqueous solution by photo-activated persulfate, Tallinn University of Technology, School of Engineering, Department of Materials and Environmental Technology.

Yuan Liang, Master's Degree, 2017, (sup) Niina Dulova; Eneliis Kattel, Photochemical degradation of a beta-lactam antibiotic in different aqueous matrices, Tallinn University of Technology, School of Engineering, Department of Materials and Environmental Technology.

Kristi Auger, Master's Degree, 2017, (sup) Eneliis Kattel; Niina Dulova, Treatment of landfill leachate by iron sludge-activated Fenton-based process, Tallinn University of Technology, School of Engineering, Department of Materials and Environmental Technology.

Sandra Salom, Master's Degree, 2016, (sup) Niina Dulova; Eneliis Kattel, Degradation of acesulfame in aqueous matrices by activated persulfate, Tallinn University of Technology, Faculty of Chemical and Materials Technology, Department of Chemical Engineering.

Marge Nõmmik, Master's Degree, 2016, (sup) Niina Dulova; Eneliis Kattel, Degradation of acesulfame in aqueous matrices by photo-Fenton process, Tallinn University of Technology, Faculty of Chemical and Materials Technology, Department of Chemical Engineering.

Sigrid Turja, Master's Degree, 2015, (sup) Niina Dulova; Eneliis Kattel, Landfill leachate treatment by activated hydrogen peroxide and persulfate, Tallinn University of Technology, Faculty of Chemical and Materials Technology, Department of Chemical Engineering.

ELULOOKIRJELDUS

Isikuandmed

Nimi: Eneliis Kattel
Sünniaeg: 26.07.1989
Sünnikoht: Tallinn, Eesti
Kodakondsus: Eesti

Kontaktandmed

E-post: eneliis.kattel@ttu.ee

Hariduskäik

2014– ...	Tallinna Tehnikaülikool, doktorantuur (keemia- ja materjalitehnoloogia)
2014–2016	TTÜ Eesti Inseneripedagoogika Keskus; loodus-, täppisteaduste ja tehnoloogiavaldkonna õppeainete täienduskoolitus (tehnikatõpetaja/-õppejõu lisaeriala)
2011–2013	Tallinna Tehnikaülikool, tehnikateaduste magistriraad
2011–2013	Tallinna Tehnikaülikool, tehnikateaduste bakalaureusekraad
1996–2008	Saku Gümnaasium, keskkaridus

Keelteoskus

Eesti keel	emakeel
Inglise keel	kõrgtase
Vene keel	algtase
Saksa keel	algtase

Täiendkursused

Juuli 2017	Osalemine suvekoolis ja kursusel "2nd Summer School on Environmental Applications of Advanced Oxidation Processes and Training School on Advanced Treatment Technologies and Contaminants of Emerging Concern (NEREUS COST Action ES1403); Porto, Portugal
Juuni 2017	Osalemine Eesti Keskkonnaministeeriumi ja Induco Ltd. Finland korraldatud töötoas "Resource Wisdom"; Eesti Keskkonnaministeerium, Tallinn, Eesti
August 2016	Osalemine kursustel "Homogeneous catalysis" ja "Fate of Organic Chemicals in the Environment; 26th Jyväskylä Summer School, University of Jyväskylä, Soome
Juuni 2016	Osalemine NEREUS Cristina Becerra-Castro nimelisel "Methods for detecting and quantifying antibiotic resistant bacteria and antibiotic resistance genes in the environment" koolitusel; IDAEA-CSIC, Barcelona, Hispaania
Mai–juuni 2012	2-nädalane intensiivprogramm teemal „Sustainable Management and Technology“; Artois University (The Institute of Technology in Bethune), Bethune, Prantsusmaa

Teenistuskäik

2017–2018	Tallinna Tehnikaülikool, doktorant-nooremteadur
2015–2017	Tallinna Tehnikaülikool, teadustöö täitja
2013–2014	Tallinna Tehnikaülikool, insener

Kaitstud lõputööd

Tehnikateaduste magistrikraad: Põlevkivi töötlemisest pärineva pürolüüsivee puhastamine Fenton-protsessiga ja osoonimisega, Tallinna Tehnikaülikool, Keemia- ja materjalitehnoloogia teaduskond, Keemiatehnika instituut, 2013.

Juhendajad: Marina Trapido, Anna Goi

Uurimistöö põhisuunad

1. Bio- ja keskkonnateadused; 1.8. Keskkonnaseisundit ja keskkonnakaitset hõlmavad uuringud; CERCS ERIALA: T270 Keskkonnatehnoloogia, reostuskontroll; PÕHISUUND: Vee ja reovee töötlus

1. Bio- ja keskkonnateadused; 1.9. Keskkonnaohtlike aineid käsitlevad uuringud; CERCS ERIALA: P305 Keskkonnakeemia; PÕHISUUND: Mikrosaasteainete lagundamine süvaoksüdatsiooniprotsessidega

4. Loodusteadused ja tehnika; 4.11. Keemia ja keemiatehnika; CERCS ERIALA: P305 Keskkonnakeemia

Osalemine uurimisprojektides

VIR16015 Hajaasustusalade reostuskoormuse vähendamine - Läänemere piirkonna külad pilootobjektidena.

IUT1-7 Keemiatehnikapõhine lähenemisviis prioriteetsete saasteainete ja uute esilekerkivate mikrosaasteainete kõrvaldamisele veest/reoveest ja pinnasest: täiustatud oksüdatsioonitehnoloogiate kasutamine ja optimeerimine.

AR12017 Bioloogiliselt raskesti lagunevate ainete kõrvaldamine reoveest füüsikaliskemiliste ja bioloogiliste meetoditega vesikeskkonna saastekoormuse vähendamiseks (CHEMBIO).

ETF7812 Klooritud süsivesinikega saastatud pinnase taastamine peroksüdeerimisega.

Teaduspreemiad ja tunnustused

2017	Association of Chemistry and the Environment (ACE) stipendium osalemiseks konverentsil "18th European Meeting on Environmental Chemistry (EMEC 18)" (26.–29.11.2017, Porto, Portugal)
------	---

2017	Kristjan Jaagu välislahetuste stipendium osalemiseks suulise ettekandega suvekoolis ja kursusel "2nd Summer School on Environmental Applications of Advanced Oxidation Processes and Training School on Advanced Treatment Technologies and Contaminants of Emerging Concern (NEREUS COST Action ES1403)" (10.–14.07.2017, Porto, Portugal)
2017	Tallinna Linnavalitsuse Jaan Poska stipendium
2016	ERF Dora Pluss programm (tegevus 1) stipendium osalemiseks suulise ettekandega konverentsil 1st International Conference on Sustainable Water Processing, 11.–14.09.2016, Sitges, Hispaania
2016	COST (European Cooperation in Science and Technology) stipendium osalemiseks Cristina Becerra-Castro nimelisel NEREUS "Methods for detecting and quantifying antibiotic resistant bacteria and antibiotic resistance genes in the environment" koolitusel (13.–15.06.2016, IDAEA-CSIC, Barcelona, Hispaania)

Juhendatud magistritööd

Maarja Sammelselg, magistrikraad, 2017, (juh) Niina Dulova; Eneliis Kattel, Amokitsilliini lagundamine erinevates vesikeskkondades foto-aktiveeritud vesinikperoksiidiga, Tallinna Tehnikaülikool, Inseneriteaduskond, Materjali- ja keskkonnatehnoloogia instituut.

Balpreet Kaur, magistrikraad, 2017, (juh) Niina Dulova; Eneliis Kattel, Amokitsilliini lagundamine vesilahuses foto-aktiveeritud persulfaadiga, Tallinna Tehnikaülikool, Inseneriteaduskond, Materjali- ja keskkonnatehnoloogia instituut.

Yuan Liang, magistrikraad, 2017, (juh) Niina Dulova; Eneliis Kattel, Beetalaktaam-antibiootikumi fotokeemiline lagundamine erinevates vesikeskkondades, Tallinna Tehnikaülikool, Inseneriteaduskond, Materjali- ja keskkonnatehnoloogia instituut.

Kristi Auger, magistrikraad, 2017, (juh) Eneliis Kattel; Niina Dulova, Prügila nõrgvee töötlemine rauasettega aktiveeritud Fentoni taolise protsessiga, Tallinna Tehnikaülikool, Inseneriteaduskond, Materjali- ja keskkonnatehnoloogia instituut.

Sandra Salom, magistrikraad, 2016, (juh) Niina Dulova; Eneliis Kattel, Atsesulfaami lagundamine veekeskkonnas aktiveeritud persulfaadiga, Tallinna Tehnikaülikool, Keemia ja materjalitehnoloogia teaduskond, Keemiatehnika instituut.

Marge Nõmmik, magistrikraad, 2016, (juh) Niina Dulova; Eneliis Kattel, Atsesulfaami lagundamine vesikeskkonnas foto-Fenton-protsessiga, Tallinna Tehnikaülikool, Keemia ja materjalitehnoloogia teaduskond, Keemiatehnika instituut.

Sigrid Turja, magistrikraad, 2015, (juh) Niina Dulova; Eneliis Kattel, Prügila nõrgvee töötlemine aktiveeritud vesinikperoksiidi ja persulfaadiga, Tallinna Tehnikaülikool, Keemia ja materjalitehnoloogia teaduskond, Keemiatehnika instituut.

